

**PARAMETRIC STUDY OF SHORT PERIODIC SPEED
CONTROL HUMPS ON A ROAD VEHICLE DYNAMIC**

BY
ISMAIL MOHAMMAD YAMIN AL-HINDI

A Thesis Presented to the
DEANSHIP OF GRADUATE STUDIES

KING FAHD UNIVERSITY OF PETROLEUM & MINERALS
DHAHRAN, SAUDI ARABIA

In Partial Fulfillment of the
Requirements for the Degree of

MASTER OF SCIENCE
In
MECHANICAL ENGINEERING


MAY 2009

KING FAHD UNIVERSITY OF PETROLEUM & MINERALS
DHAHRAN 31261, SAUDI ARABIA

DEANSHIP OF GRADUATE STUDIES

This thesis, written by **Ismail Mohammad Yamin Al-Hindi** under the direction of his thesis advisor and approved by his thesis committee, has been presented to and accepted by the Dean of Graduate Studies, in partial fulfillment of the requirements for the degree of **MASTER OF SCIENCE IN MECHANICAL ENGINEERING**.

Thesis Committee


Dr. Yaagoub Al-Nassar
(Thesis Advisor)


Dr. Amro Al-Qutub
Department Chairman


Dr. Muhammad Hawwa
(Member)


Dr. Salfin Zummo
Dean of Graduate Studies


Dr. Hussain Al-Qahtani
(Member)

21/6/09
Date

Dedicated

To

My

Beloved Father and Mother,

Loving Wife, Daughter,

Sisters and Brothers

ACKNOWLEDGMENT

All praises and glory to Allah the Almighty who alone enabled this work to be accomplished.

Acknowledgment is due to the King Fahd University of Petroleum & Minerals for graduate research work.

I wish to express my appreciation with deep gratitude to Dr. Yaagoub Al-Nassar who served as my major advisor for his guidance, encouragement and support in this work. I am especially grateful for his extensive long hours and days spent with me. I benefit from his rich knowledge and experience. I also wish to thank the other members of my thesis committee Dr. Muhammad Hawwa and Dr. Hussain Al-Qahtani for their support and cooperation.

TABLE OF CONTENTS

	Page
ACKNOWLEDGMENT	iv
TABLE OF CONTENTS	v
LIST OF TABLES	vii
LIST OF FIGURES	viii
ABSTRACT (ENGLISH)	xi
ABSTRACT (ARABIC)	xiii
CHAPTER 1. INTRODUCTION.....	1
1.1 BACKGROUND	1
1.2 SAUDI TRAFFIC STANDARDS: BRIEF REVIEW	5
1.3 HEALTH AND SAFETY ISSUES	8
1.4 ERGONOMIC STANDARDS.....	9
1.5 VIBRATION DOSE VALUE, VDV	10
1.6 THESIS OBJECTIVE.....	11
1.7 SCOPE OF THE PRESENT STUDY	12
CHAPTER 2. LITERATURE REVIEW.....	14
2.1 ON GENERAL EVALUATION OF SPEED CONTROL HUMPS	14
2.2 ON MODELING APPROACH OF SPEED CONTROL HUMPS.....	15
CHAPTER 3. MATHEMATICAL MODELING AND FORMULATION	18
3.1 VEHICLE MODELING.....	18
3.2 MATHEMATICAL FORMULATION	21
3.3 SOLUTION STRATEGY	25
CHAPTER 4. SIMULATION STRATEGY	26

4.1 INTRODUCTION	26
4.2 HUMP PARAMETERS.....	27
CHAPTER 5. RESULTS AND DISCUSSION.....	33
5.1 EFFECT OF VARYING HEIGHT OF THE HUMP.....	33
5.2 EFFECT OF VEHICLE SPEED.....	38
5.3 EFFECT OF DIFFERENT SPACING BETWEEN HUMPS.....	43
5.3.1 EFFECT OF DIFFERENT SPACING RATIOS OF CRITICAL SPACING	43
5.3.1 TIRE SIZES EFFECT ON THE HUMP SPACING.....	48
5.4 EFFECT OF MULTIPLICITY OF THESE CIRCULAR SHORT PERIODIC HUMPS.....	61
5.5 LINEAR VS. BILINEAR BEHAVIOR IN THE SUSPENSION SYSTEM	70
CHAPTER 6. CONCLUSION AND RECOMMENDATION	73
6.1 CONCLUSION.....	73
6.2 RECOMMENDATION	74
6.3 FUTURE WORK.....	75
APPENDICES.....	76
APPENDIX ‘A’	77
APPENDIX ‘B’.....	81
APPENDIX ‘C’	84
NOMENCLATURE.....	88
REFERENCES.....	91
VITA	94

LIST OF TABLES

Table 1.1: General rules where to construct humps and corresponding speed limit.....	8
Table 3.1: Mass, damping coefficient, spring coefficient, moment of inertia, and dimensions for front and rear of the vehicle main body.....	20
Table 4.1: Critical spacing for different tire sizes as follows:.....	32

LIST OF FIGURES

Figure 1.1: Short periodic humps	2
Figure 1.2: Short periodic humps at Dammam-Dhahran highway and Doha	3
Figure 1.3: Short periodic humps at Tanajib/ Safaniyah main road intersection	3
Figure 1.4: Short periodic humps at Ras-Tanura	3
Figure 1.5: Vehicle crossing over short bump	5
Figure 1.6: In-Kingdom Standard for speed hump.....	6
Figure 1.7: In-Kingdom Standard for Flat-Top hump.....	6
Figure 1.8: In-Kingdom Standard for Raised Intersection speed hump.....	7
Figure 3.1: 3-D Model of the vehicle and the driver.....	19
Figure 4.1: Vehicle tire crossing over single circular short periodic hump.	28
Figure 4.2: Effective profile of the hump when tire size is R_{T2}	28
Figure 4.3: Vehicle tire crossing over two short humps when: (a) $S = 0$, (b) $S < S_{cr}$, (c) $S = S_{cr}$, and (d) $S > S_{cr}$	29
Figure 4.4: Actual interface between the vehicle tire size, R_{T2} , for 2 humps	30
Figure 4.5: Actual interface between the vehicle tire size, R_{T2} , for 10 humps	30
Figure 5.1: VDV vs. Speed for tire size R_{T2} crossing over 2 humps for Driver when: (a) $S = 0$, (b) $S = 1.0 \times S_{cr}$, and (c) $S = 2.0 \times S_{cr}$	35
Figure 5.2: VDV vs. Speed for tire size R_{T2} crossing over 5 humps for Driver when: (a) $S = 0$, (b) $S = 1.0 \times S_{cr}$, and (c) $S = 2.0 \times S_{cr}$	36
Figure 5.3: VDV vs. Speed for tire size R_{T2} crossing over 10 humps for Driver when: (a) $S = 0$, (b) $S = 1.0 \times S_{cr}$, and (c) $S = 2.0 \times S_{cr}$	37
Figure 5.4: Max Accl. vs. Speed for single hump, h_2 for Driver	40
Figure 5.5: Max Jerk vs. Speed for single hump, h_2 for Driver	40
Figure 5.6: VDV vs. Speed for single hump, h_2 for Driver.....	40
Figure 5.7: Max Accl. vs. Speed for single hump, h_2 for Main Body.....	41
Figure 5.8: Max Jerk vs. Speed for single hump, h_2 for Main Body.....	41

Figure 5.9: VDV vs. Speed for single hump, h_2 for Main Body	41
Figure 5.10: VDV vs. Speed for Driver with h_2 , tire size R_{T2} for (a) 2 humps and (b) 10 humps when $S = 0$, $S = S_{cr}$, and $S = 2.0$ of S_{cr}	42
Figure 5.11: VDV vs. Speed for 2 humps, h_2 , tire size R_{T2} for (a) Driver and (b) Main Body	45
Figure 5.12: VDV vs. Speed for 5 humps, h_2 , tire size R_{T2} for (a) Driver and (b) Main Body	46
Figure 5.13: VDV vs. Speed for 10 humps, h_2 , tire size R_{T2} for (a) Driver and (b) Main Body	47
Figure 5.14: VDV vs. Spacing for Driver, for: 2 humps, h_2 , different tire sizes $R_{T1}/ R_{T2}/ R_{T3}$, speeds of (a) 30 km/hr, (b) 50 km/hr, (c) 80 km/hr and (d) 100 km/hr	50
Figure 5.15: VDV vs. Spacing for Main Body, for: 2 humps, h_2 , different tire sizes $R_{T1}/ R_{T2}/ R_{T3}$, speeds of (a) 30 km/hr, (b) 50 km/hr, (c) 80 km/hr and (d) 100 km/hr	52
Figure 5.16: VDV vs. Spacing for Driver, for: 5 humps, h_2 , different tire sizes $R_{T1}/ R_{T2}/ R_{T3}$, speeds of (a) 30 km/hr, (b) 50 km/hr, (c) 80 km/hr and (d) 100 km/hr	54
Figure 5.17: VDV vs. Spacing for Main Body, for: 5 humps, h_2 , different tire sizes $R_{T1}/ R_{T2}/ R_{T3}$, speeds of (a) 30 km/hr, (b) 50 km/hr, (c) 80 km/hr and (d) 100 km/hr	56
Figure 5.18: VDV vs. Actual Spacing for Driver, for: 10 humps, h_2 , different tire sizes $R_{T1}/ R_{T2}/ R_{T3}$, speeds of (a) 30 km/hr, (b) 50 km/hr, (c) 80 km/hr and (d) 100 km/hr	58
Figure 5.19: VDV vs. Spacing for Main Body, for: 10 humps, h_2 , different tire sizes $R_{T1}/ R_{T2}/ R_{T3}$, speeds of (a) 30 km/hr, (b) 50 km/hr, (c) 80 km/hr and (d) 100 km/hr	60
Figure 5.20: VDV vs. Speed for multiple humps, for Driver for h_2 , different tire sizes (a) R_{T1} , (b) R_{T2} , and (c) R_{T3} with fixed spacing = 0 m	62

Figure 5.21: VDV vs. Speed for multiple humps, for Main Body for h_2 , different tire sizes (a) R_{T1} , (b) R_{T2} , and (c) R_{T3} with fixed spacing = 0 m	63
Figure 5.22: VDV vs. Speed for multiple humps, for Driver for h_2 , different tire sizes (a) R_{T1} , (b) R_{T2} , and (c) R_{T3} with fixed spacing = 0.25 m	64
Figure 5.23: VDV vs. Speed for multiple humps, for Main Body for h_2 , different tire sizes (a) R_{T1} , (b) R_{T2} , and (c) R_{T3} with fixed spacing = 0.25 m	65
Figure 5.24: VDV vs. Speed for multiple humps, for Driver for h_2 , different tire sizes (a) R_{T1} , (b) R_{T2} , and (c) R_{T3} with fixed spacing = 0.5 m	66
Figure 5.25: VDV vs. Speed for multiple humps, for Main Body for h_2 , different tire sizes (a) R_{T1} , (b) R_{T2} , and (c) R_{T3} with fixed spacing = 0.5 m	67
Figure 5.26: VDV vs. Speed for multiple humps, for Driver for h_2 , different tire sizes (a) R_{T1} , (b) R_{T2} , and (c) R_{T3} with fixed spacing = 1.0 m	68
Figure 5.27: VDV vs. Speed for multiple humps, for Main Body for h_2 , different tire sizes (a) R_{T1} , (b) R_{T2} , and (c) R_{T3} with fixed spacing = 1.0 m	69
Figure 5.28: VDV vs. Speed for Driver for: 10 humps, h_2 , tire size R_{T2} for Stiffness coefficient for linear and bilinear comparison.....	71
Figure 5.29: VDV vs. Speed for Main Body for: 10 humps, h_2 , tire size R_{T2} for Stiffness coefficient for linear and bilinear comparison.....	71
Figure 5.30: VDV vs. Speed for Driver for: 10 humps, h_2 , tire size R_{T2} for Damping coefficient for linear and bilinear comparison.....	72
Figure 5.31: VDV vs. Speed for Main Body for: 10 humps, h_2 , tire size R_{T2} for Damping coefficient for linear and bilinear comparison.....	72

ABSTRACT

Student Name: Ismail Mohammad Yamin Al-Hindi

Thesis Title: Parametric Study of Short Periodic Speed Control Humps on a Road Vehicle Dynamic

Major Field: Mechanical Engineering

Date of Degree: Jumada I 1430 H (May 2009)

The purpose of speed control humps is to introduce shocks and high vibration levels when a vehicle passes over them in order to force the driver to slow down. Circular short periodic speed control humps are not observed to be effective in controlling speeding vehicles in many different areas such as road intersections, highways, checkpoints, exits, and bridge intersections as conventional speed control humps. However, no study is recommending to construct such humps or study of the relationship between the driver's vibration and the vehicle main body's due to passing over these humps. Moreover, most of the constructed circular short periodic humps used in different locations are not supported by efficient warning signs ahead in many locations.

The main objective of this parametric study is to assess the effects of circular short periodic speed control humps due different height, vehicle speed, hump spacing, and multiplicity on the dynamic behavior of the vehicle as a whole and on the driver in particular. Vehicle safety and driver comfort are most important in evaluating the effectiveness of speed control humps. The assessment is based on two standard methods of measuring whole body vibration: the British standard BS 6841 and the new

ISO/DIS standard 2631-5. A mathematical 3-D vehicle model representation is used. The effects of the individual parameters on the dynamic response of the system are evaluated using the MATLAB program and the solver ODE45 (Runge Kutta) numerical method to solve the system of equations. This study focuses on the amount of vibration transmitted to the main vehicle body and the driver. This study shows that the vibration dose value (VDV) decreases as the crossing speed increases. However, this observation does not mean they are not harming the vehicle body. In fact, the time span of the car will be reduced due to fatigue failures and bolts looseness due to highly frequency vibration.

Keywords: *Short Periodic Humps, Speed Control Humps, Parametric Identification, Vehicle nonlinearities, Vehicle Safety, Vehicle Driver.*

ملخص الرسالة

الإسم: إسماعيل بن محمد يامين بن عبداللطيف الهندي
عنوان الرسالة: دراسة ديناميكية المركبة على المطبات المتكررة القصيرة.
التخصص: الهندسة الميكانيكية
تاريخ الدرجة: جمادي الأولى ١٤٣٠ هـ (الموافق مايو ٢٠٠٩ م)

الهدف من مطبات التحكم بالسرعة هو رفع مستوى الصدمات والإهتزازات وعدم الإرتياحية عندما تعبر المركبة فوق المطبات بسرعة تتجاوز السرعة المسموحة بها. من المشاهدات والواقع الملموس إن المطبات المتكررة القصيرة غير فعالة في تهدئة سرعة المركبة وتنبية السائق مقارنة بالمطبات التقليدية, كما أن أغلب المطبات المتكررة القصيرة غير مدعومة بالإشارات والإرشادات التحذيرية لأماكن وجودها والتي من شأنها أن تدفع السائق لتهدئة سرعة المركبة. كذلك لم يثبت حتى الآن من قبل أي دراسة أو بحث العلاقة بين إهتزاز السائق في المركبة عندما تعبر فوق هذه المطبات المتكررة.

إن الهدف الرئيس من هذه الدراسة المرورية هو تقييم المطبات المتكررة القصيرة عند مرور المركبة فوقها وجدواها في التحكم بالسرعة ومدى تأثيرها على جسم المركبة والسائق من خلال التغير في إرتفاعها, والمسافات الفاصلة بينها, وتعددتها, وسرعة المركبة. وتقوم هذه الدراسة ببناءً على المواصفات القياسية في قياس الإهتزازات للجسم الكلي للسائق وهما: BS 6841 و ISO/DIS 2631-5. ولقد تم تقصي آثار هذه المطبات بإستعمال نموذج رياضي ثلاثي الأبعاد يمثل فيها المركبة والسائق من خلال برنامج MATLAB وحل معادلات النظام بإستخدام ODE45 والمعروف بـ Runge Kutta. لقد اظهرت نتائج هذه الدراسة أن هذه المطبات المتكررة القصيرة لاتجدي كثيراً في تحذير السائق من وجود تقاطعات مرورية أو نقاط تفتيش حيث أن السرعة العالية هي التي تعطي الجرعات الإهتزازية الأقل للسائق وجسم المركبة بينما هذا يعكس بدوره على سلامة المركبة وطول عمرها في حالة عبور المركبة بصورة متكررة عليها. بينما السرعة المتدنية تنعكس سلباً على راحة السائق وذلك من خلال مدى الإهتزازات الكبيرة مقارنة بالسرعات العالية.

كلمات دليلة: المطبات المتكررة القصيرة, مطبات للتحكم بالسرعة, دراسة حدودية, سلامة المركبة, سلامة وراحة السائق.

CHAPTER 1

INTRODUCTION

1.1 BACKGROUND

Speed humps are roadway geometric design features intended to reduce vehicle speed and they are in common use throughout the world. These traffic control devices offer several advantages over other traffic control methods such as one-way streets and turn or entry prohibitions, the most important advantage being a reduction in overall vehicular speed and collisions. The objective of speed control humps is to introduce shocks and high vibration levels when a vehicle passes over them if its speed is higher than the allowable speed limit. Speed humps constitute an efficient method to reduce car speed in residential areas. This results in reducing accidents rate. However, different speed limits require different speed hump profiles. Another important design factor is the side effect on the driver's health; for example, old people with back problems should be considered in the design of speed humps.

The ideal speed control hump should be made such that at and below the design speed, all drivers should be able to cross the hump without damaging the carried load and vehicle components, or loss of control and they should suffer no discomfort.

Above the design speed, the driver should suffer his violation through risk of loss of control or loss of driver's comfort. Unfortunately, at least in our eastern province of Saudi Arabia, the type of humps commonly constructed a head of police check point is often short periodic hump profile as shown in Figure 1.1. Actual photo pictures are taken from different road sites in Dammam, Dhahran, Tanajib, and Ras Tanura (see Figures 1.2., 1.3, and 1.4).

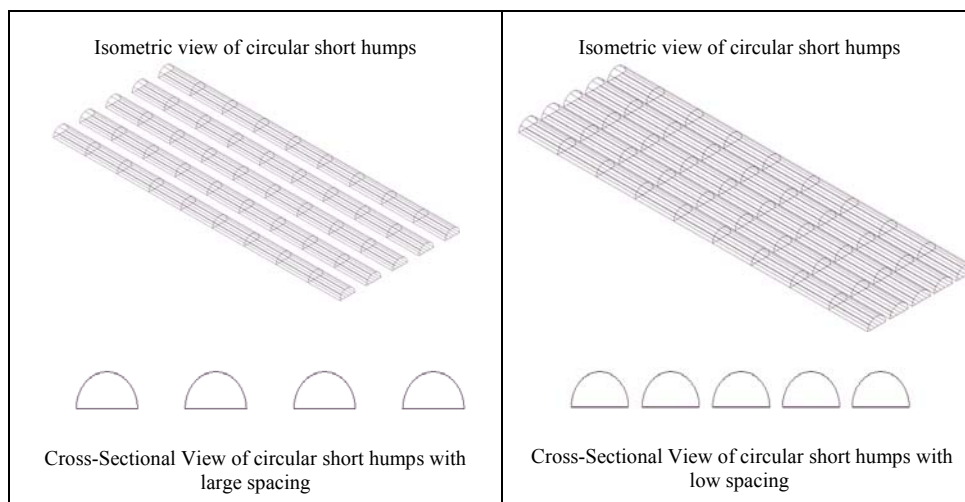


Figure 1.1: Short periodic humps.



Figure 1.2: Short periodic humps at Dammam-Dhahran highway and Doha.



Figure 1.3: Short periodic humps at Tanajib/ Safaniyah main road intersection.



Figure 1.4: Short periodic humps at Ras-Tanura.

In-Kingdom Local Traffic Departments are trying hard to minimize accidents at intersection road by constructing different speed control humps. Among these humps are circular, flat top, and short periodic profile. Circular short periodic speed control humps are observed to be not effective in controlling speeding vehicles in many different areas such as road intersections, highways, checkpoints, exits, and bridge intersections as conventional speed control humps. However, there is no research, standards or study up to date recommending such type of humps to be constructed nor study of the relationship between whole body vibration due to passing over a short periodic humps. Moreover, most of these humps used are not supported by efficient warning signs in many locations. Vehicle safety and driver comfort are the most significant and sufficient in evaluating the effectiveness of speed control humps. The primary purpose of this parametric study is to evaluate numerically the effects of short periodic speed control humps on vehicle dynamic at both low and high speed. The parameters of this study will include height, spacing, multiplicity, and vehicle speed as well as it includes variances in stiffness and damping such as linear and bilinear behavior. The development of a 3-D vehicle model is required in this study. Therefore, the results obtained from the simulation will provide the acceptable geometrical short periodic design if they are needed to be constructed at any rate. In conclusions, the results are analyzed with recommendations and suggestion for safe and comfortable driving along the roads.

1.2 SAUDI TRAFFIC STANDARDS: BRIEF REVIEW

Due to the importance of traffic safety on the roads for the vehicle and driver, Saudi Traffic Department has established engineering standards for constructing speed control humps:

1.1.1 Basic Requirement for Hump Design and Construction:

There are several types of hump design mainly speed bumps, speed humps, flat-top humps and raised intersection humps. The detail construction data each of these types are given [26] as follow:

- Speed bump:

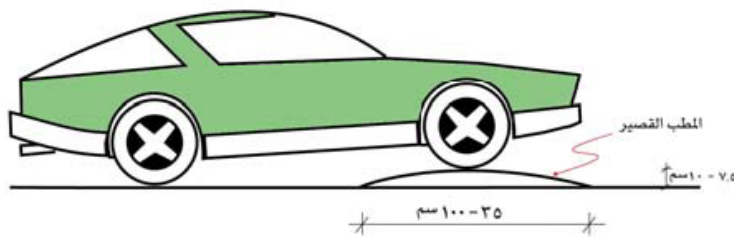


Figure 1.5: Vehicle crossing over short bump [27].

– Speed hump:

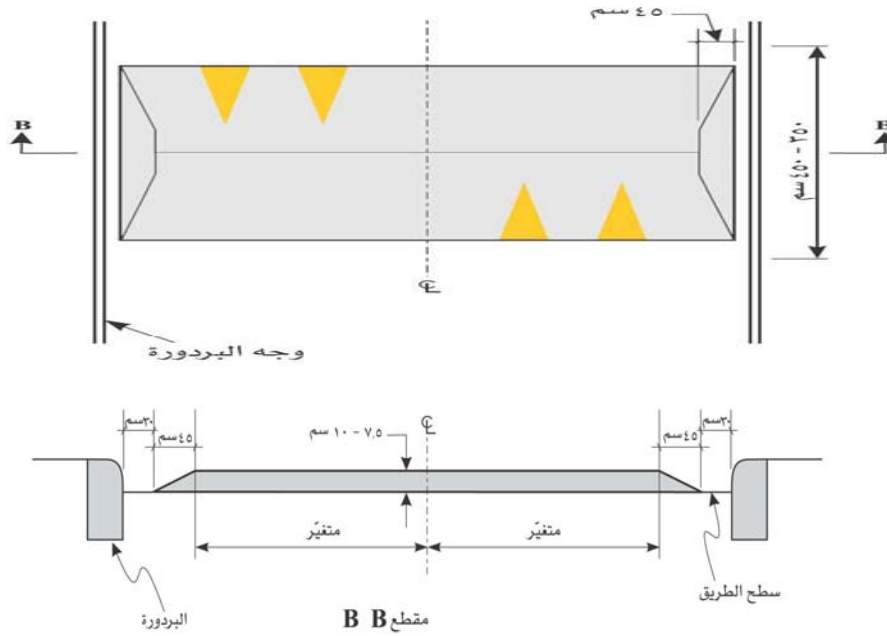


Figure 1.6: In-Kingdom Standard for constructing speed hump [27].

– Flat-Top hump:

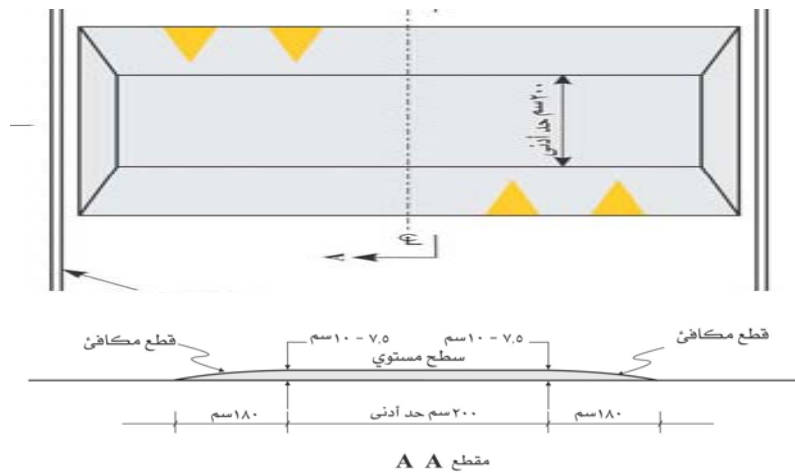


Figure 1.7: In-Kingdom Standard for constructing Flat-Top hump [27].

- Raised Intersection hump:

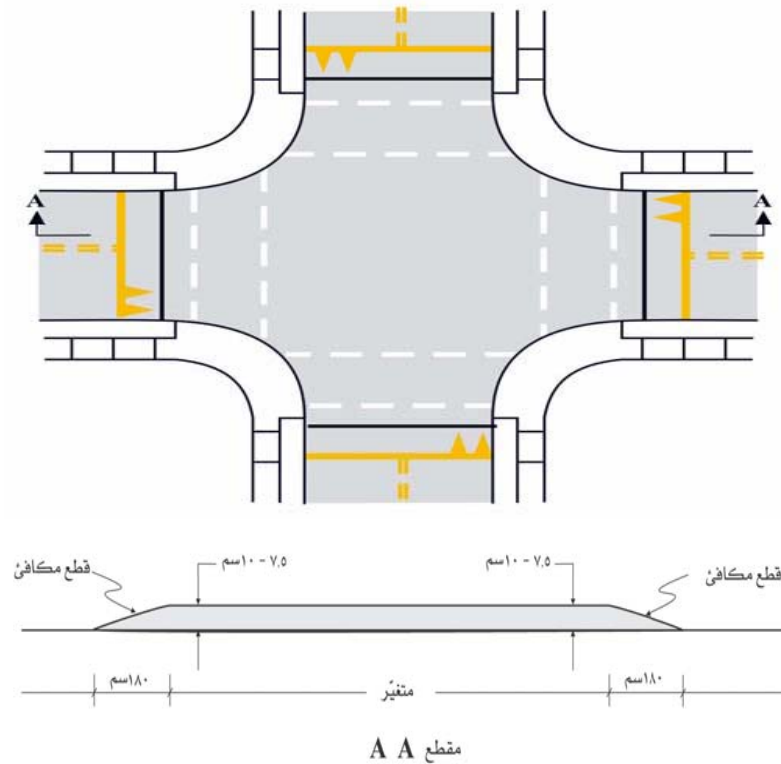


Figure 1.8: In-Kingdom Standard for Raised Intersection speed hump [27].

1.1.2 Locations where humps to be constructed:

Table 1.1 list some guidelines for the locations where speed control humps should be constructed and safe speed for crossing according to the In-Kingdom Traffic Standard.

Table 1.1: General rules where to construct humps and corresponding speed limit [27]:

Type of Road Category	Speed limit
<ul style="list-style-type: none"> – Local Streets – Residential Roads – Intersection Roads 	60 km/hr or Less

1.3 HEALTH AND SAFETY ISSUES

It is a fact that accident rates In-Kingdom with respect to other countries, are high due to the violation of speed limits and a shortage of traffic forces. Therefore, using speed control humps is a very efficient way of slowing down cars, especially in residential areas, and may help reduce traffic accidents. Based upon the study by Saadon [18], speed control humps, which are 4 m wide and 10 cm high, are replacing 1 m wide and 15 cm high humps on many residential roads. This is because the second speed bumps are found to be ineffective in controlling speed limits at the desired value

A speed control hump is a local elevation of the road surface of limited height, usually from 0.075 m to 0.10 m, in order to decrease driving speeds to an acceptable limit known as the critical speed. A speed hump works by transmitting an upward force to a vehicle, and its occupants, as it traverses the hump. The force induces a front-to-back pitching acceleration that increases as the vehicle travels faster. Watts [25] stated that the ideal speed control humps should be crossed without damage to load or

vehicle, loss of control, or driver discomfort, which means ideally zero vertical acceleration. If the speed control humps is crossed with a speed that is above the critical speed, the driver should suffer some discomfort without damaging the load or vehicle or risking loss of control. Drivers in vehicles are exposed to whole body mechanical vibration during their daily ride. Whole-body vibrations originate from two different types of force. A random and sudden forces designated as a shock as stated by Granlund [11]. When the tires hit a bump or sink into a pothole, shock occurs. If this shock is strong enough, it can cause severe spinal injury which is discussed in the book by Dupuis and Zerlett [7].

1.4 ERGONOMIC STANDARDS

Health risks to vehicle drivers from speed control humps shocks were analyzed using two standards: the British standard BS-6841 [5] and the new ISO/DIS 2631-5 standard [15]. A speed control humps experiment entails a variety of testing conditions: different hump profiles and dimensions, different vehicle speeds, and various seat locations within the vehicle. These conditions cause various types of repeated shocks to the vehicle and the driver. To date there has been no published research on whole body vibration of speed control humps and their possible hazard on human health.

1.5 VIBRATION DOSE VALUE, VDV

Vibration measurements were analyzed using the procedure described in both the British Standard BS 6841 [17] and the International Standard ISO/DIS 2631-5 [18]. International Standard ISO 2631-1 [26] is a more recent standard than BS 6841 that provides similar but not identical procedures for evaluation of vibration and shock. The differences between the ISO 2631-1 [26] and BS 6841 are due to variations in the shapes of the frequency weightings, the phase responses of the frequency weighting filters, the method of combining multiaxis vibration, and the assessment method [24].

For the British Standard BS 6841, the analysis includes the application of frequency weightings, the use of multiplying factors in different axes, and the calculation of vibration dose values (VDVs). For the International Standard ISO/DIS 2631-5 [18], the analysis includes the use of different multiplication factors in different axes.

According to the British Standard BS 6841 [17], the VDV is defined as the cumulative vibration and shock measures that a person is exposed to during a given period of time. The VDV reflects the magnitude, and duration of the total exposure to vibration.

The VDV is described by the following equation:

$$VDV = \sqrt[4]{\int_{t_1}^{t_2} a_w^4(t) dt} \quad (1.1)$$

where $a_w(t)$ is the weighted filtered signal

t_1 is the initial time of the calculation period

t_2 is the final times of the calculation period

In our case, we obtain this value numerically directly in time domain from our simulation.

1.6 THESIS OBJECTIVE

It has been witnessed that most of the drivers including myself are crossing these humps with high speed to avoid the large fluctuation when crossing at low speed. This observation supports our study that these humps are not effective to force driver to slow down but rather they play as signs for entering or exiting intersection or highways.

Short periodic speed control humps seems to be very dangerous to the road vehicle compared to the normal humps used internationally in many locations. Due to their wide existence in various locations of our east province at police check points on

the main highways, industrial security check points, residential areas, and at the entrances to the highways, this study is aiming to evaluate their dynamic and vibrational effects on the vehicle and the driver. In fact, these humps are not used for controlling vehicle speeds but rather they are used as warning signs for slowing down. Furthermore, circular short periodic humps are selected to measure the effects of their geometrical parameters of the hump on the vehicle dynamics in terms of their height, width, spacing, vehicle speed, and multiplicity. As well as, it includes variances in stiffness and damping coefficients such as linear and bilinear behavior.

The motivation of the work when crossing these short humps we feel the vibration is very annoying going either with low or high speed. In this study, we would like to see that if there is any optimal parameter so these short humps can be utilize effectively with driver comfort and vehicle safety can be achieved.

1.7 SCOPE OF THE PRESENT STUDY

This study primarily is a parametric approach to evaluate the effects of short periodic speed control humps on vehicle dynamic for a range of speeds from low to high speed. The geometrical circular hump parameters to be thoroughly investigated are as follow:

- Height of the hump: h_1 (7.5 cm) and h_2 (10 cm) height will be studied.
- Spacing between the humps: 0 m, 0.25 m, 0.5 m, and 1.0 m as well as $0 S_{cr}$, $0.5 S_{cr}$, $1.0 S_{cr}$, $1.5 S_{cr}$, $2.0 S_{cr}$, where S_{cr} is the critical spacing associated with three

different tire radius sizes namely R_{T1} (13 in \approx 33 cm), R_{T2} (15 in \approx 38 cm), and R_{T3} (19 in \approx 48 cm) and more definition of the critical spacing is explained in chapter 5.

- Vehicle speed: a range of speed is used from 0 to 100 kh/hr for all the simulations.
- Multiplicity of short humps: different numbers of humps are selected to evaluate their repetition starting with single hump to 2, 3, 5, 7, and 10 humps respectively.
- Variances in stiffness and damping coefficients in the suspension system to incorporate linear and bilinear dynamic behavior and their effect on the vehicle and driver's comfort when passing over these short periodic humps:

$$c^*_{ij} = \begin{cases} c_{ij} & \text{if } \dot{z}_{ij} \geq \dot{z}^*_{ij} \\ \beta \times c_{ij} & \text{if } \dot{z}_{ij} \leq \dot{z}^*_{ij} \end{cases}$$

$$k^*_{ij} = \begin{cases} k_{ij} & \text{if } z_{ij} \geq z^*_{ij} \\ \beta \times k_{ij} & \text{if } z_{ij} \leq z^*_{ij} \end{cases}$$

where ij refer to FR (Front Right), FL (Front Left), RR (Rear Right), RL (Rear Left)

CHAPTER 2

LITERATURE REVIEW

2.1 ON GENERAL EVALUATION OF SPEED CONTROL HUMPS

Ever since the creation of the first industrial machines powered by motors, a new nuisance for human beings has made its appearance: vibrations. In many areas, we are all the time more subjected to serious harmful and damaging effects of vibrations by different speed control humps of different profiles. Among of these are circular, harmonic, parabolic, sinusoidal, flat-top, short periodic humps and others that are used haphazardly.

When investigating about first designs on speed control humps and their related studies, several previous works where explored on speed control humps according to the study by Griffin et al. [12], Rakheja [20], Barak [1] and Saadoon [22], who had verified that mechanical vibrations cause numerous pathological demonstrations due to the fact that they are directly transmitted to the human body through direct contact with solid materials on the road. These vibrations are particularly evident in the area of road vehicles. Since the early days of the 20th century, efforts have steadily increased to

eliminate or reduce this type of vibration. For instance, one such effort has been the suspension system installed between the excitation input and the vehicle body.

During the history of imposing speed humps since the 1970s, several hump profiles were used. The shape of the speed hump has been optimized for the response characteristics of different types of vehicles passing over the hump. There are several research studies on the problem of designing a hump geometry that can satisfy vehicle safety and driver comfort from the dimensions point of view only as reported by Maemori, [17].

2.2 ON MODELING APPROACH OF SPEED CONTROL HUMPS

Through extensive literature search, it is found that very few studies have been reported on the use of hump profile as a design variable. Also, there has not been any study on the series of short humps or the humps dimensions than has been reported. Other works, focused on the optimum shape design of speed control humps but they lack the practicality of implementation in terms of cost and construction according to Pedersen [18]. Furthermore, continuous efforts were investigated the dynamic behavior of the vehicle crossing normal seen humps for different rise and return profiles such as: (sinusoidal, harmonic, cycloidal, circular and modified harmonic) by using 5 degrees-of-freedom of 2-D vehicle model. It is clear that hump geometry plays a major role in the dynamic effects on the vehicle and driver. The most important hump geometrical

parameters are hump profile, and dimensions which include height and width as in the work reported by Kassem and Al-Nassar [16]. Another design factor is the hump layout, or the number of humps in one road and their spacing as reported in the study of Fwa and Liaw, [9]. The analytical study demonstrated that the reasonable accuracy for the dynamic behavior of actual road vehicle running on rough road using two degrees-of-freedom model that studied by Gobbi and Mastinu [10]. Moreover, the dynamic behavior was investigated of the vehicle crossing of different profile humps from different rise and return profiles such as: (sinusoidal, harmonic, cycloidal, circular and modified harmonic) using 12 degrees-of-freedom as studied by Khorshid and Alfares [8].

It is clearly noted that a 2-D model did not allow analyzing all the motions generated by an actual vehicle studied the effects of vibration on the comfort and road holding capability of road vehicles as observed in the variation of different parameters such as suspension coefficients, road disturbances, and the seat position as studied by Bouazara and Richard [4]. Consequently, more studies were investigated for the entire vehicle model in a 3-D with eight degrees-of-freedom for random excitation road by vertical, pitching and rolling motions in terms of acceleration, velocity and movement, for various vehicle solid components one can see this in the work of Bouazara and Richard [2]. In order to utilize this model for better understanding, a true movement generated by ground vehicles with the rolling motion of particular interest has been reported by Crolla [6], Hrovat [14] and Bouazara [3].

Another interesting work is carried out by Metallidis et al. [19]. In their work, a parametric identification and fault detection studies have been performed in nonlinear vehicle system for two (1-D), four (2-D), and seven (3-D) degrees-of-freedom which subjected to harmonic road excitations. In addition, more optimization studies were carried out for the suspension damping and stiffness parameters of nonlinear quarter-car models subjected to also random road excitation involving passive damping with constant or dual-rate characteristics as in the study of Verros et al. [20].

CHAPTER 3

MATHEMATICAL MODELING AND FORMULATION

3.1 VEHICLE MODELING

A mathematical model is required to study the parametric effects of short periodic speed control humps on vehicle and driver. A model that suits this study of whole-body vibration of road vehicles is adopted from the work by Bouazara and Richard [2]. The vehicle model is supported by identical front and rear suspensions which consist of a secondary spring, a damper, an unsprung mass and a primary spring. The system is made up of the following parameters: m_G , m_D , m_{FR} , m_{FL} , m_{RR} , and m_{RL} are the masses for the driver, car body, and wheel axes FR, FL, RR, and RL, respectively; C_D , C_{FR} , C_{FL} , C_{RR} , C_{RL} are damping coefficients and K_D , K_{FR} , K_{FL} , K_{RR} , K_{RL} are the stiffness coefficients for the seat and vehicle suspensions; K_{F1} , K_{F2} , K_{R1} , K_{R2} , are the tire stiffness coefficients. The model data was given in Table 3.1. This 3-D vehicle model has eight degrees-of-freedom as shown in Figure 3.1.

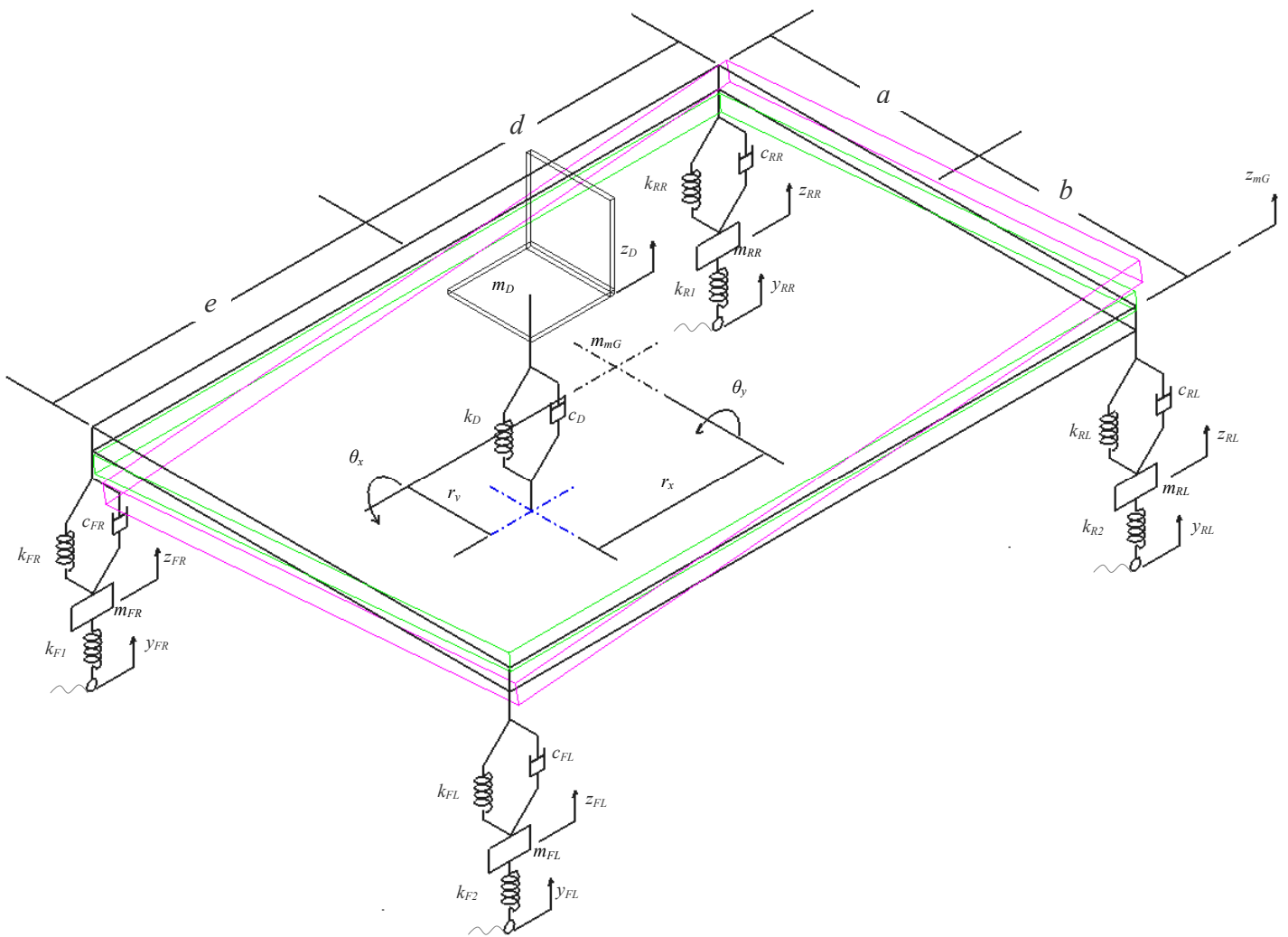


Figure 3.1: 3-D Model of the vehicle and the driver [2].

Table 3.1: Mass, damping coefficient, spring coefficient, moment of inertia, and dimensions for front and rear of the vehicle main body [2]:

Mass	m_{FR}	m_{FL}	m_{RR}	m_{RL}	m_D
	40 kg	40 kg	35.5 kg	35.5 kg	75 kg
	m_G				
	730 kg				
Damping Coefficient	C_{FR}	C_{FL}	C_{RR}	C_{RL}	C_D
	1290 Ns/m	1290 Ns/m	1620 Ns/m	1620 Ns/m	2000 Ns/m
Stiffness Coefficient	K_{FR}	K_{FL}	K_{RR}	K_{RL}	K_D
	19.96 kN/m	19.96 kN/m	17.5 kN/m	17.5 kN/m	100 kN/m
	K_{F1}	K_{F2}	K_{R1}	K_{R2}	
	175.5 kN/m	175.5 kN/m	175.5 kN/m	175.5 kN/m	
Moment of Inertia	I_{Gxx}	I_{Gyy}			
	1230 kg m ²	1230 kg m ²			
Dimension	e	d	a	b	
	1.011 m	1.803 m	0.755 m	0.755 m	
	r_y	r_x			
	0.5 m	0.5 m			

The vehicle behavior is expressed by vertical, pitching and rolling motions in terms of acceleration, velocity and movement, for various vehicle solid components. In this analysis, we do not consider yaw motion because it has been shown that its effect is negligible on vehicle comfort and road holding capability as explained by Hrovat [14].

3.2 MATHEMATICAL FORMULATION

In order to obtain the differential equations of motion of the system represented in Figure 3.1, we follow energy approach in which kinetic energy, potential energy and damping forces of the system need to develop as follow:

Kinetic Energy:

$$T = T_{F_R} + T_{F_L} + T_{R_R} + T_{R_L} + T_G + T_D + \frac{I}{2}(I_G)_{xx} \dot{\theta}_x^2 + \frac{I}{2}(I_G)_{yy} \dot{\theta}_y^2$$

$$T = \frac{1}{2}m_{F_R}(\dot{z}_{F_R}^2)_z + \frac{1}{2}m_{F_L}(\dot{z}_{F_L}^2)_z + \frac{1}{2}m_{R_R}(\dot{z}_{R_R}^2)_z + \frac{1}{2}m_{R_L}(\dot{z}_{R_L}^2)_z + \frac{1}{2}m_G(\dot{z}_G^2)_z + \frac{1}{2}m_D(\dot{z}_D^2)_z$$

$$+ \frac{I}{2}(I_G)_{xx} \dot{\theta}^2 + \frac{I}{2}(I_G)_{yy} \dot{\phi}^2 \quad (3.1)$$

where $\dot{\theta}_x = \dot{\theta}$ and $\dot{\theta}_y = \dot{\phi}$

Potential Energy:

$$\begin{aligned}
V &= V_{F_1} + V_{F_R} + V_{F_2} + V_{F_L} + V_{R_1} + V_{R_R} + V_{R_2} + V_{R_L} + V_D \\
V &= \frac{1}{2}k_{F_1}(z_{F_R} - y_{F_R})^2 + \frac{1}{2}k_{F_R}[z_{F_R} - (z_G - a\theta - e\phi)]^2 \\
&\quad + \frac{1}{2}k_{F_2}(z_{F_L} - y_{F_L})^2 + \frac{1}{2}k_{F_L}[z_{F_L} - (z_G + b\theta - e\phi)]^2 \\
&\quad + \frac{1}{2}k_{R_1}(z_{R_R} - y_{R_R})^2 + \frac{1}{2}k_{R_R}[z_{R_R} - (z_G - a\theta + d\phi)]^2 \\
&\quad + \frac{1}{2}k_{R_2}(z_{R_L} - y_{R_L})^2 + \frac{1}{2}k_{R_L}[z_{R_L} - (z_G + b\theta + d\phi)]^2 \\
&\quad + \frac{1}{2}k_D[z_G - r_y\theta + r_x\phi - z_D]^2
\end{aligned} \tag{3.2}$$

Generalized Forces & Moments for the Damping Coefficients:

$$\begin{aligned}
Q_{m_{F_R}}^f &= -c_{F_R}(\dot{z}_{F_R} - \dot{z}_G + a\dot{\theta} + e\dot{\phi}) \\
Q_{m_{F_L}}^f &= -c_{F_L}(\dot{z}_{F_L} - \dot{z}_G - b\dot{\theta} + e\dot{\phi}) \\
Q_{m_{R_R}}^f &= -c_{R_R}(\dot{z}_{R_R} - \dot{z}_G + a\dot{\theta} - d\dot{\phi}) \\
Q_{m_{R_L}}^f &= -c_{R_L}(\dot{z}_{R_L} - \dot{z}_G - b\dot{\theta} - d\dot{\phi}) \\
Q_{m_D}^f &= -c_D(\dot{z}_D - \dot{z}_G + r_y\dot{\theta} - r_x\dot{\phi}) \\
Q_{m_G}^f &= c_{F_R}(\dot{z}_{F_R} - \dot{z}_G + a\dot{\theta} + e\dot{\phi}) - c_{F_L}(\dot{z}_{F_L} - \dot{z}_G - b\dot{\theta} + e\dot{\phi}) \\
&\quad - c_{R_R}(\dot{z}_{R_R} - \dot{z}_G + a\dot{\theta} - d\dot{\phi}) - c_{R_L}(\dot{z}_{R_L} - \dot{z}_G - b\dot{\theta} - d\dot{\phi}) \\
&\quad - c_D(\dot{z}_D - \dot{z}_G + r_y\dot{\theta} + r_x\dot{\phi} - \dot{z}_D) \\
Q_{\theta}^M &= -c_{F_R}(\dot{z}_G - a\dot{\theta} - e\dot{\phi} - \dot{z}_{F_R})a + c_{F_L}(\dot{z}_G + b\dot{\theta} - e\dot{\phi} - \dot{z}_{F_L})b \\
&\quad - c_{R_R}(\dot{z}_G - a\dot{\theta} + d\dot{\phi} - \dot{z}_{R_R})a + c_{R_L}(\dot{z}_G + b\dot{\theta} + d\dot{\phi} - \dot{z}_{R_L})b \\
&\quad + c_D(\dot{z}_D - \dot{z}_G + r_y\dot{\theta} - r_x\dot{\phi})r_y
\end{aligned}$$

$$\begin{aligned}
Q_\phi^M = & -c_{FR} (\dot{z}_G - a\dot{\theta} - e\dot{\phi} - \dot{z}_{FR})e - c_{FL} (\dot{z}_G + b\dot{\theta} - e\dot{\phi} - \dot{z}_{FL})e \\
& + c_{RR} (\dot{z}_G - a\dot{\theta} + d\dot{\phi} - \dot{z}_{RR})d + c_{RL} (\dot{z}_G + b\dot{\theta} + d\dot{\phi} - \dot{z}_{RL})d \\
& - c_D (\dot{z}_D - \dot{z}_G + r_y\dot{\theta} - r_x\dot{\phi})r_x
\end{aligned} \tag{3.3}$$

After obtaining the above expressions, the equations of motion are developed using the following Lagrange equation,

$$\frac{d}{dt} \left(\frac{\partial T}{\partial \dot{z}_i} \right) - \frac{\partial T}{\partial z_i} + \frac{\partial V}{\partial z_i} = Q_{m_i}^f \tag{3.4}$$

where i stands for any of eight degrees of freedom ($FR, FL, RR, RL, D, G, \theta_x$ and θ_y)

Consequently, eight equations of motion of the system in the vehicle are: front right wheel, front left wheel, rear right wheel, rear left wheel, main body of vehicle, driver, pitch and roll. After developing each equation with respect to the location in the vehicle, the linearized equations of motion for this system are obtained directly as for small angle θ_x and θ_y :

$$\begin{aligned}
m_{FR} \ddot{z}_{FR} - c_{FR} \dot{z}_G + c_{FR} \dot{z}_{FR} + c_{FR} a \dot{\theta}_x + c_{FR} e \dot{\theta}_y \\
- k_{FR} z_G + (k_{FR} + k_{F1}) z_{FR} + k_{FR} a \theta_x + k_{FR} e \theta_y = k_{F1} y_{FR}
\end{aligned} \tag{3.5}$$

$$\begin{aligned}
m_{FL} \ddot{z}_{FL} - c_{FL} \dot{z}_G + c_{FL} \dot{z}_{FL} - c_{FL} b \dot{\theta}_x + c_{FL} e \dot{\theta}_y \\
- k_{FL} z_G + (k_{FL} + k_{F2}) z_{FL} - k_{FL} b \theta_x + k_{FL} e \theta_y = k_{F2} y_{FL}
\end{aligned} \tag{3.6}$$

$$\begin{aligned}
m_{RR} \ddot{z}_{RR} - c_{RR} \dot{z}_G + c_{RR} \dot{z}_{RR} + c_{RR} a \dot{\theta}_x - c_{RR} d \dot{\theta}_y \\
- k_{RR} z_G + (k_{RR} + k_{R1}) z_{RR} + k_{RR} a \theta_x - k_{RR} d \theta_y = k_{R1} y_{RR}
\end{aligned} \tag{3.7}$$

$$\begin{aligned}
m_{RL} \ddot{z}_{RL} - c_{RL} \dot{z}_G + c_{RL} \dot{z}_{RL} - c_{RL} b \dot{\theta}_x - c_{RL} d \dot{\theta}_y \\
- k_{RL} z_G + (k_{RL} + k_{R2}) z_{RL} - k_{RL} b \theta_x - k_{RL} d \theta_y = k_{R2} y_{RL}
\end{aligned} \tag{3.8}$$

$$\begin{aligned}
m_D \ddot{z}_D - c_D \dot{z}_G + c_D \dot{z}_D - c_D r_y \dot{\theta}_x + c_D r_x \dot{\theta}_y \\
- k_D z_G + k_D z_D - k_D r_y \theta_x + k_D r_x \theta_y = 0
\end{aligned} \tag{3.9}$$

$$\begin{aligned}
m_G \ddot{z}_G + (c_{FR} + c_{FL} + c_{RR} + c_{RL} + c_D) \dot{z}_G \\
- c_{FR} \dot{z}_{FR} - c_{FL} \dot{z}_{FL} - c_{RR} \dot{z}_{RR} - c_{RL} \dot{z}_{RL} - c_D \dot{z}_D \\
+ (-c_{FR} a + c_{FL} b - c_{RR} a + c_{RL} b + c_D r_y) \dot{\theta}_x \\
+ (-c_{FR} e - c_{FL} e + c_{RR} d + c_{RL} d - c_D r_x) \dot{\theta}_y \\
+ (k_{FR} + k_{FL} + k_{RR} + k_{RL} + k_D) z_G \\
- k_{FR} z_{FR} - k_{FL} z_{FL} - k_{RR} z_{RR} - k_{RL} z_{RL} - k_D z_D \\
+ (-k_{FR} a + k_{FL} b - k_{RR} a + k_{RL} b + k_D r_y) \theta_x \\
+ (-k_{FR} e - k_{FL} e + k_{RR} d + k_{RL} d - k_D r_x) \theta_y = 0
\end{aligned} \tag{3.10}$$

$$\begin{aligned}
(I_G)_{xx} \ddot{\theta}_x + (-c_{FR} a + c_{FL} b - c_{RR} a + c_{RL} b + c_D r_y) \dot{z}_G \\
+ c_{FR} a \dot{z}_{FR} - c_{FL} b \dot{z}_{FL} + c_{RR} a \dot{z}_{RR} - c_{RL} b \dot{z}_{RL} - c_D r_y \dot{z}_D \\
+ (c_{FR} a^2 + c_{FL} b^2 + c_{RR} a^2 + c_{RL} b^2 + c_D r_y^2) \dot{\theta}_x \\
+ (c_{FR} a e - c_{FL} e b - c_{RR} a d + c_{RL} b d - c_D r_x r_y) \dot{\theta}_y \\
+ (-k_{FR} a + k_{FL} b - k_{RR} a + k_{RL} b + k_D r_y) z_G \\
+ k_{FR} a z_{FR} - k_{FL} b z_{FL} + k_{RR} a z_{RR} - k_{RL} b z_{RL} - k_D r_y z_D \\
+ (k_{FR} a^2 + k_{FL} b^2 + k_{RR} a^2 + k_{RL} b^2 + k_D r_y^2) \theta_x \\
+ (k_{FR} a e - k_{FL} e b - k_{RR} a d + k_{RL} b d - k_D r_x r_y) \theta_y = 0
\end{aligned} \tag{3.11}$$

$$\begin{aligned}
(I_G)_{yy} \ddot{\theta}_y + (-c_{FR} e - c_{FL} e + c_{RR} d + c_{RL} d - c_D r_x) \dot{z}_G \\
+ c_{FR} e \dot{z}_{FR} + c_{FL} e \dot{z}_{FL} - c_{RR} d \dot{z}_{RR} - c_{RL} d \dot{z}_{RL} + c_D r_x \dot{z}_D \\
+ (c_{FR} e a - c_{FL} e b - c_{RR} d a + c_{RL} d b - c_D r_x r_y) \dot{\theta}_x \\
+ (c_{FR} e^2 + c_{FL} e^2 + c_{RR} d^2 + c_{RL} d^2 + c_D r_x^2) \dot{\theta}_y \\
+ (-k_{FR} e - k_{FL} e + k_{RR} d + k_{RL} d - k_D r_x) z_G \\
+ k_{FR} e z_{FR} + k_{FL} e z_{FL} - k_{RR} d z_{RR} - k_{RL} d z_{RL} + k_D r_x z_D \\
+ (k_{FR} e a - k_{FL} e b - k_{RR} d a + k_{RL} d b - k_D r_x r_y) \theta_x \\
+ (k_{FR} e^2 + k_{FL} e^2 + k_{RR} d^2 + k_{RL} d^2 + k_D r_x^2) \theta_y = 0
\end{aligned} \tag{3.12}$$

3.3 SOLUTION STRATEGY

Upon using the MATLAB program, the solver ODE45 (Runge Kutta) is used to solve the system of equations. However, this method or solver requires the system of equations to be of the first order. Therefore, each of the equations is replaced by two first order equations as shown in conversion Equation 3.13. The required initial conditions are the initial positions and velocities. The system of equations is shown in detail in the appendix.

$$\left. \begin{array}{ll}
 y_{(1)} = z_{FR}; & y_{(2)} = z_{FL}; & y_{(9)} = \dot{z}_{FR}; & y_{(10)} = \dot{z}_{FL}; \\
 y_{(3)} = z_{RR}; & y_{(4)} = z_{RL}; & y_{(11)} = \dot{z}_{RR}; & y_{(12)} = \dot{z}_{RL}; \\
 y_{(5)} = z_D; & y_{(6)} = z_G; & y_{(13)} = \dot{z}_D; & y_{(14)} = \dot{z}_G; \\
 y_{(7)} = \theta_x; & y_{(8)} = \theta_y; & y_{(15)} = \dot{\theta}_x; & y_{(16)} = \dot{\theta}_y; \\
 \\
 \frac{\partial y_{(1)}}{\partial t} = y_{(9)}; & \frac{\partial y_{(2)}}{\partial t} = y_{(10)}; & \frac{\partial y_{(9)}}{\partial t} = \ddot{z}_{FR}; & \frac{\partial y_{(10)}}{\partial t} = \ddot{z}_{FL}; \\
 \frac{\partial y_{(3)}}{\partial t} = y_{(11)}; & \frac{\partial y_{(4)}}{\partial t} = y_{(12)}; & \frac{\partial y_{(11)}}{\partial t} = \ddot{z}_{RR}; & \frac{\partial y_{(12)}}{\partial t} = \ddot{z}_{RL}; \\
 \frac{\partial y_{(5)}}{\partial t} = y_{(13)}; & \frac{\partial y_{(6)}}{\partial t} = y_{(14)}; & \frac{\partial y_{(13)}}{\partial t} = \ddot{z}_D; & \frac{\partial y_{(14)}}{\partial t} = \ddot{z}_G; \\
 \frac{\partial y_{(7)}}{\partial t} = y_{(15)}; & \frac{\partial y_{(8)}}{\partial t} = y_{(16)}; & \frac{\partial y_{(15)}}{\partial t} = \ddot{\theta}_x; & \frac{\partial y_{(16)}}{\partial t} = \ddot{\theta}_y;
 \end{array} \right\} \quad (3.13)$$

CHAPTER 4

SIMULATION STRATEGY

4.1 INTRODUCTION

In this chapter the effects of short periodic speed control humps on vehicle dynamic at both low and high speed are to be thoroughly investigated. And, these parameters are:

- Effect of varying height of the hump.
- Effect of vehicle speed.
- Effect of different spacing between the humps.
- Effect of multiplicity of these short humps.
- Linear vs. bilinear behavior in the suspension system.

In all the parametric study cases, the following plots are produced:

- Hump profiles of different height of humps vs. speed for different repeated humps.
- Max vertical acceleration of the driver and main body vs. speed.
- Max Jerk of the driver and main body vs. speed.
- VDV of the driver and main body vs. speed for different spacing and different tire sizes.

- VDV of the driver and main body vs. speed for multiplicity of humps.
- VDV vs. speed of the driver and main body for linear and bilinear behavior of stiffness and damping coefficient.

4.2 HUMP PARAMETERS

Dimensions and configuration of the circular short periodic hump play a major role in its dynamic effects on the vehicle and driver. And, the following parametric studies parameters are of particular importance:

4.2.1 HEIGHT OF HUMP

It has been observed that low humps are ineffective comparing to high humps which can be very dangerous and they might cause rigorous damage to the vehicle underneath. Two heights have been considered in this study which are h_1 and h_2 . The maximum height for these humps has been identified as shown in Figure 4.1. The main factor in choosing a suitable height for the hump is the dynamic response of the vehicle as shown in Figure 4.2.

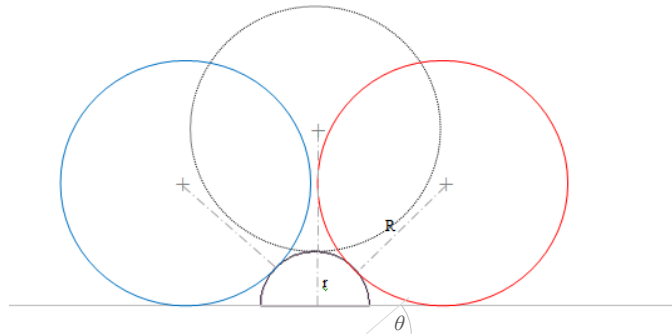


Figure 4.1: Vehicle tire crossing over single circular short periodic hump.

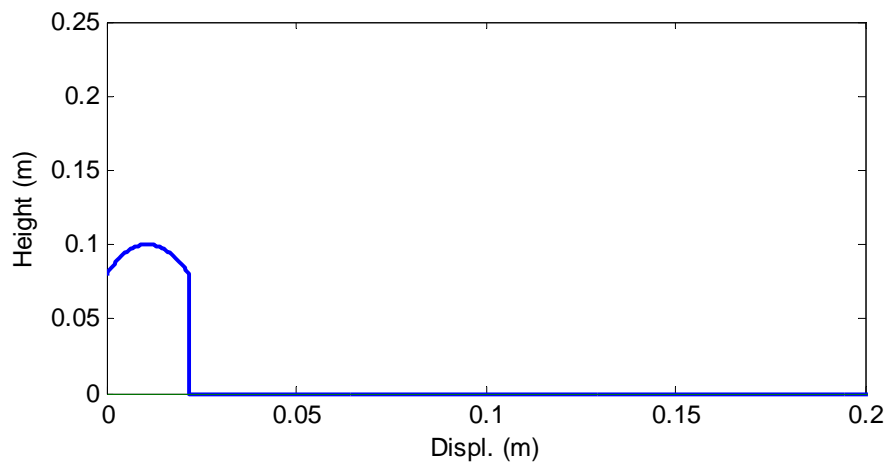
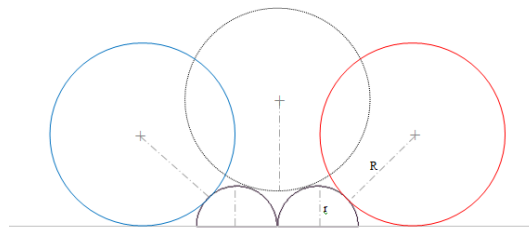


Figure 4.2: Effective profile of the hump when tire size is R_{T2} .



(a) Zero hump spacing

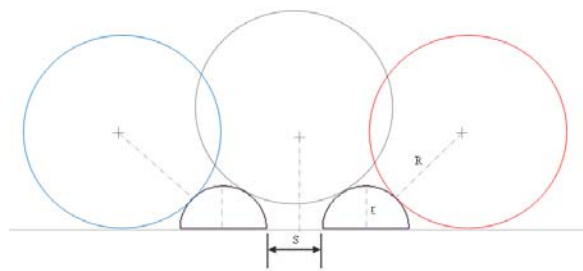
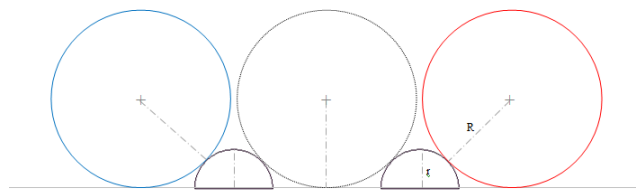
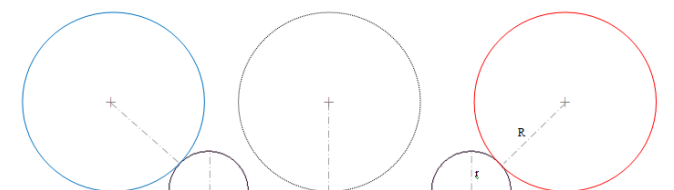
(b) Hump spacing, S , less than S_{cr} (c) Critical hump spacing, S_{cr} (d) Hump spacing, S , greater than S_{cr}

Figure 4.3: Vehicle tire crossing over two short humps when: (a) $S = 0$, (b) $S < S_{cr}$, (c) $S = S_{cr}$, and (d) $S > S_{cr}$.

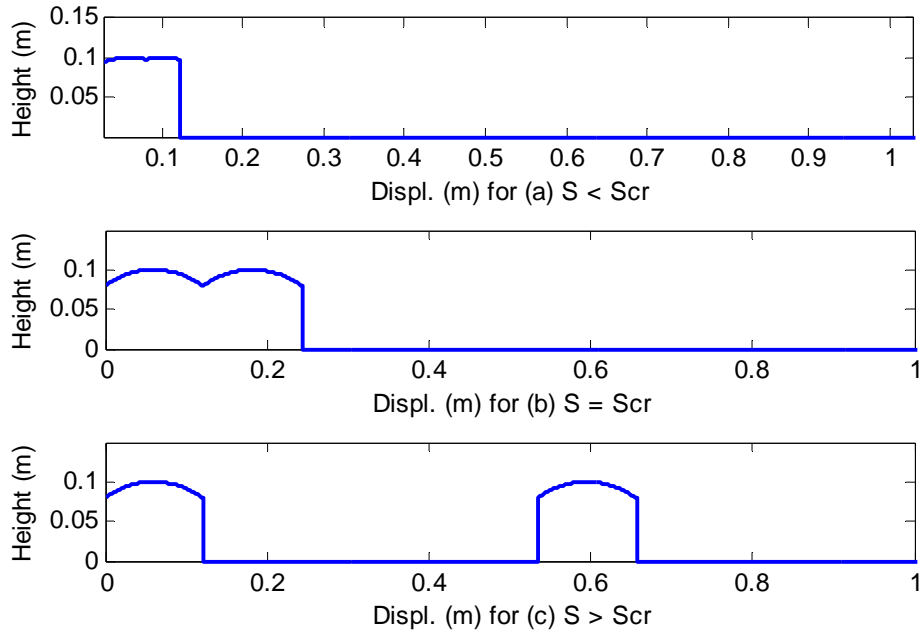


Figure 4.4: Actual interface between the vehicle tire size, R_{T2} , for 2 humps when: (a) $S < S_{cr}$, (b) $S = S_{cr}$, and (c) $S > S_{cr}$.

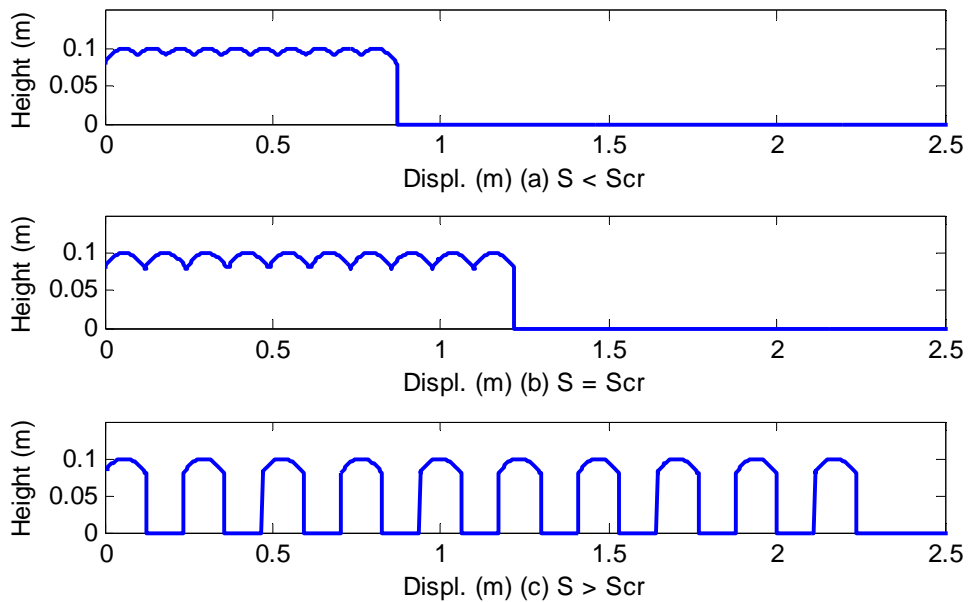


Figure 4.5: Actual interface between the vehicle tire size, R_{T2} , for 10 humps when: (a) $S < S_{cr}$, (b) $S = S_{cr}$, and (c) $S > S_{cr}$.

4.2.2 VEHICLE SPEED

Effect of speed has been measured against vertical acceleration, jerk, and whole-body vibration dose value (VDV) for both the vehicle and the driver at a range of speeds from 0 km/hr to 100 km/hr. Furthermore, maximum acceleration and maximum jerk vs. speeds demonstrated high effects for the dynamic behavior of the driver at low speed and the vehicle safety decrease at high speed. VDV increases at low speeds and decreases at high speeds.

4.2.3 DIFFERENT SPACING BETWEEN HUMPS

For the feasibility of this study, seven hump spacing have been studied and calculated in which of two less than the critical spacing (0, and 0.5), one is equal to the critical spacing and two greater than the critical spacing (1.5, and 2.0). There are three critical spacing have been identified in this study for three different vehicle tire sizes R_{T1} , R_{T2} , and R_{T3} of different hump height as shown in Table 4.1.

Critical spacing can be obtained using the following expression see Figure 4.3 (c):

$$S_{critical} = 2 \times (R + r) \times \cos \theta - 2 \times r \quad (4.1)$$

Table 4.1: Critical spacing for different tire sizes as follows:

Hump height	h_1	h_2
S_{cr1} for Tire Size R_{T1}	0.3197 cm	0.3515 cm
S_{cr2} for Tire Size R_{T2}	0.3511 cm	0.3872 cm
S_{cr2} for Tire Size R_{T3}	0.4086 cm	0.4527 cm

4.2.4 MULTIPLICITY OF CIRCULAR SHORT PERIODIC HUMPS

With different spacing between each hump, number of humps has major effect on whole-body vibration. The multiplicities of humps are chosen to be one, two, three, five, seven, and ten humps. The hump profile refers to the geometry of the cross section of the hump. Such profile can be shown in Figure 4.3. In order to choose a specific no. of humps for this study, it can be selected depending on the dynamic effects on vehicle and driver which is the subject of this parametric study. It is observed that these humps are used in groups as shown in Figure 4.4 and Figure 4.6 using different spacing between humps.

CHAPTER 5

RESULTS AND DISCUSSION

5.1 EFFECT OF VARYING HEIGHT OF THE HUMP

Two different heights are used in this parametric study namely h_1 and h_2 . The effect of varying the heights on the amount vibrational dose value, VDV, behavior of the driver are given in figures 5.1, 5.2, and 5.3 for a range of approaching speeds. Only single tire radius size is considered in this analysis (tire radius size of R_{T2}). Furthermore, three different spacing have been considered to be presented namely, 0, critical spacing, and double of the critical spacing with multiplicity of 2, 5, and 10 successive short humps. The first three groups of figures (Figures 5.1 (a), (b), and (c)) represent 0, critical spacing, and twice the critical spacing for 2 repeated humps. While the second three groups of figures (Figures 5.2 (a), (b), and (c)) represent 0, critical spacing, and twice the critical spacing for 5 repeated humps. Finally, the last three groups of figures (Figure 5.3 (a), (b), and (c)) represent 0, critical spacing, and twice the critical spacing for 10 repeated humps. As a general observation, the amount of vibrational dose represented by VDV measure shows that the higher the humps, the more vibration does transfer to the driver. The effect of approaching speed shows that VDV value decreases as the approaching speed increases. This does not imply that it is recommended to speed up when crossing these short humps since higher crossing

speeds excite higher frequencies on the vehicle body which can create unforeseen defects in the vehicle components as looseness of bolts for example. It is clear that the optimal crossing speed is less than 50 km/hr. It is also observed that when the spacing is twice the critical spacing whether the numbers of humps are 2, 5, or 10 the behavior of VDV is almost the same with respect to crossing speed of 30 km/hr and above.

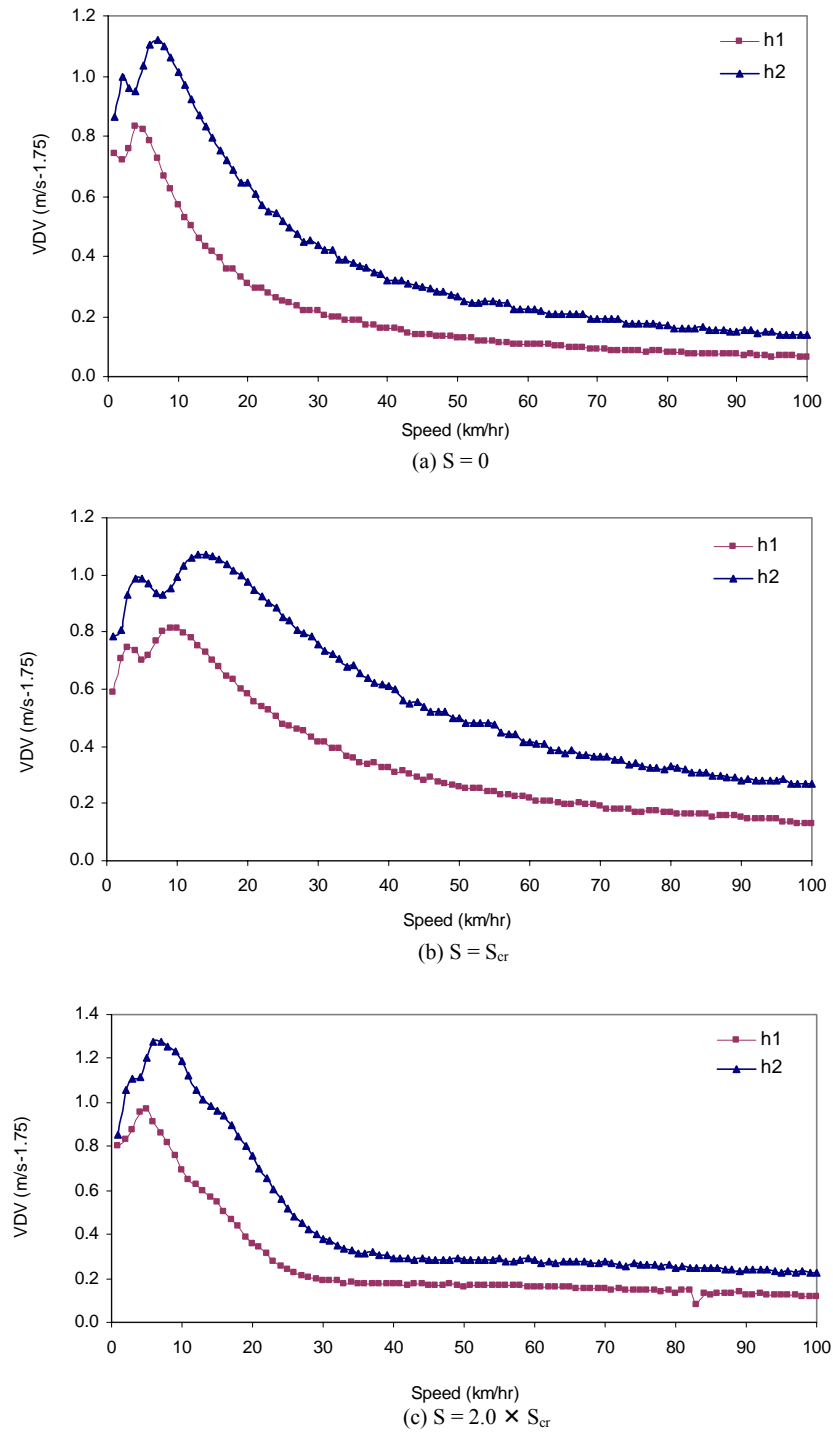


Figure 5.1: VDV vs. Speed for tire size R_{T2} crossing over 2 humps for Driver when: (a) $S = 0$, (b) $S = S_{cr}$, and (c) $S = 2.0 \times S_{cr}$

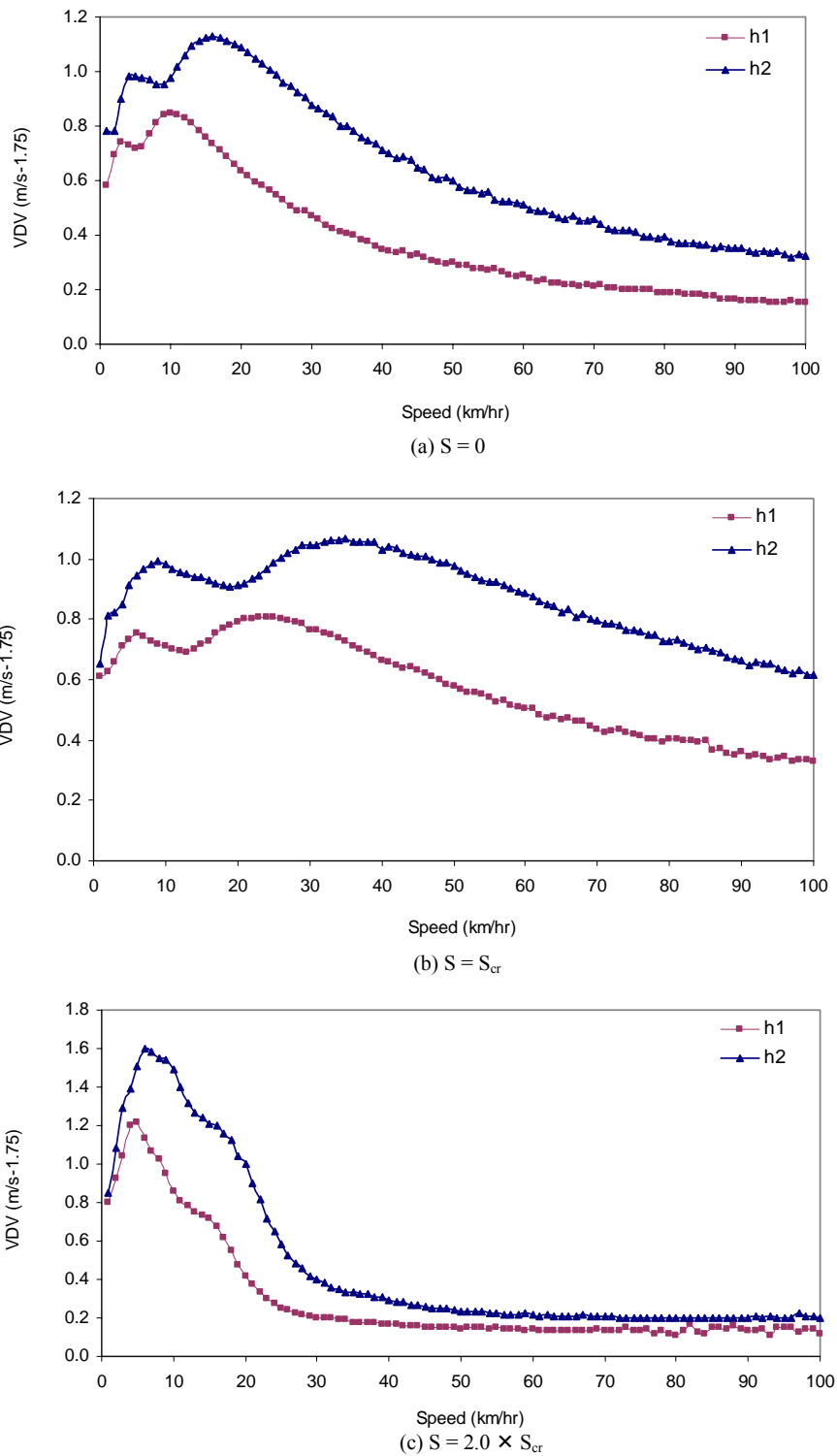


Figure 5.2: VDV vs. Speed for tire size R_{T2} crossing over 5 humps for Driver when: (a) $S = 0$, (b) $S = S_{cr}$, and (c) $S = 2.0 \times S_{cr}$.

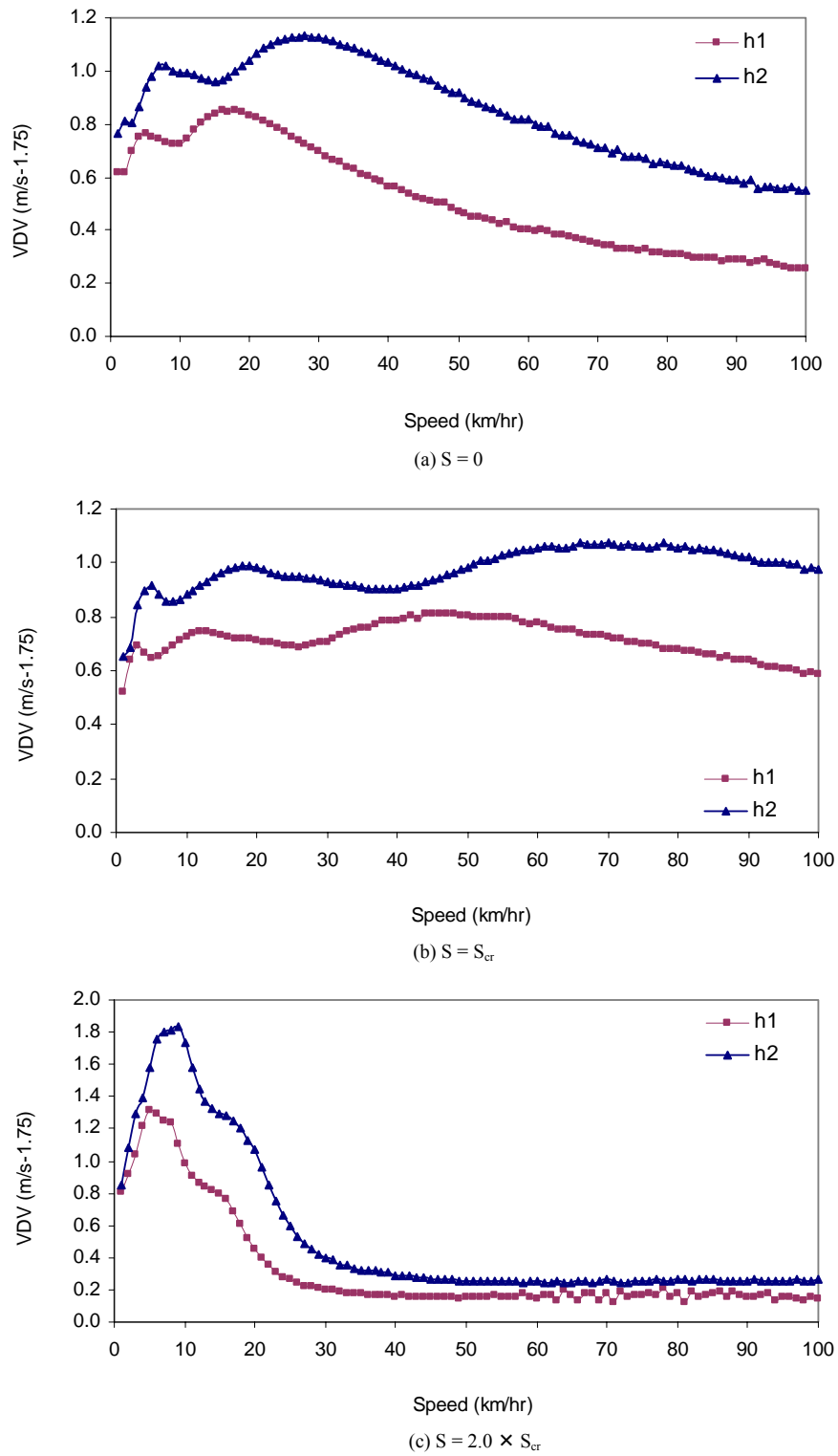


Figure 5.3: VDV vs. Speed for tire size R_{T2} crossing over 10 humps for Driver when: (a) $S = 0$, (b) $S = S_{cr}$, and (c) $S = 2.0 \times S_{cr}$.

5.2 EFFECT OF VEHICLE SPEED

In this section, the effect of vehicle crossing speed over a single hump is being examined first. Figure 5.4, 5.5, 5.7, and 5.8 represent maximum absolute values of acceleration and jerk, and VDV for the vehicle and the driver. Three tire sizes, namely R_{T1} , R_{T2} , and R_{T3} are considered with fixing the height of the hump to be h_2 . One should note that the acceleration and jerk magnitudes tend to decrease with increasing of hump crossing speed. Also, the main body of the vehicle is exposed to a maximum jerk level 300 m/s^3 twice as much as the driver received level 140 m/s^3 .

Next, the effect of vehicle crossing speeds for 2 and 10 repeated humps are investigated. For clarity purpose, four constant crossing speeds are selected to display the dynamic behavior of the driver. They are 20 km/hr, 50 km/hr, 70 km/hr, and 100 km/hr. Effect of three hump spacing are examined. These are zero spacing, critical spacing, and double of the critical spacing. In all these simulation cases, hump height of h_2 and tire radius size of R_{T2} have been kept as fixed parameters. It is difficult to extract concrete observation from the time response behavior of the driver except that the displacement, acceleration, and jerk are more pronounced at low crossing speeds. Another remark it can be observed that series of repeated humps resulted as observed in a single hump and that is that the acceleration and jerk magnitudes tend to decrease with increasing of hump spacing and crossing speed. Again here, higher crossing speeds are not recommended although the driver is receiving minimum shocks and low discomfortable level but the vehicle body is certainly suffer a lot from these

disturbances due to frequently crossing and the high level of vibrational frequencies which leads to different failure modes or probability of accidents.

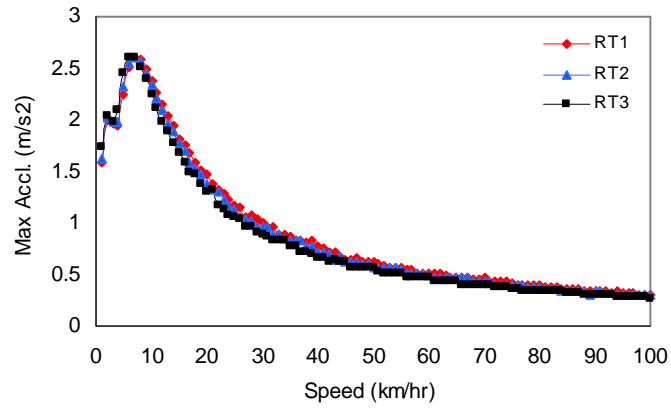


Figure 5.4: Max Accl. vs. Speed for single hump, h_2 for Driver for tire size R_{T1} / R_{T2} / R_{T3} having absolute positive values.

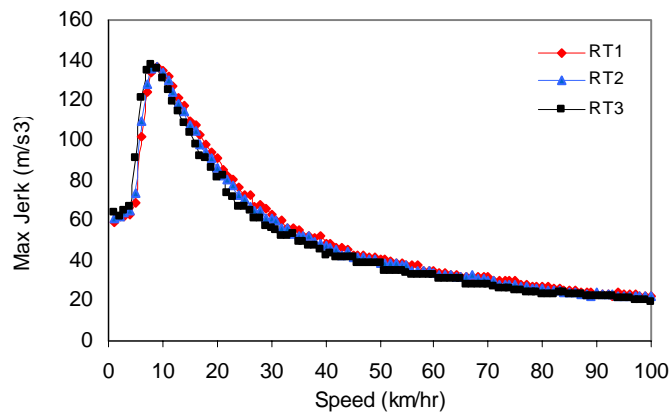


Figure 5.5: Max Jerk vs. Speed for single hump, h_2 for Driver for tire size R_{T1} / R_{T2} / R_{T3} having absolute positive values.

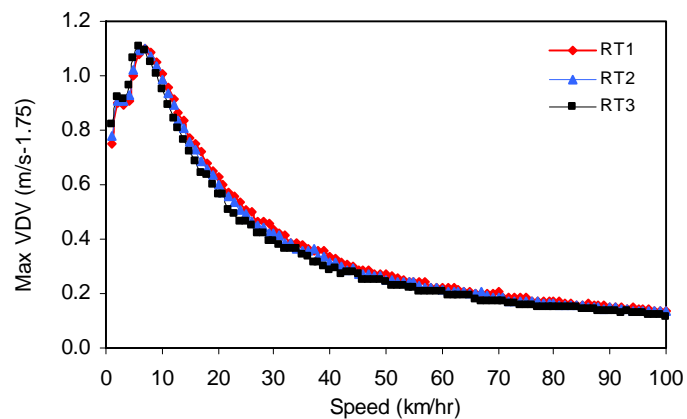


Figure 5.6: VDV vs. Speed for single hump, h_2 for Driver for tire size R_{T1} / R_{T2} / R_{T3}

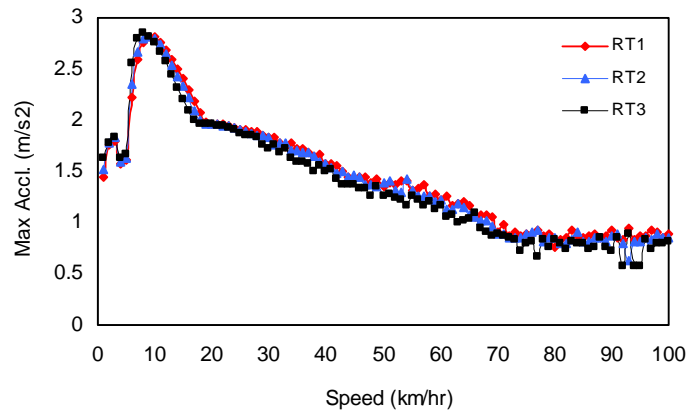


Figure 5.7: Max Accel. vs. Speed for single hump, h_2 for Main Body for tire size R_{T1} / R_{T2} / R_{T3} having absolute positive values.

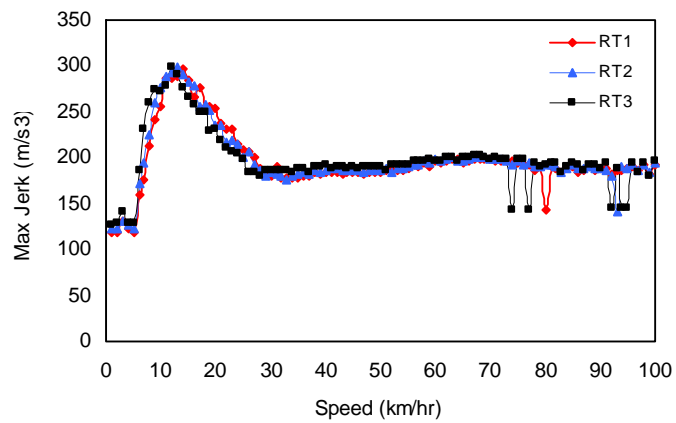


Figure 5.8: Max Jerk vs. Speed for single hump, h_2 for Main Body for tire size R_{T1} / R_{T2} / R_{T3} having absolute positive values.

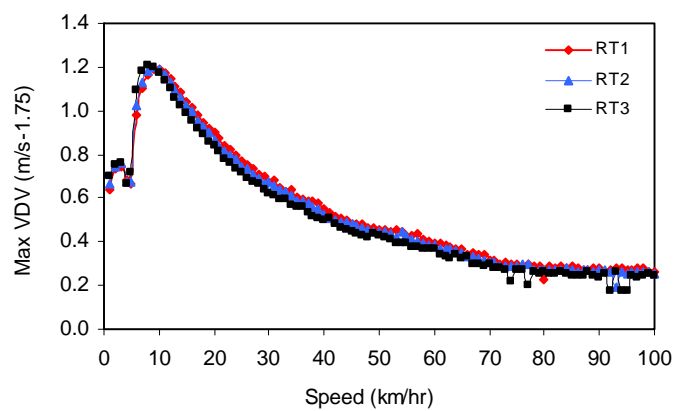
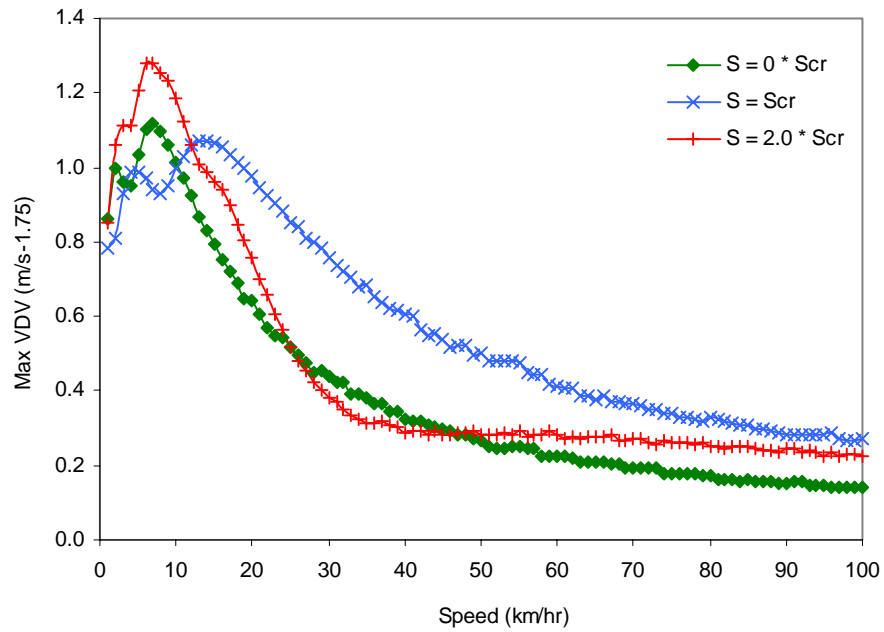
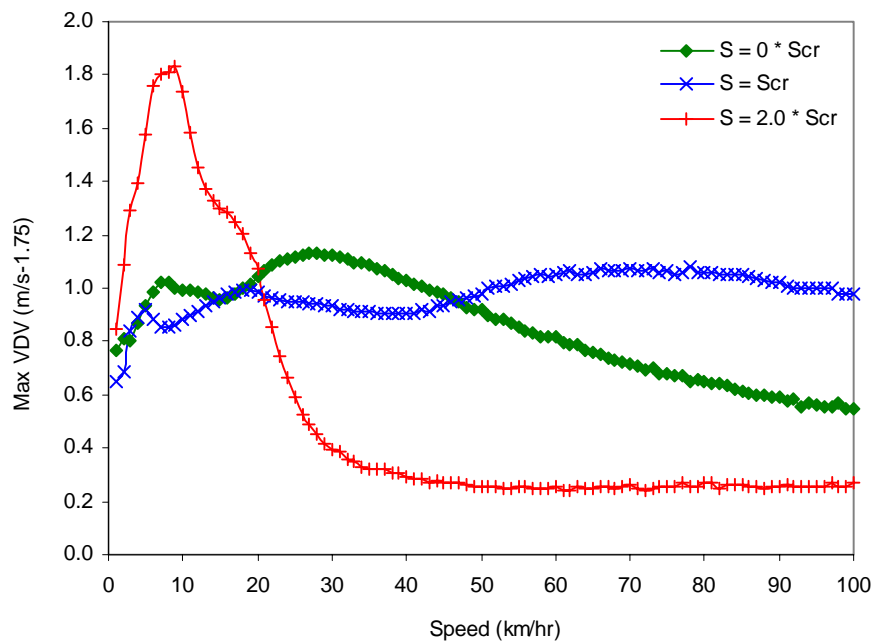


Figure 5.9: VDV vs. Speed for single hump, h_2 for Main Body for tire size R_{T1} / R_{T2} / R_{T3}



(a) 2 humps



(b) 10 humps

Figure 5.10: VDV vs. Speed for Driver with h_2 , tire size R_{T2} for (a) 2 humps and (b) 10 humps when $S = 0$, $S = S_{cr}$, and $S = 2.0$ of S_{cr}

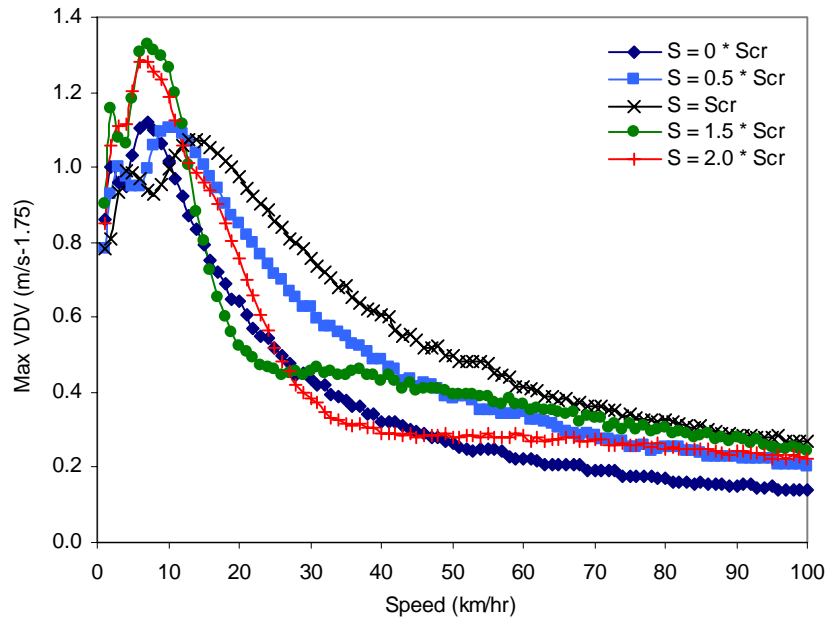
5.3 EFFECT OF DIFFERENT SPACING BETWEEN HUMPS

5.3.1 Effect of different spacing ratios of critical spacing

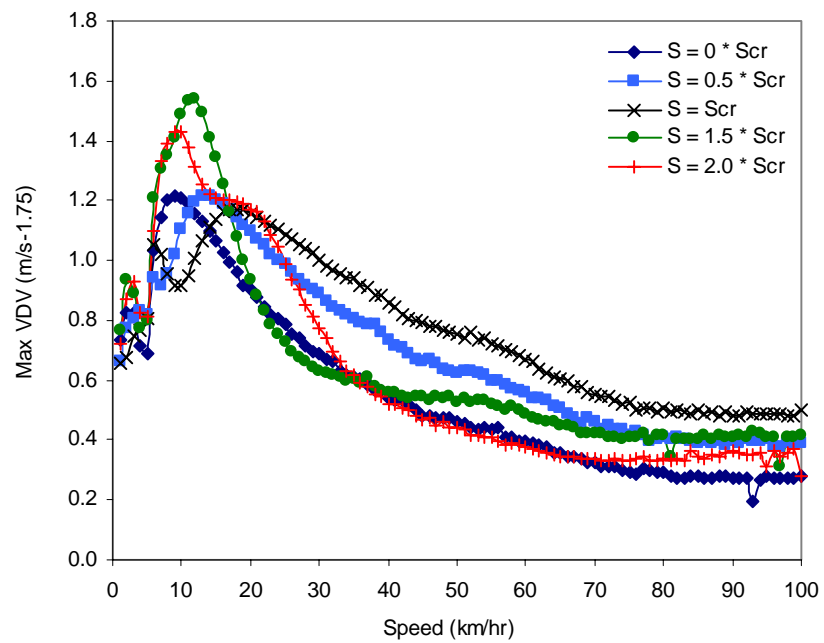
In this section, the effect of different spacing between humps is investigated. All simulation cases considered here are for a hump length of h_2 and tire radius size of R_{T2} . Various ratios hump spacing of critical spacing are examined namely 0, 0.5, S_{cr} , 1.5, and 2.0. The dynamic behavior resulted are expressed in terms of VDV value representing the main body of the vehicle and the driver. Also, in these cases the effect of spacing when there are 2, 5, or 10 repeated humps is considered. Figure 5.11 represent the case for 2 humps for (a) the driver and (b) the vehicle main body. While Figure 5.12 represent the case for 5 humps. Finally, Figure 5.13 represents the case for 10 humps.

The common points among all these figures is that the critical spacing is relatively the worst case in general in which the VDV is maximum with respect to other hump spacing ratio of the critical spacing for most of the approaching speeds. For the case of 2 repeated humps, spacing below the critical spacing provides relatively less VDV amount. While for the case of 5 repeated humps, spacing greater than the critical gives less VDV amount. And, if 2 and 5 repeated humps are compared to other ratios in the case of 10 repeated humps, zero spacing shows greater VDV amount. Another observation is that as the spacing is getting bigger beyond the critical spacing, the VDV level is decreasing into small compared to the other spacing ratios in which large spacing ratio posses lower VDV value. In order

to select proper spacing, one has to consider the number of humps to be used and the optimal approaching speed. From these simulation, it is observed that the usual approaching speed is 20 km/hr and higher since VDV gives low values. Therefore, our evaluation will be focused on this speed and higher only. For 2 repeated humps and at speed of 20 km/hr and higher, zero spacing gives relatively low VDV values. If one turns to the case of 5, 10 repeated humps, it is noted that the proper spacing is when $S = 2.0 \times S_{cr}$ at an approximate speed of 30 km/hr and higher for the driver comfort and 50 km/hr for the vehicle body.

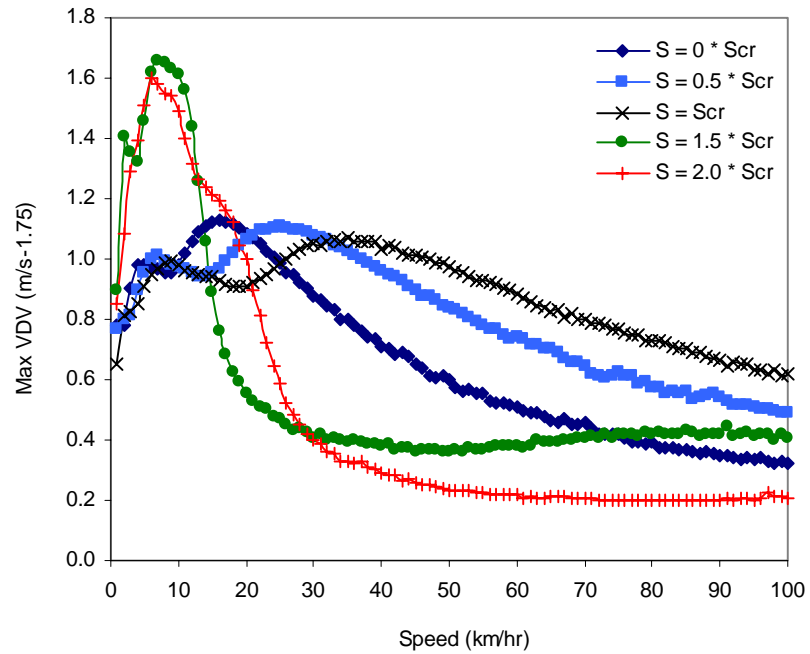


(a) Driver

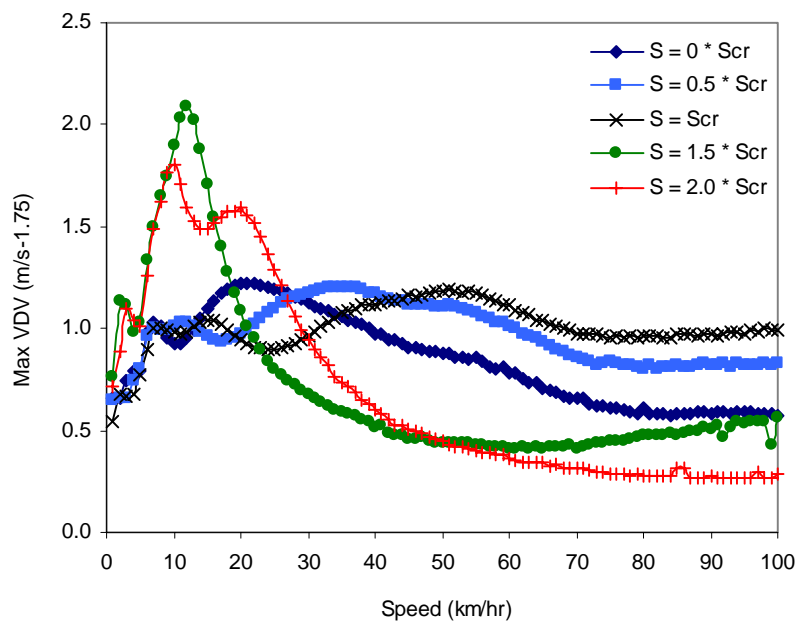


(b) Main Body

Figure 5.11: VDV vs. Speed for: 2 humps, h_2 , tire size R_{T2} for (a) Driver and (b) Main Body



(a) Driver



(b) Main Body

Figure 5.12: VDV vs. Speed for: 5 humps, h_2 , tire size R_{T2} for (a) Driver and (b) Main Body

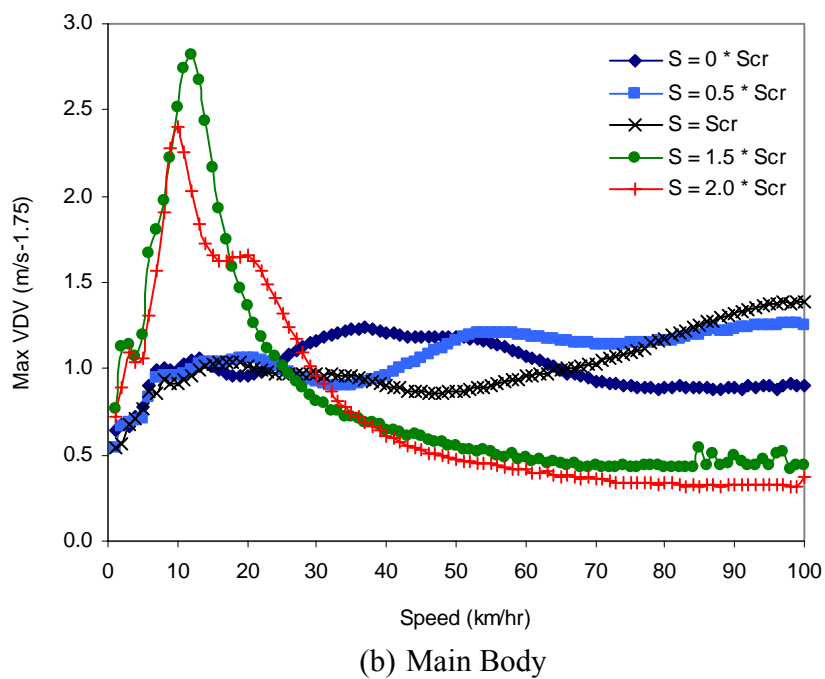
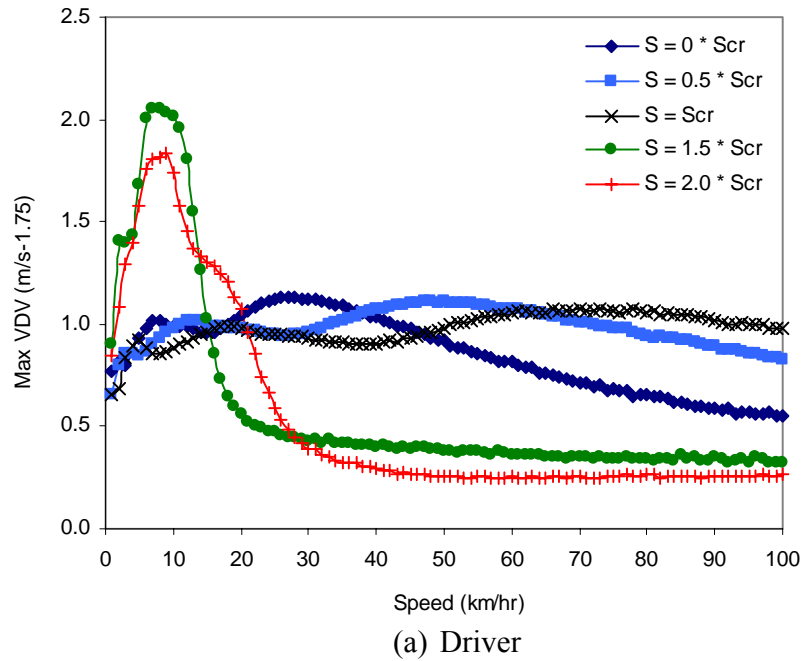
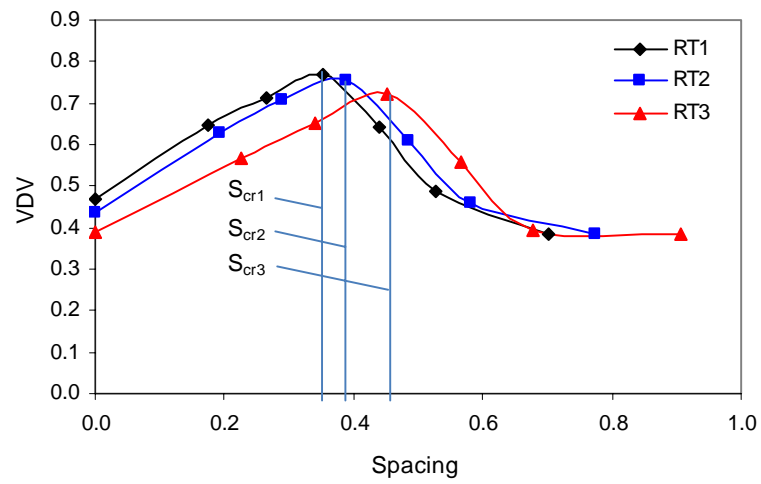


Figure 5.13: VDV vs. Speed for: 10 humps, h_2 , tire size R_{T2} for (a) Driver and (b) Main Body

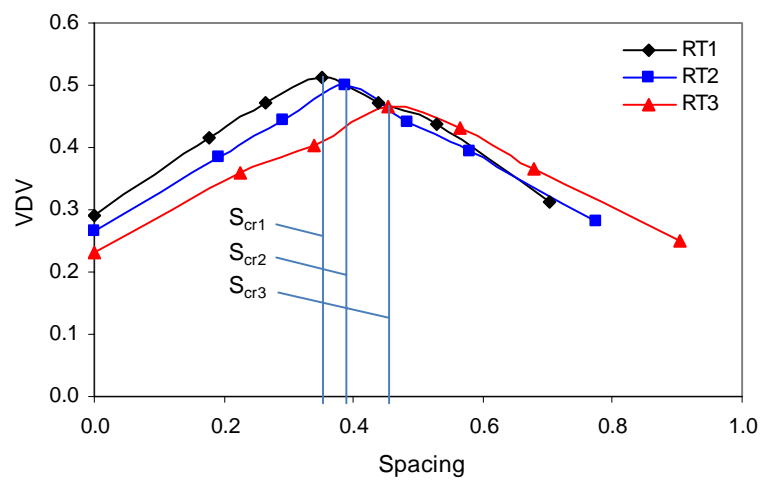
5.3.1 Tire sizes effect on the hump spacing

The three tire sizes of R_{T1} , R_{T2} , and R_{T3} are considered to evaluate their effect on the spacing between humps. Figures 5.14 to 5.19 give the VDV values with respect to the spacing between humps for case 2, 5, and 10 repeated humps. The simulation is carried out for selected speeds of 30 km/hr, 50 km/hr, 80 km/hr, and 100 km/hr. By examining these figures, they clearly support the early argument that zero spacing gives low VDV value for 2 humps case while 5, 7, and 10 humps having more spacing provide less VDV values. Also, the critical spacing associated with tire sizes show more discomfort level for both the driver and vehicle main body. From Figures 5.14, 5.15, 5.16, and 5.17, one can observe that for 2 and 5 repeated humps, smaller tire size gives high VDV values than other tires sizes when hump spacing is below the critical spacing. Whereas the VDV values flip over in a way that it becomes larger with large tire size for spacing greater than the critical spacing for different selected speeds as shown in Figures 5.18, and 5.19.

(a) Speed = 30 km/hr



(b) Speed = 50 km/hr



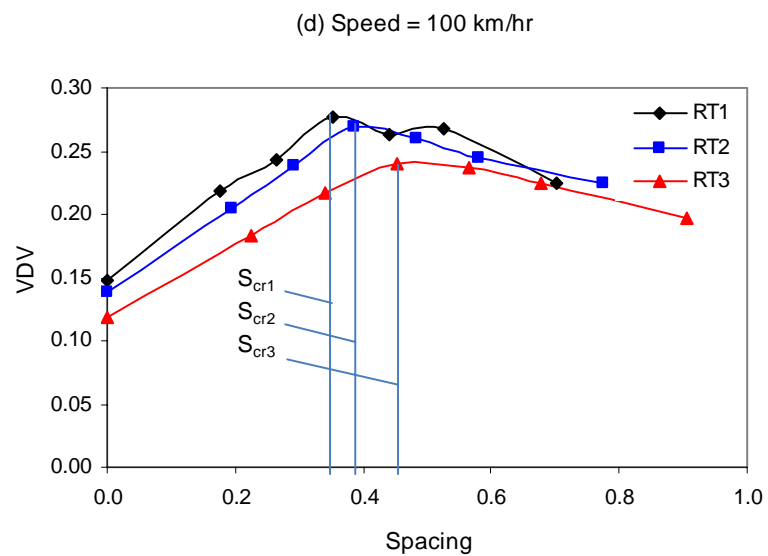
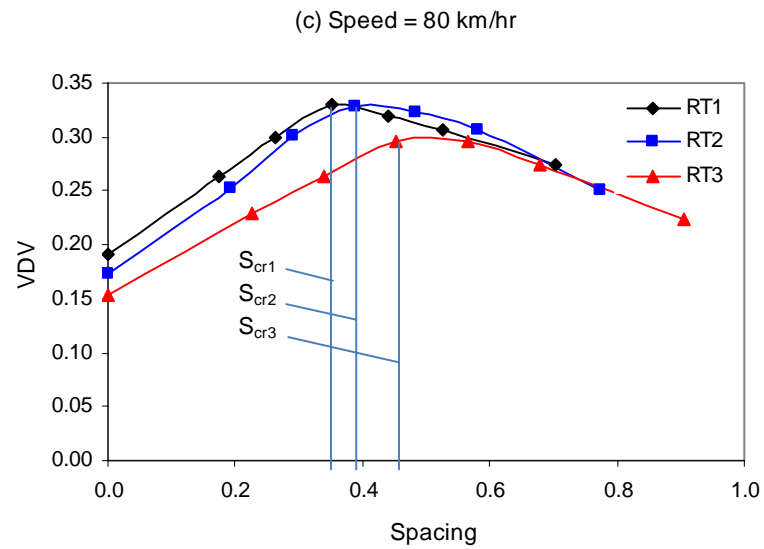
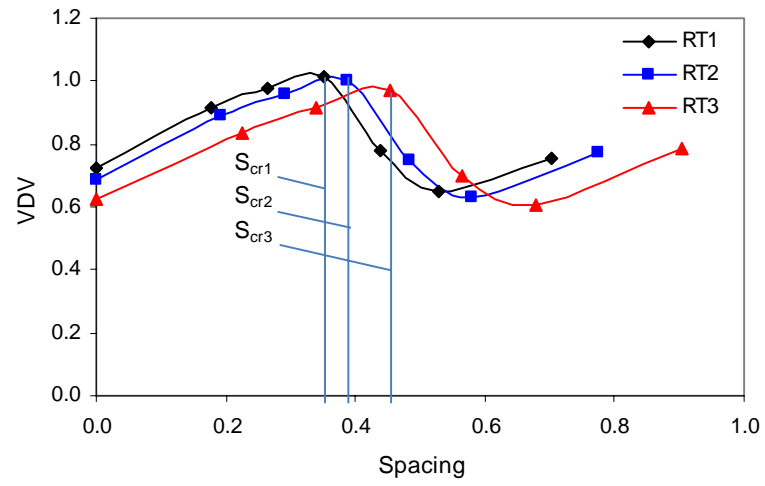
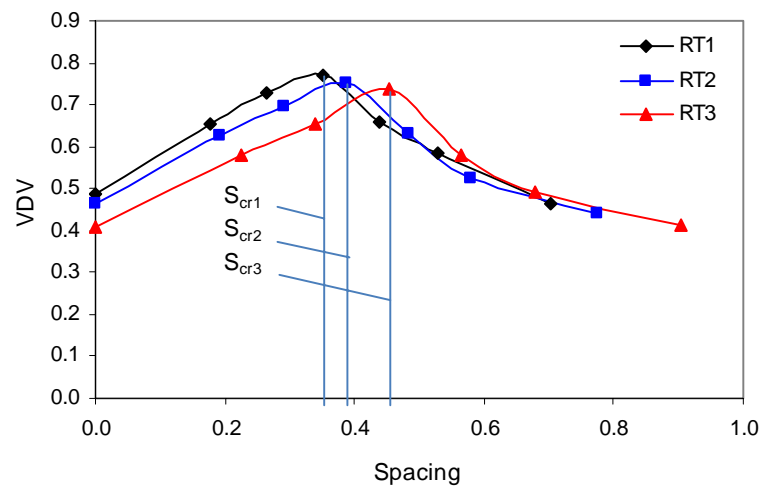


Figure 5.14: VDV vs. Spacing for Driver, for: 2 humps, h_2 , different tire sizes $R_{T1}/R_{T2}/R_{T3}$, speeds of (a) 30 km/hr, (b) 50 km/hr, (c) 80 km/hr and (d) 100 km/hr

(a) Speed = 30 km/hr



(b) Speed = 50 km/hr



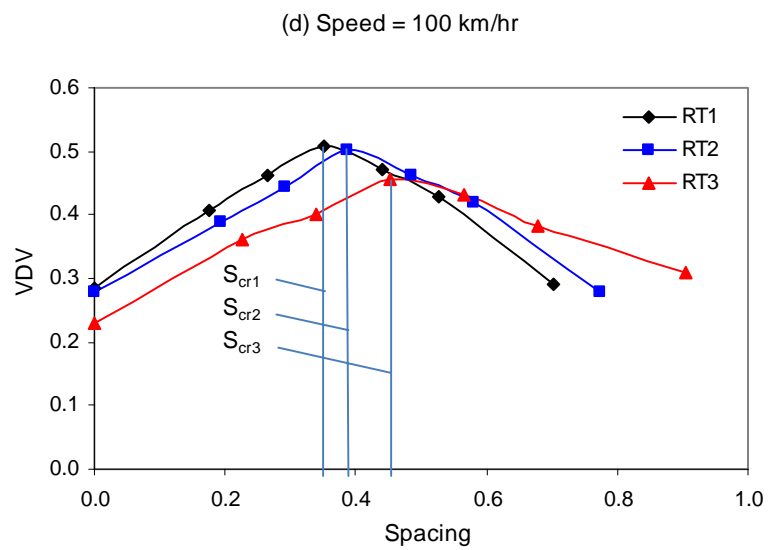
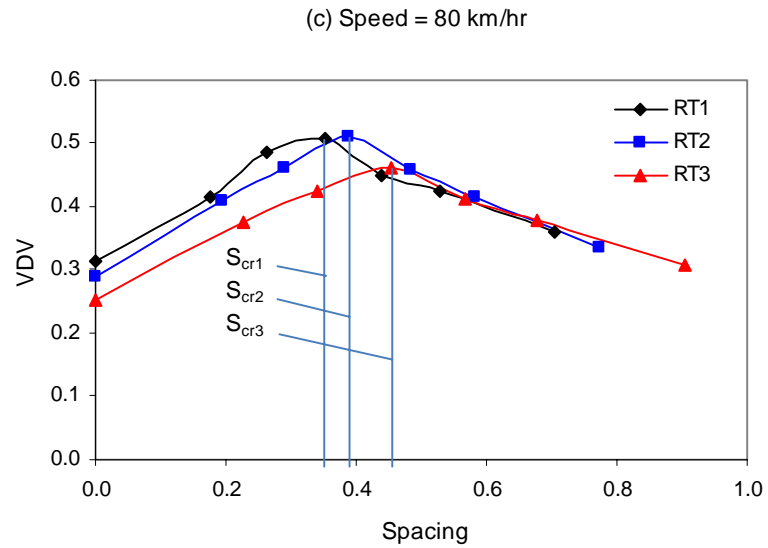
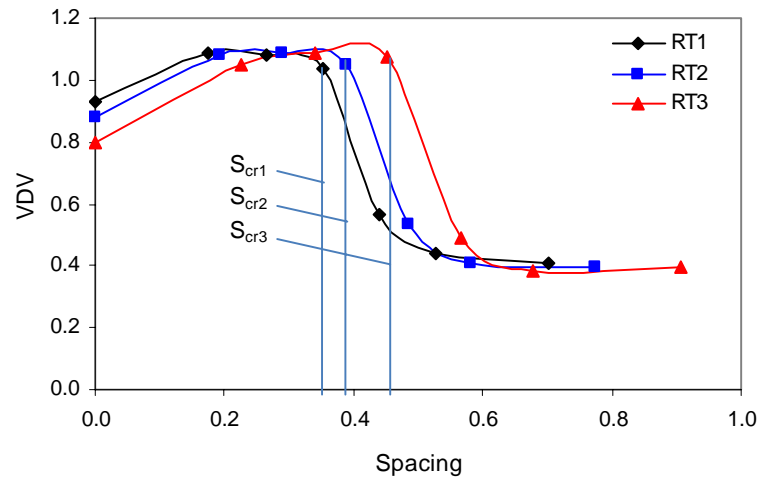
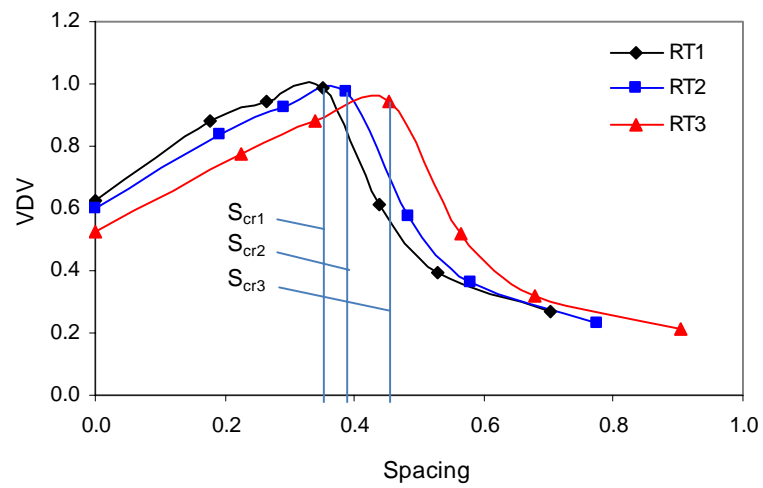


Figure 5.15: VDV vs. Spacing for Main Body, for: 2 humps, h_2 , different tire sizes $R_{T1}/R_{T2}/R_{T3}$, speeds of (a) 30 km/hr, (b) 50 km/hr, (c) 80 km/hr and (d) 100 km/hr

(a) Speed = 30 km/hr



(b) Speed = 50 km/hr



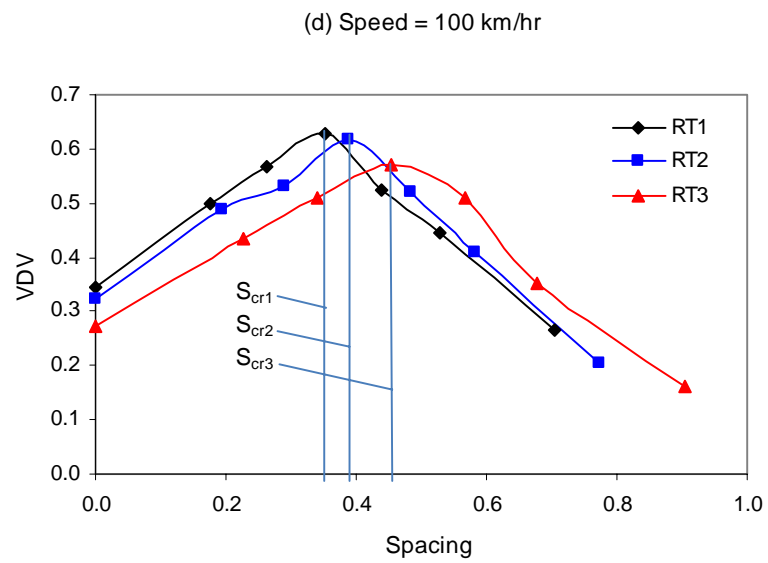
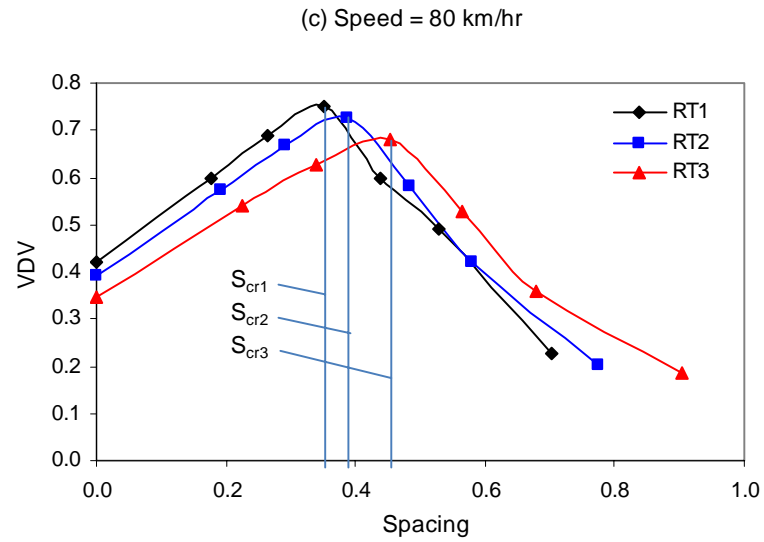
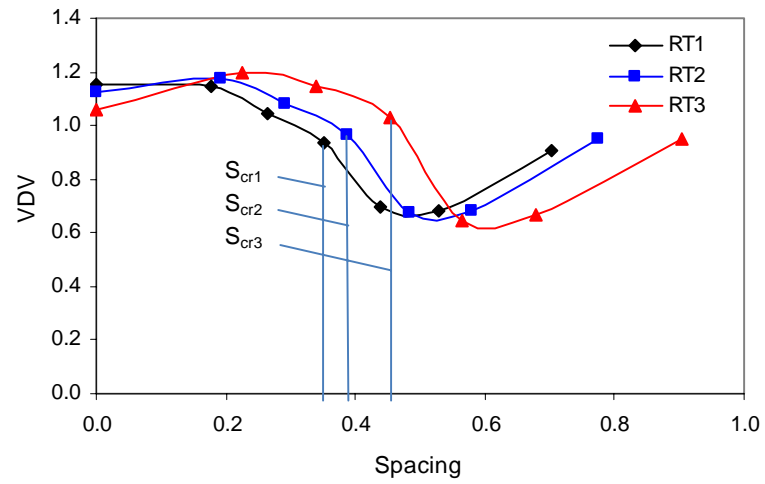
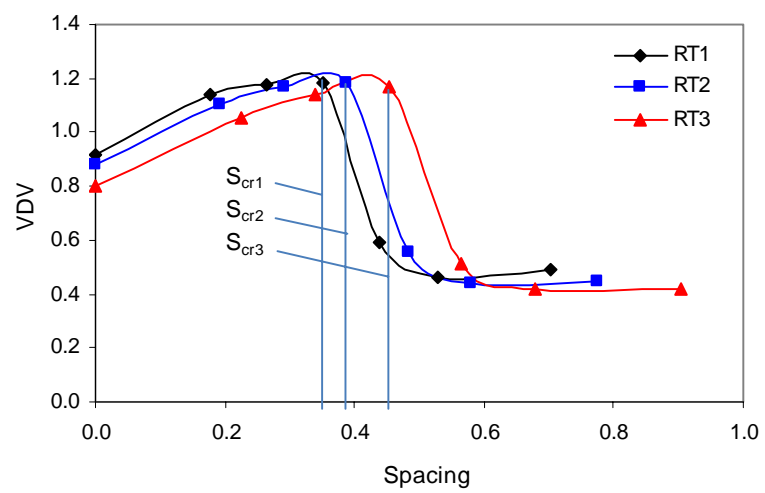


Figure 5.16: VDV vs. Spacing for Driver, for: 5 humps, h_2 , different tire sizes $R_{T1}/ R_{T2}/ R_{T3}$, speeds of (a) 30 km/hr, (b) 50 km/hr, (c) 80 km/hr and (d) 100 km/hr

(a) Speed = 30 km/hr



(b) Speed = 50 km/hr



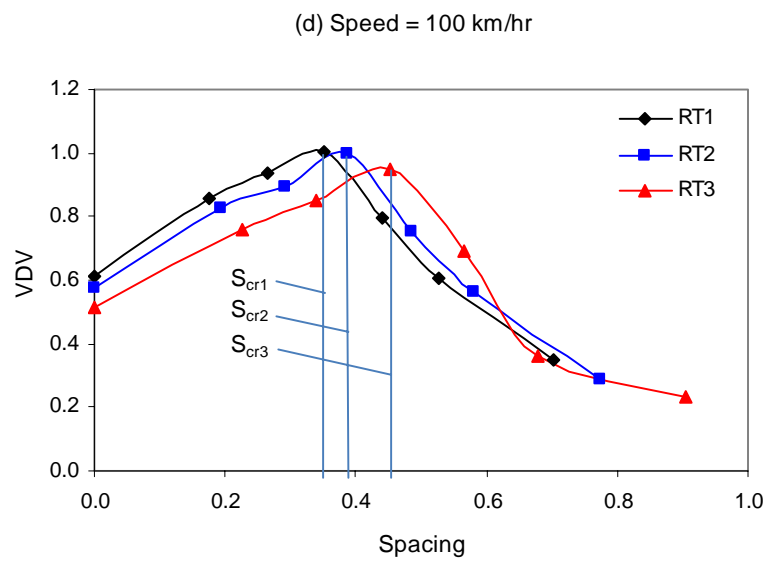
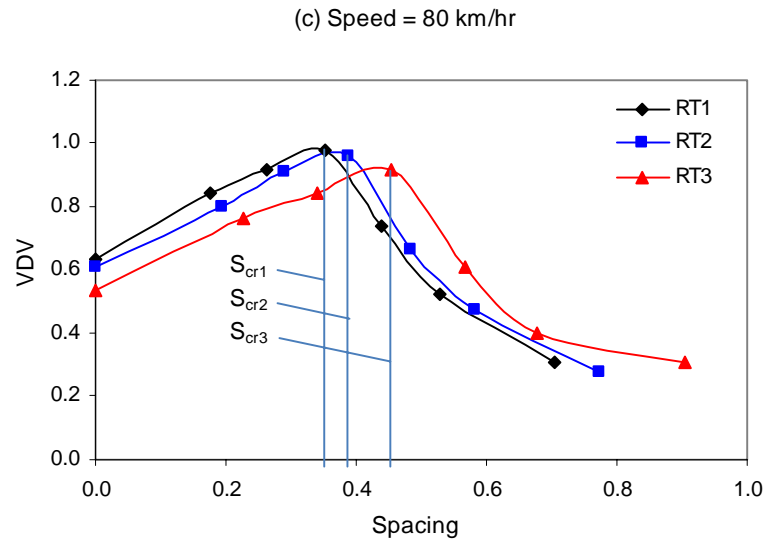
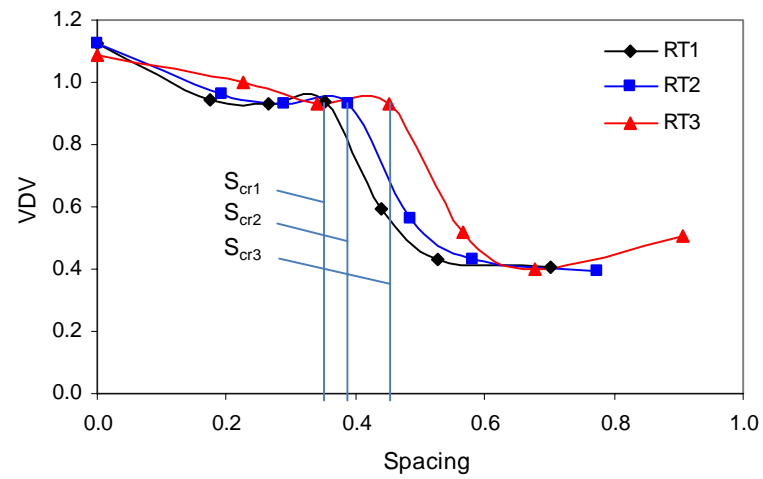
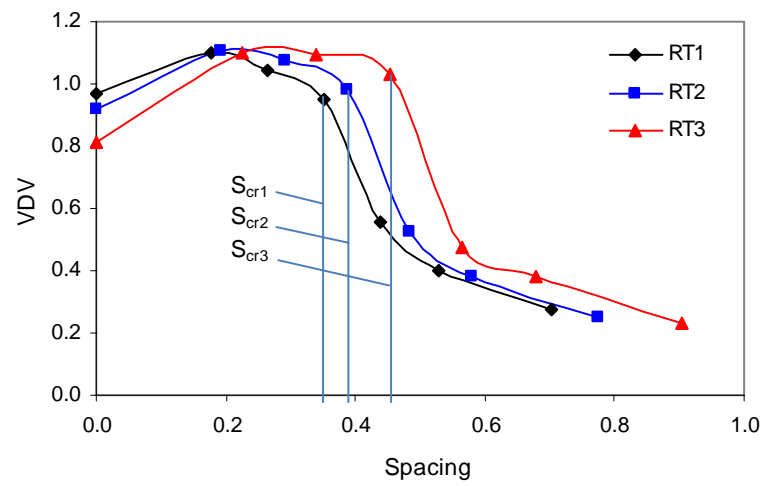


Figure 5.17: VDV vs. Spacing for Main Body, for: 5 humps, h_2 , different tire sizes $R_{T1}/R_{T2}/R_{T3}$, speeds of (a) 30 km/hr, (b) 50 km/hr, (c) 80 km/hr and (d) 100 km/hr

(a) Speed = 30 km/hr



(b) Speed = 50 km/hr



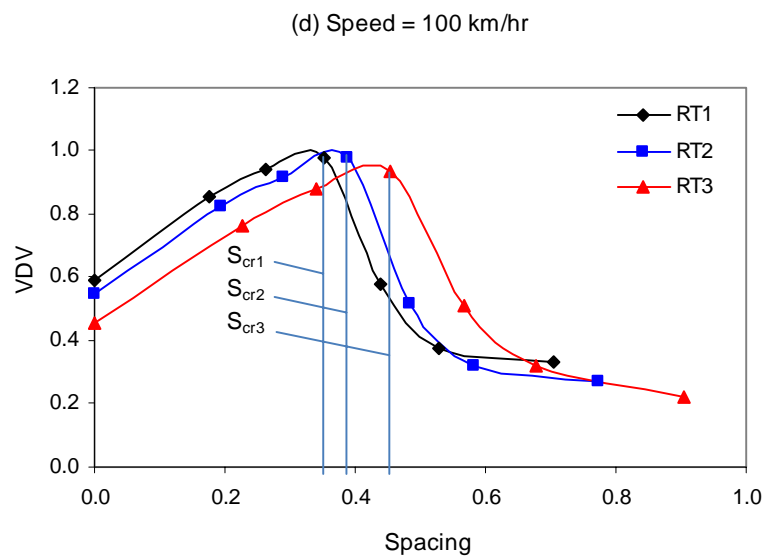
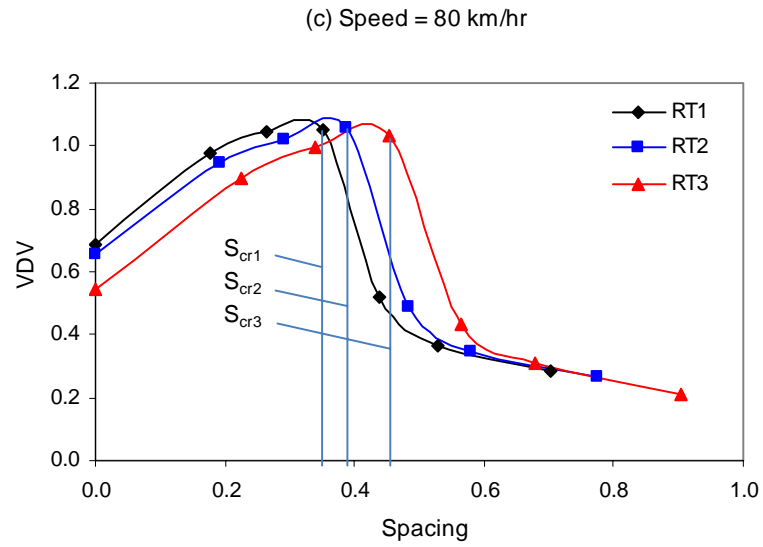
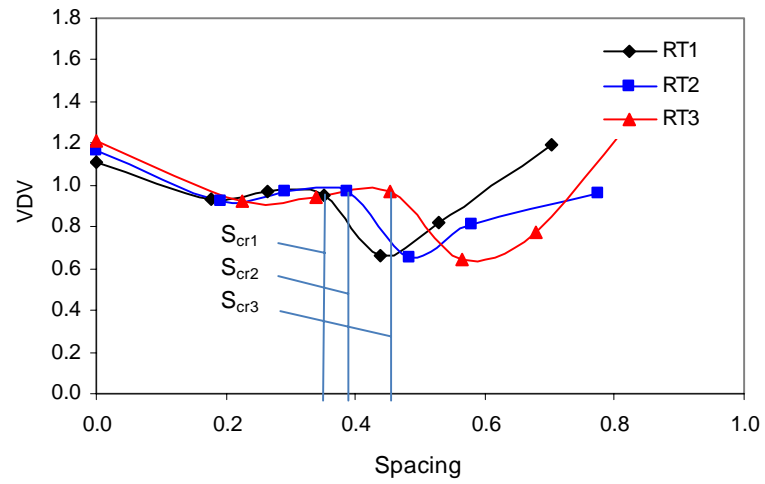
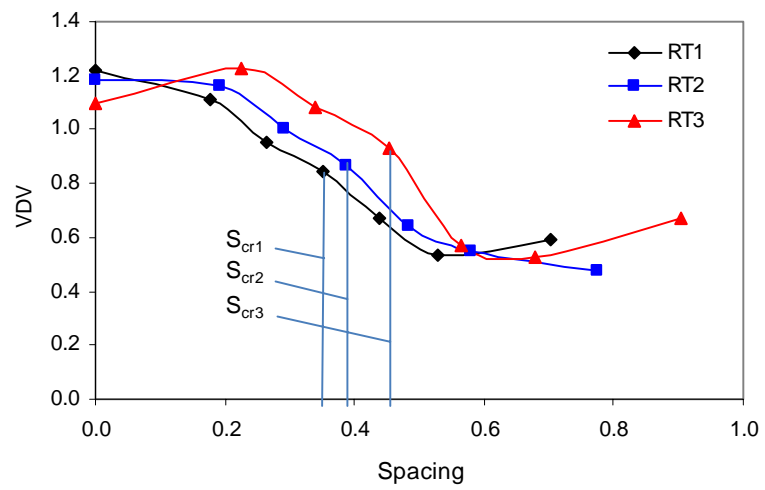


Figure 5.18: VDV vs. Actual Spacing for Driver, for: 10 humps, h_2 , different tire sizes R_{T1} / R_{T2} / R_{T3} , speeds of (a) 30 km/hr, (b) 50 km/hr, (c) 80 km/hr and (d) 100 km/hr

(a) Speed = 30 km/hr



(b) Speed = 50 km/hr



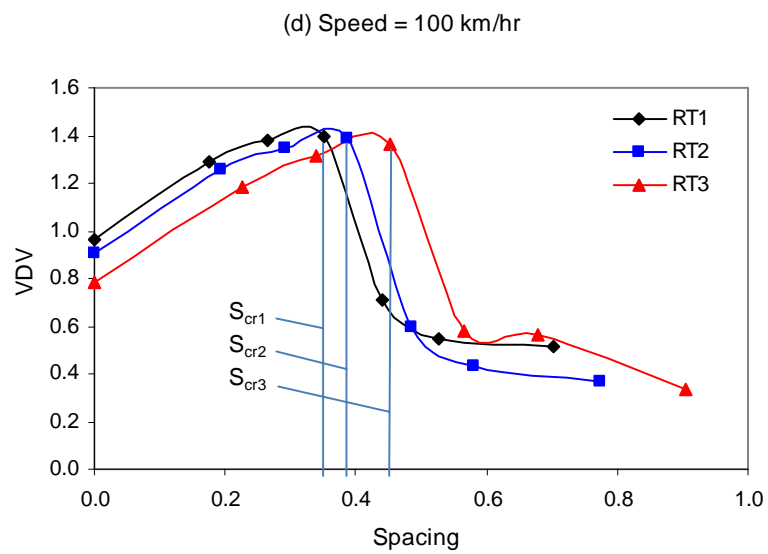
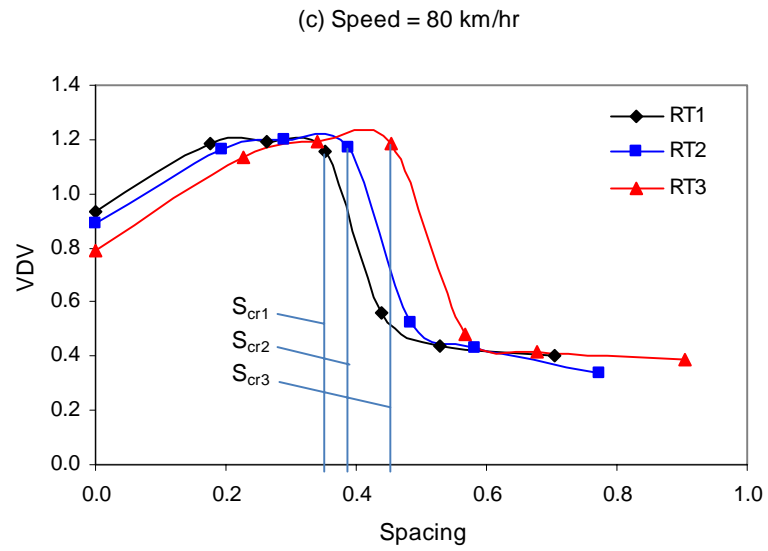


Figure 5.19: VDV vs. Spacing for Main Body, for: 10 humps, h_2 , different tire sizes R_{T1} / R_{T2} / R_{T3} , speeds of (a) 30 km/hr, (b) 50 km/hr, (c) 80 km/hr and (d) 100 km/hr

5.4 EFFECT OF MULTIPLICITY OF THESE CIRCULAR SHORT PERIODIC HUMPS

In this part of the parametric study, the effect of the hump multiplicity is examined. The multiplicities of humps are 1, 2, 3, 5, 7, and 10. Four spacing are considered namely 0 m, 0.25 m, 0.5 m, and 1.0 m. The first two spacing are less than the critical spacing for all the three tire sizes considered while the other two are greater than the critical spacing. Figures 5.20, 5.22, 5.24, and 5.26 give the VDV amount of the driver when the spacing are for 0 m, 0.25 m, 0.5 m, and 1.0 m respectively. Also, Figures 5.21, 5.23, 5.25, and 5.27 give the VDV amount of the vehicle main body. Examining resulted figures of VDV vs. speed, one can observe that when spacing is less than the critical spacing, VDV values are high for higher multiplicities of humps. This is true for all tire sizes for both the driver and vehicle body except for low approaching speeds. However, when the spacing between these humps is higher than the critical spacing, the multiplicity effect almost vanishes as the spacing is increased with approaching speeds of 40 km/hr and higher. The speed range of 20 km/hr to 40 km/hr, VDV values decrease and all converge to almost one stream of a magnitude of VDV.

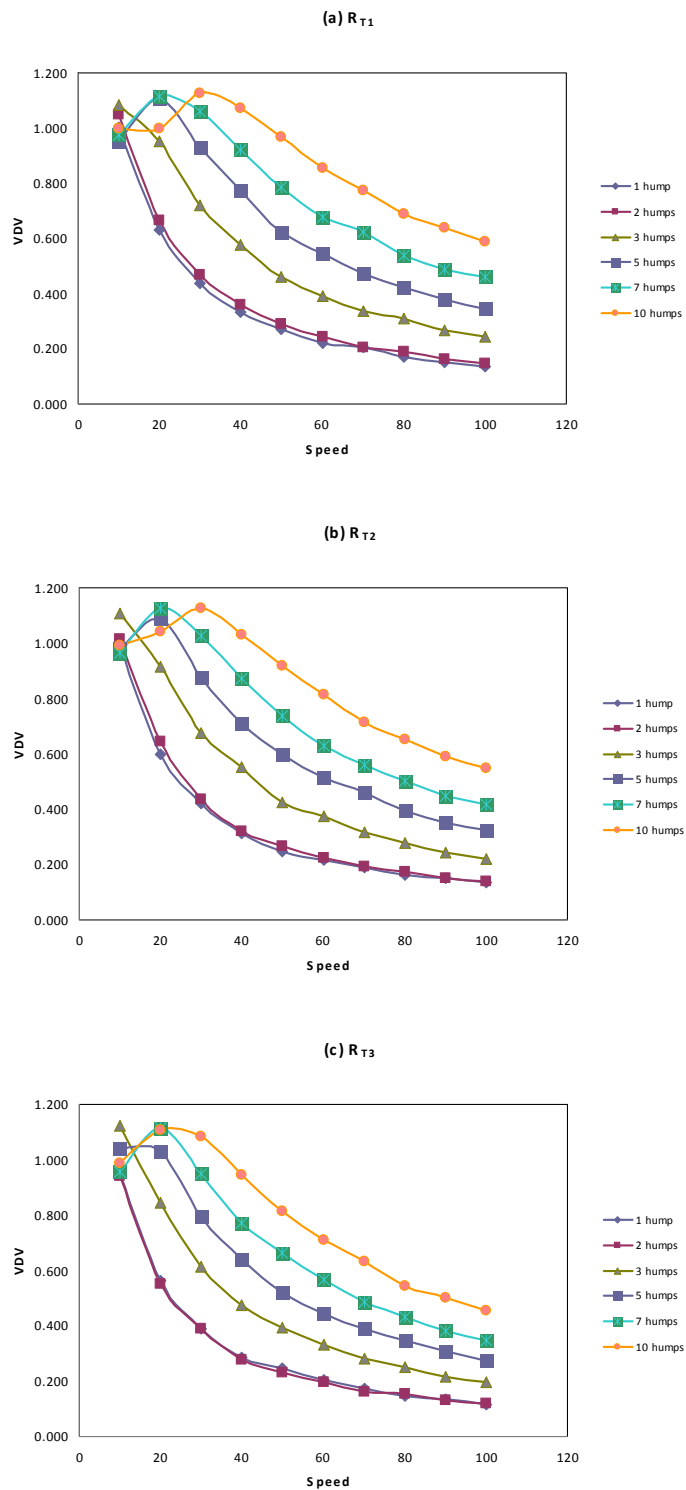


Figure 5.20: VDV vs. Speed for multiple humps, for Driver for: h_2 , different tire sizes (a) R_{T1} , (b) R_{T2} , and (c) R_{T3} with fixed spacing = 0 m

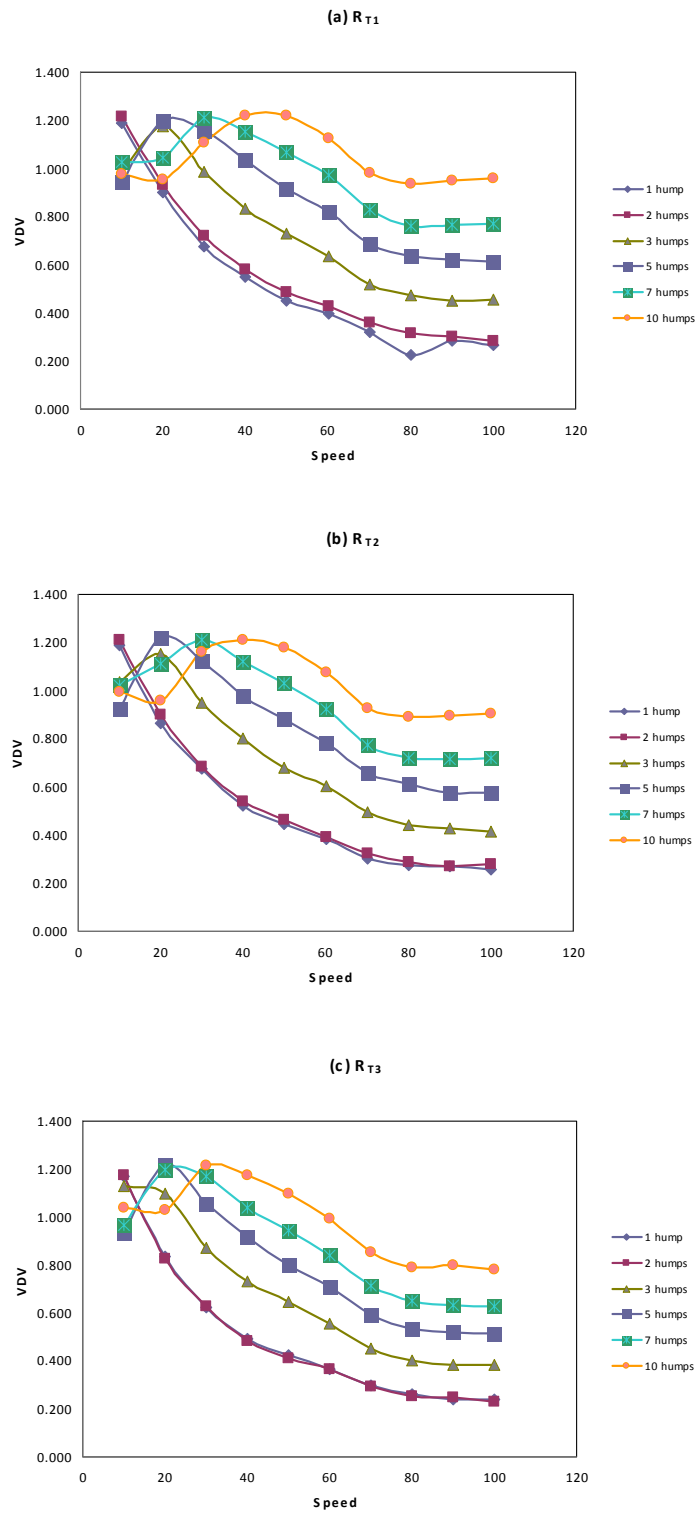


Figure 5.21: VDV vs. Speed for multiple humps, for Main Body for: h_2 , different tire sizes (a) R_{T1} , (b) R_{T2} , and (c) R_{T3} with fixed spacing = 0 m

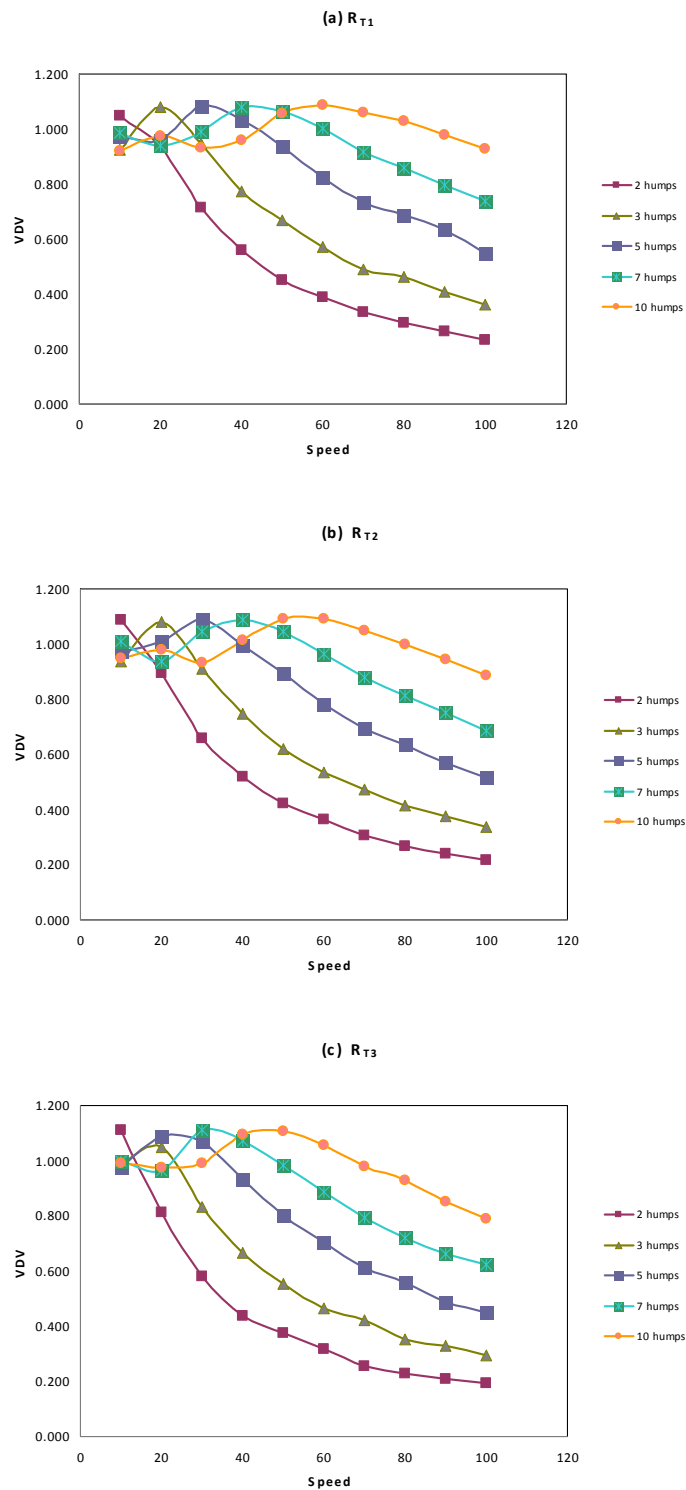


Figure 5.22: VDV vs. Speed for multiple humps, for Driver for: h_2 , different tire sizes (a) R_{T1} , (b) R_{T2} , and (c) R_{T3} with fixed spacing = 0.25 m

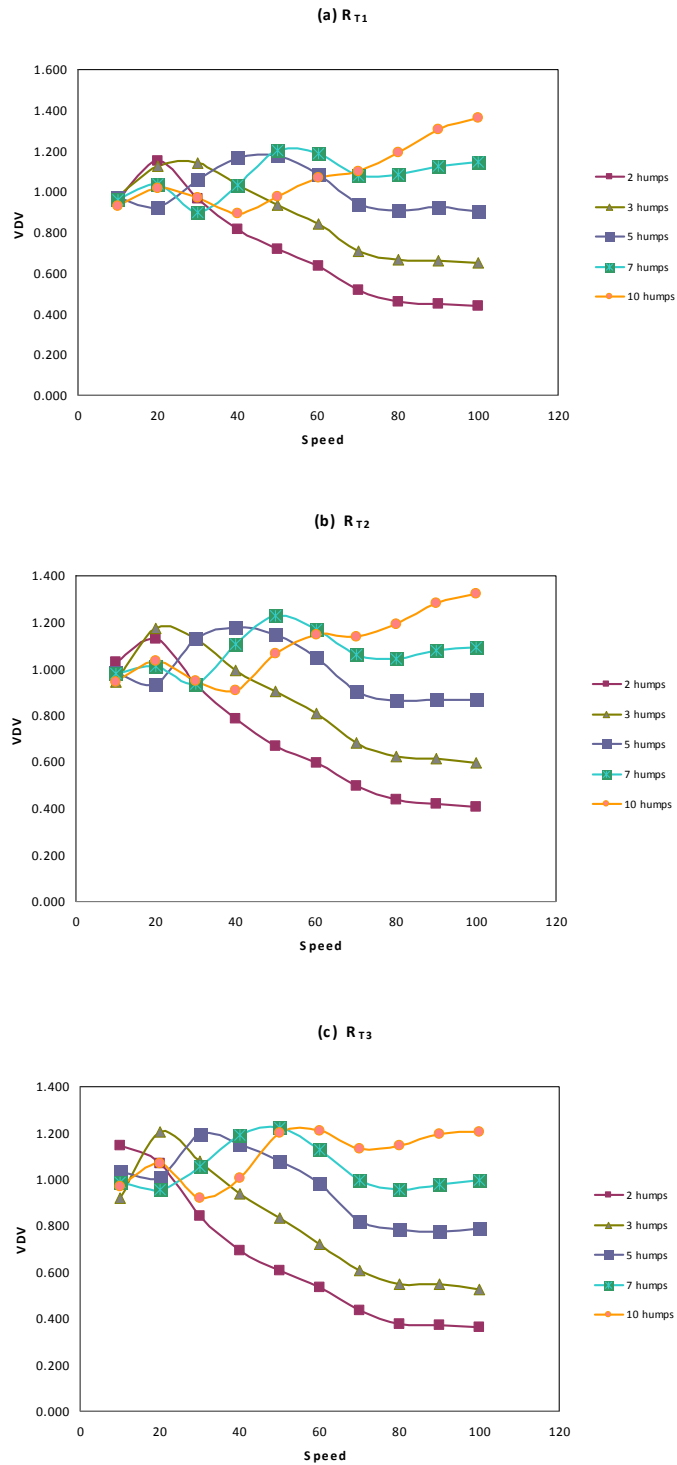


Figure 5.23: VDV vs. Speed for multiple humps, for Main Body for: h_2 , different tire sizes (a) R_{T1} , (b) R_{T2} , and (c) R_{T3} with fixed spacing = 0.25 m

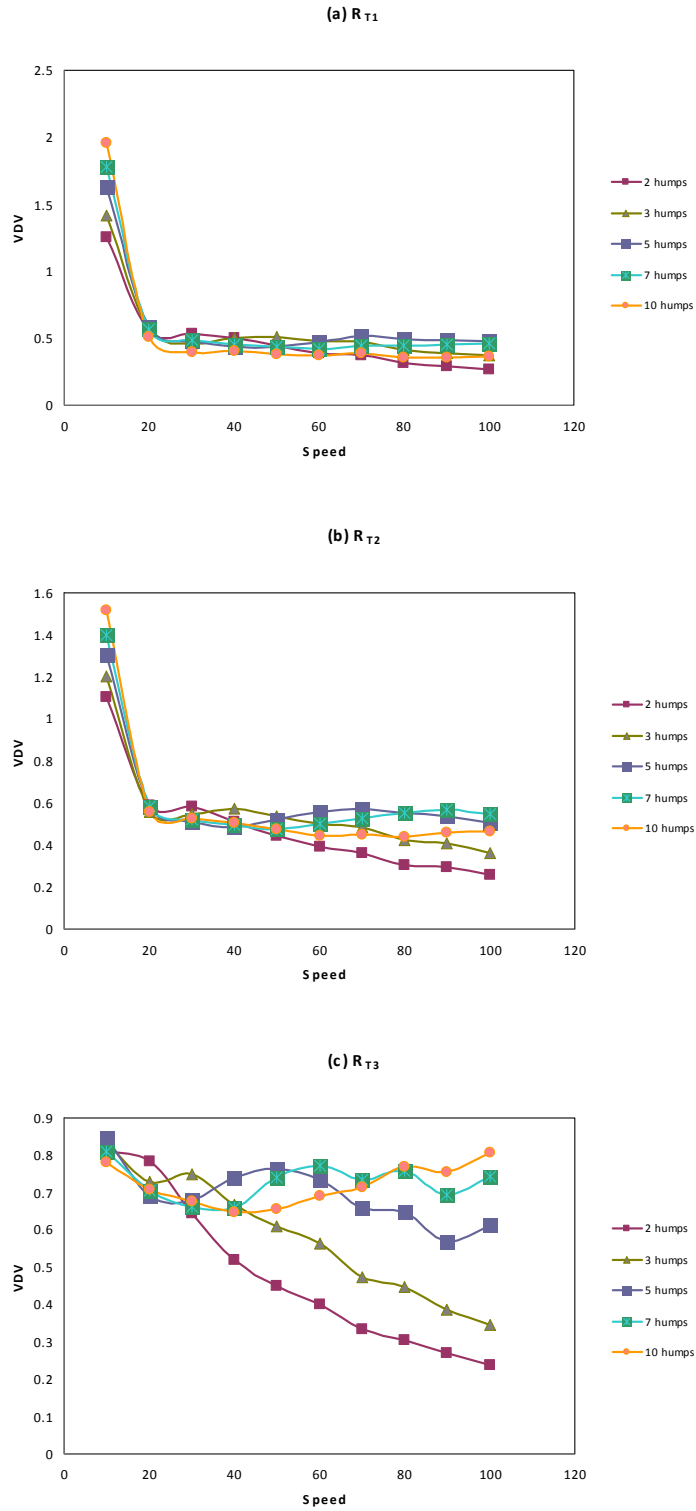


Figure 5.24: VDV vs. Speed for multiple humps, for Driver for: h_2 , different tire sizes (a) R_{T1} , (b) R_{T2} , and (c) R_{T3} with fixed spacing = 0.5 m

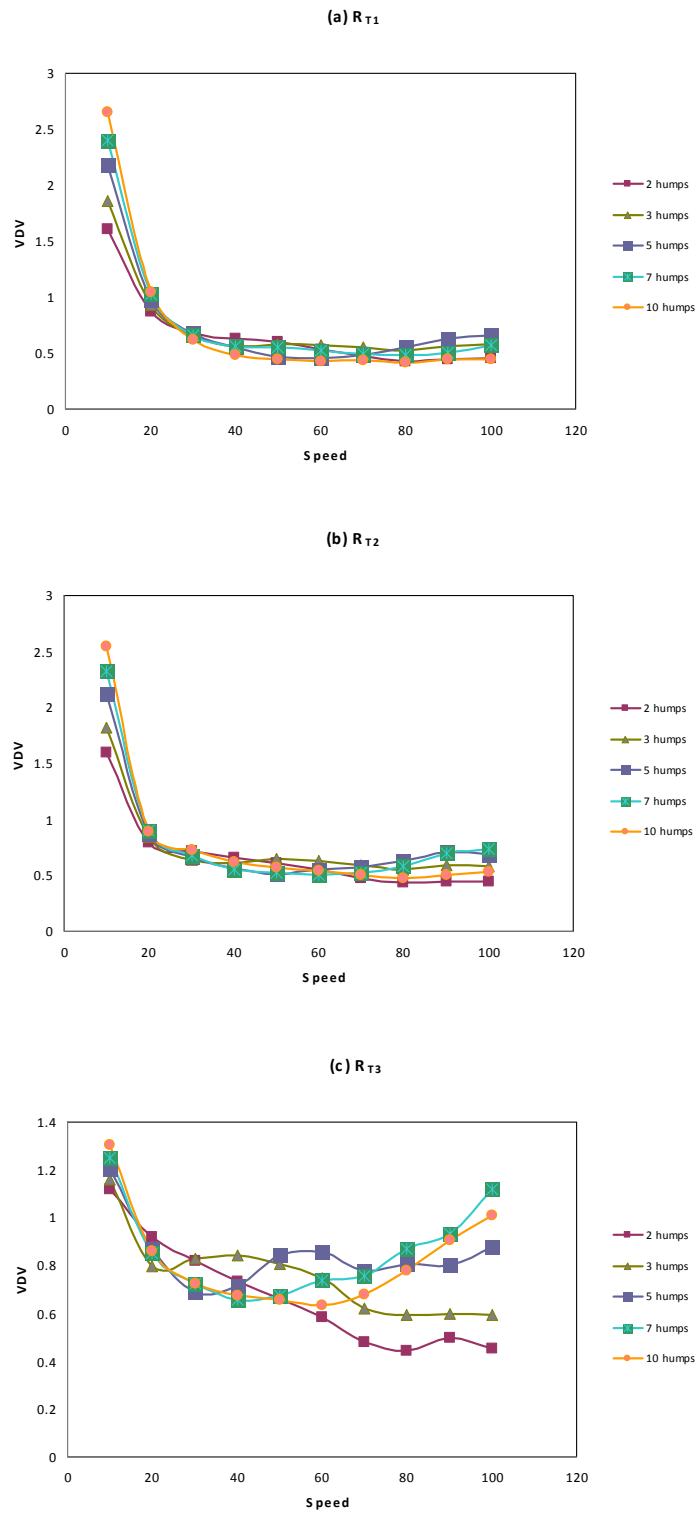


Figure 5.25: VDV vs. Speed for multiple humps, for Main Body for: h_2 , different tire sizes (a) R_{T1} , (b) R_{T2} , and (c) R_{T3} with fixed spacing = 0.5 m

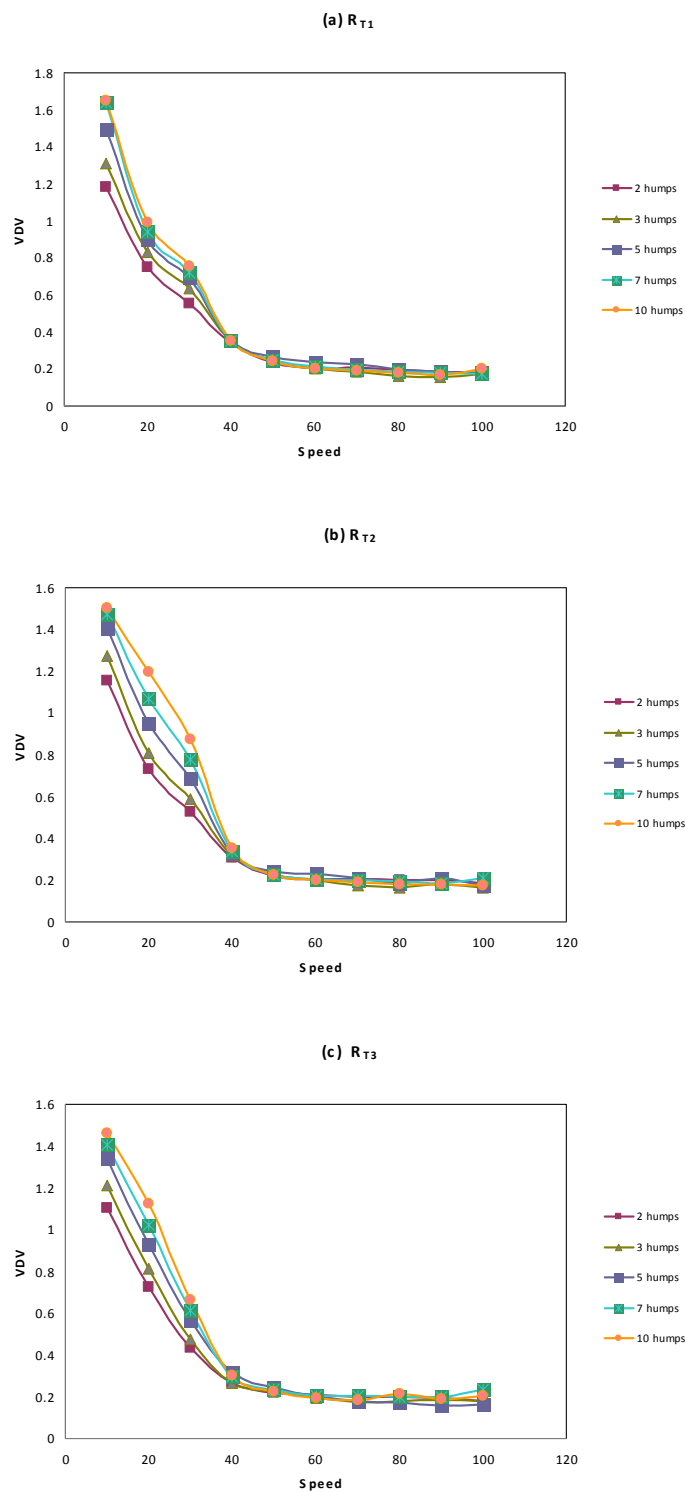


Figure 5.26: VDV vs. Speed for multiple humps, for Driver for: h_2 , different tire sizes (a) R_{T1} , (b) R_{T2} , and (c) R_{T3} with fixed spacing = 1.0 m

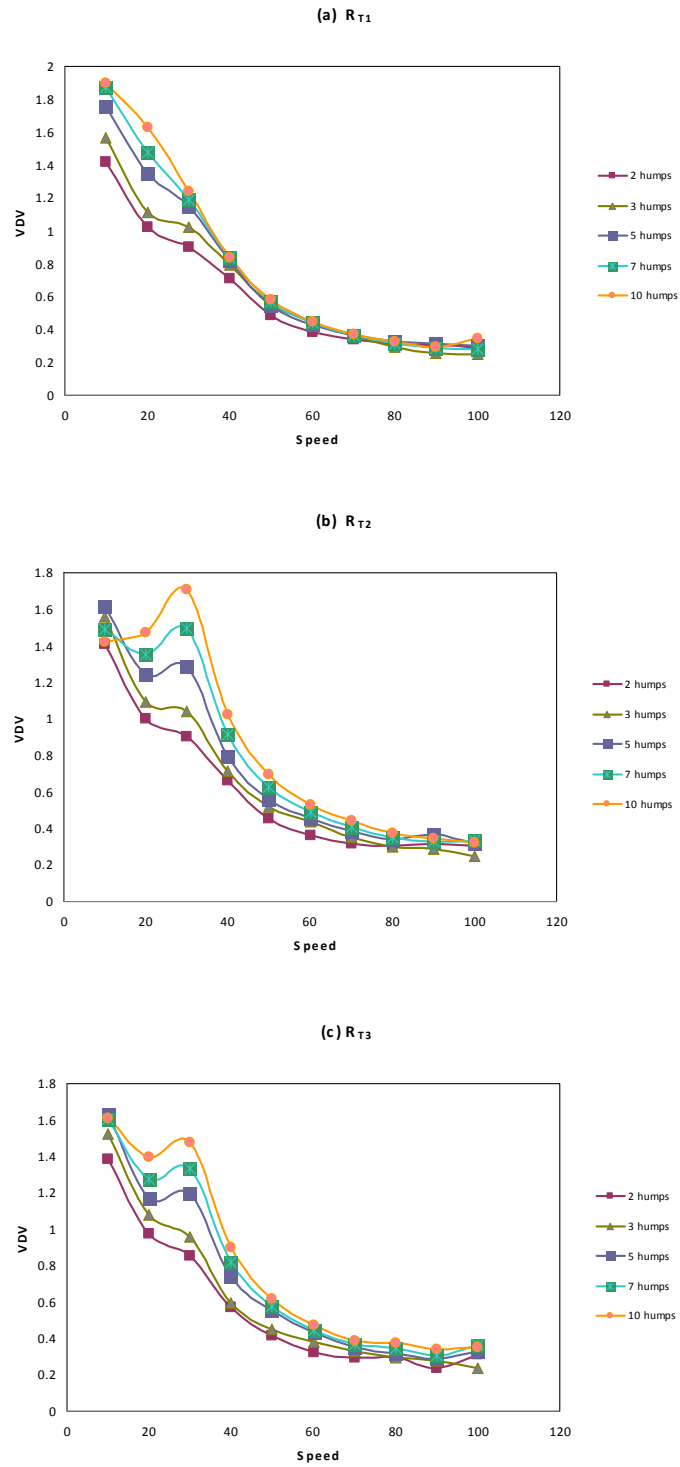


Figure 5.27: VDV vs. Speed for multiple humps, for Main Body for: h_2 , different tire sizes (a) R_{T1} , (b) R_{T2} , and (c) R_{T3} with fixed spacing = 1.0 m

5.5 LINEAR VS. BILINEAR BEHAVIOR IN THE SUSPENSION SYSTEM

In order to study the significance of the variances in stiffness and damping coefficients in the suspension system, linear and bilinear response behavior is examined. All simulation cases considered here are for a hump length of h_2 , tire size of R_{T2} , and a multiplicity of 10 repeated humps only are investigated. The goal is to measure the bilinear effect namely 2, 3, and 4 of the linear magnitude. Figures 5.42 and 5.44 give the VDV amount of the driver when the variances in stiffness and damping coefficients is incorporated while Figures 5.43 and 5.45 give the VDV amount of the vehicle body. Now back to Figures 5.42, and 5.43, for all ratios of stiffness, all VDV values are comparable to linear behavior due to the fact that the coefficients used in our model are of high values. However, Figures 5.44, and 5.45 show relatively increasing in VDV value as the ratios of damping increases.

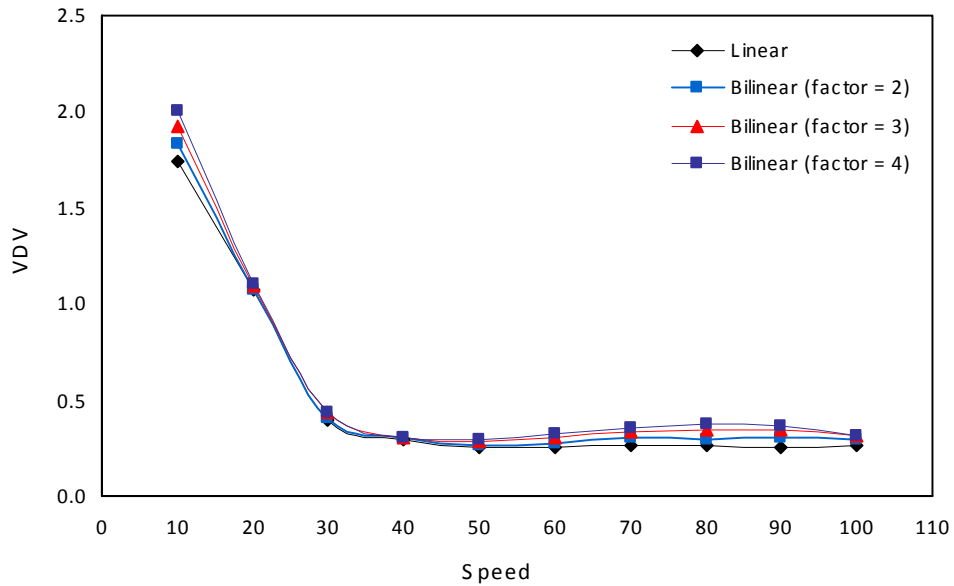


Figure 5.28: VDV vs. Speed for Driver for: 10 humps, h_2 , tire size R_{T2} for Stiffness coefficient for linear and bilinear comparison.

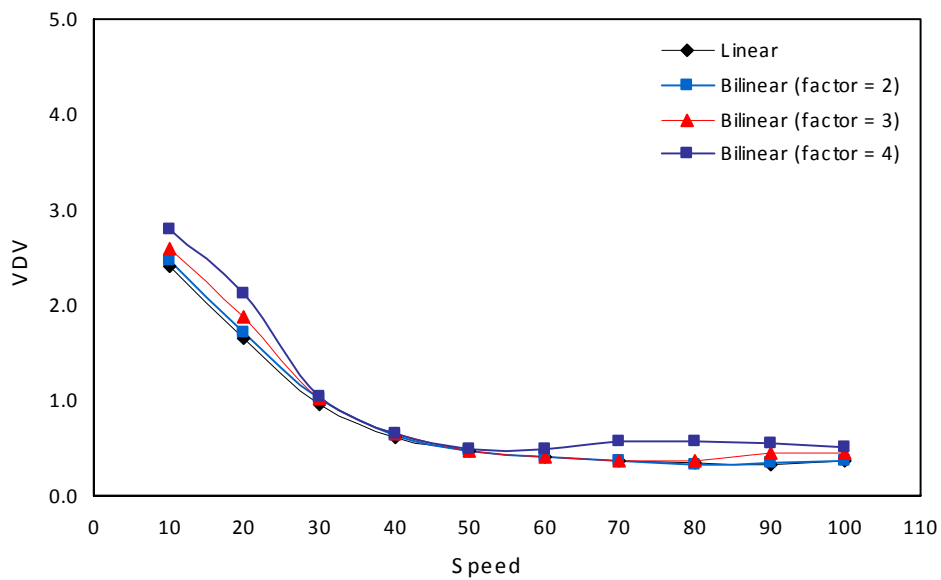


Figure 5.29: VDV vs. Speed for Main Body for: 10 humps, h_2 , tire size R_{T2} for Stiffness coefficient for linear and bilinear comparison.

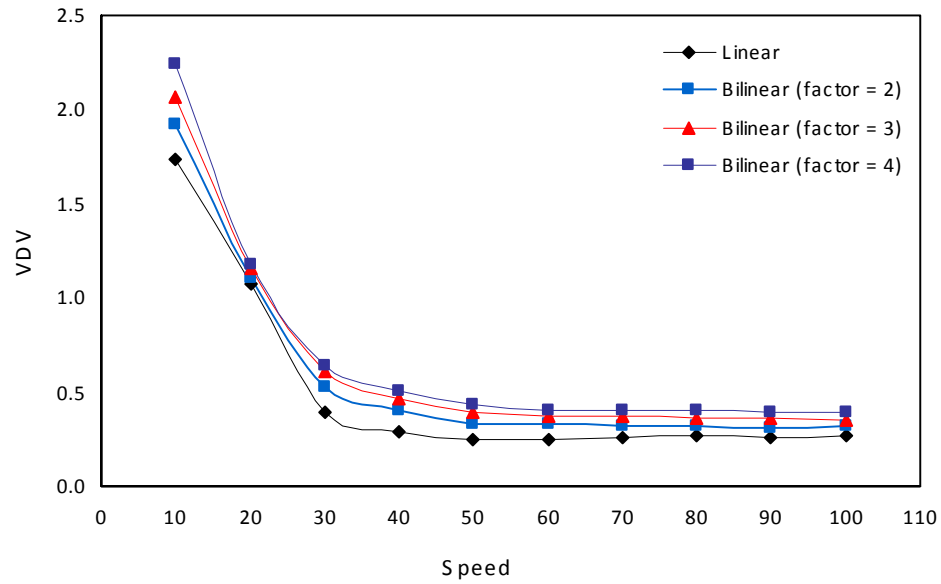


Figure 5.30: VDV vs. Speed for Driver for: 10 humps, h_2 , tire size R_{T2} for Damping coefficient for linear and bilinear comparison.

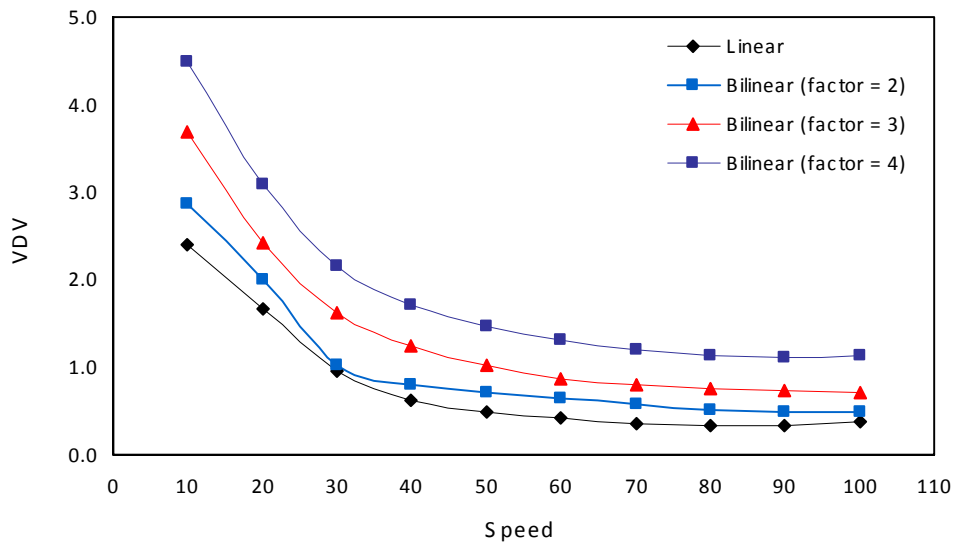


Figure 5.31: VDV vs. Speed for Main Body for: 10 humps, h_2 , tire size R_{T2} for Damping coefficient for linear and bilinear comparison.

CHAPTER 6

CONCLUSION AND RECOMMENDATION

6.1 CONCLUSION

A 3-D vehicle model has been studied from the dynamics behavior and vibrational effects for both the vehicle and the driver, while crossing circular short periodic speed control humps to measure the effects of their geometrical parameters of the hump on the vehicle dynamics in terms of their height, vehicle speed, spacing and multiplicity as well as the variances in stiffness and damping coefficients such as linear and bilinear behavior. Based on the analysis of the extensive parametric analytical study, the following conclusions and recommendations can be specified:

- Circular short periodic speed control humps are not effective in controlling the vehicle speed.
- It is clear that vehicle and driver are exposed to serious shock magnitudes when crossing circular short periodic speed control humps at low speeds.
- If these humps need to be constructed, close to critical spacing should be avoided.
- The optimal approaching speed is less than 50 km/hr.

- If the vehicle speed is less than 50 km/hr, the driver will experience discomfort and if the vehicle speed is higher than the 50 km/hr, the VDV is decreasing and vehicle safety effect is increasing. In fact, these humps are trade between discomfort of the driver and vehicle safety.

6.2 RECOMMENDATION

- In order to force the driver to slow down, these humps are not recommended.
- If the driver is approaching these humps with high speed, it can be dangerous and could have resulted in accident.
- We even would like to emphasize that constructing common standard humps is better than these short humps.
- If these humps ought to be constructed, the driver must be informed of their existence at an enough distance ahead through warning signs to allow all drivers to slow down their speeds.
- If these humps are to be constructed, height of the short periodic hump should be low.
- These humps usually are used to warn the drivers and force them to slow down and this study show that these are serving the main purpose.

6.3 FUTURE WORK

After conducting this parametric study of circular short periodic humps, one can add more to improve driver comfort and vehicle safety for these humps and this can be achieved by:

- Studying the same model including the child seats (back seats).
- Repeating also, the root mean quadrant to find the comfort level of the driver defined by: the British standard BS 6841 and ISO/DIS standard 2631-5 as:

$$r.m.q. = \left(\frac{1}{T} \int a^4(t) dt \right)^{\frac{1}{4}}$$

and compared with VDV results and extract the best evaluation criteria for such a study.

- Considering repeated grooves rather than circular periodic humps in term or their depth, width and spacing with different approaching speeds.

APPENDICES

Appendix 'A'

The main MATLAB program is used to solve the system of equations using the solver ODE45 (Runge Kutta) numerical method is shown below with a file name Accl_Jerk_VDV_1km_minmax.m. All the inputs are clearly shown between the dashed lines in order to find the maximum positive acceleration, maximum positive jerk and VDV.

Accl_Jerk_VDV_1kmh_minmax.m

```

global K_FR K_FL K_RR K_RL K_F1 K_F2 K_R1 K_R2 K_D
global C_FR C_FL C_RR C_RL C_D
global m_FR m_FL m_RR m_RL m_G m_D
global r_x r_y
global a b e d
global I_xx I_yy
global car_speed hump_w r
global car_span
global hump_s
global R_tire R
global th_cr x_star h_star1
global S_cr
global th_2 x_star2 h_star2

% -----
% Enter speed in km/hr (skh) and decimal of this speek (dskh):
skh = 1; dskh = 1;
car_speed = skh*(1000/3600);
car_span = 2.8140;
% -----
% Enter hump raduis or height for 7.5 cm or 10 cm:
r = 0.10;
% -----
% Select diameter of vehicle tire (inch) 13, 15, 19:
R_tire = 15;
R = R_tire * 2.54 / 100;
% -----
% Select hump span of S_cr: 0, 0.5, equal, 1.5, 2.0:
th_cr = asin(R/(R+r));
S_cr = 2 * (R+r) * cos(th_cr) - 2 * r;
hump_s = 0.75 * S_cr;
% -----
th_2 = acos(((hump_s/2)+r)/(R+r));
x_star = r * cos(th_cr);
x_star2 = r * cos(th_2);
h_star1 = R * (1 - sin(th_cr));
h_star2 = r * (sin(th_2));
grav=9.81;

```

```

% -----
% Calculating the acceleration using different velocities:

mm = 100/dskh;
for i=1:mm
t0=0;tfinal=2;
nm=1001;
dt=(tfinal-t0)/nm;
tspan=[t0:dt:tfinal];
Initial_Cond = [0;0;0;0;0;0;0;0;0;0;0;0;0;0;0;0];
[t,y] = ode45(@LE_8DOF_f,tspan,Initial_Cond);

sp(i) = car_speed;
spkh(i)= skh;

axD(:,1) = (1/grav) * ( 1 / m_D ) * ( ...
- C_D * ( y(:,13) - ( y(:,14) - r_x * y(:,16) + r_y * y(:,15) ) ) ...
- K_D * ( y(:,5) - ( y(:,6) - r_x * y(:,8) + r_y * y(:,7) ) ) );

axG(:,1) = (1/grav) * ( 1 / m_G ) * ( ...
- C_FR * ( y(:,14) - e * y(:,16) - a * y(:,15) - y(:,9) ) ...
- C_FL * ( y(:,14) - e * y(:,16) + b * y(:,15) - y(:,10) ) ...
- C_RR * ( y(:,14) + d * y(:,16) - a * y(:,15) - y(:,11) ) ...
- C_RL * ( y(:,14) + d * y(:,16) + b * y(:,15) - y(:,12) ) ...
- C_D * ( y(:,14) - r_x * y(:,16) + r_y * y(:,15) - y(:,13) ) ...
- K_FR * ( y(:,6) - e * y(:,8) - a * y(:,7) - y(:,1) ) ...
- K_FL * ( y(:,6) - e * y(:,8) + b * y(:,7) - y(:,2) ) ...
- K_RR * ( y(:,6) + d * y(:,8) - a * y(:,7) - y(:,3) ) ...
- K_RL * ( y(:,6) + d * y(:,8) + b * y(:,7) - y(:,4) ) ...
- K_D * ( y(:,6) - r_x * y(:,8) + r_y * y(:,7) - y(:,5) ) );

max_Da = max(axD);
min_Da = min(axD);
max_Ga = max(axG);
min_Ga = min(axG);
del_Da(i) = max_Da - abs(min_Da);
del_Ga(i) = max_Ga - abs(min_Ga);

if abs(max_Da) > abs(min_Da)
    maxDa(i) = max_Da;
else
    maxDa(i) = min_Da;
end

if abs(max_Ga) > abs(min_Ga)
    maxGa(i) = max_Ga;
else
    maxGa(i) = min_Ga;
end

subplot(2,1,1),plot(t,axD(:,1)), hold on

```

```

TITLE('Acc. vs. Time for Driver')
XLABEL('Time')
YLABEL('Acc._D')
subplot(2,1,2),plot(t,axG(:,1)), hold on
TITLE('Acc. vs. Time for Main Body')
XLABEL('Time')
YLABEL('Acc._G')
AXy5(:,i)=axD(:,1);
AXy6(:,i)=axG(:,1);

car_speed = car_speed + dskh*(1000/3600);
skh = skh + dskh;

for k=1:1002
vv1(k,i)=axD(k,1)^4;
vv2(k,i)=axG(k,1)^4;
end
Z1 = trapz(t,vv1(:,i));
Z2 = trapz(t,vv2(:,i));
vdvD(i) = Z1^(1/4);
vdvG(i) = Z2^(1/4);
end
% -----
% Calculating the Jerk:
nn=size(t);
ttt=0.0;
for ii=1:mm
for k=1:nn-1
del(k) = t(k+1,1)-t(k,1);
tt(k) = ttt+del(k);
JXy5(k,ii) = (AXy5(k+1,ii) - AXy5(k,ii)) / del(k);
JXy6(k,ii) = (AXy6(k+1,ii) - AXy6(k,ii)) / del(k);
ttt=tt(k);
end
max_Dj = max(JXy5(:,ii));
min_Dj = min(JXy5(:,ii));
max_Gj = max(JXy6(:,ii));
min_Gj = min(JXy6(:,ii));
del_Dj(ii) = max_Dj - abs(min_Dj);
del_Gj(ii) = max_Gj - abs(min_Gj);

if abs(max_Dj) > abs(min_Dj)
maxDj(ii) = max_Dj;
else
maxDj(ii) = min_Dj;
end

if abs(max_Gj) > abs(min_Gj)
maxGj(ii) = max_Gj;
else
maxGj(ii) = min_Gj;
end
end
end
% -----

```

```

% Plotting Acc. and Jerk vs. Velocity:
figure(2);
    subplot(2,1,1),plot(spkh,maxDa,'b-')
    TITLE('Acc. vs. Speed for Driver')
    XLABEL('Speed')
    YLABEL('Acc.')
    subplot(2,1,2),plot(spkh,maxGa,'r-')
    TITLE('Acc. vs. Speed for Main Body')
    XLABEL('Speed')
    YLABEL('Acc.')
figure(3);
    subplot(2,1,1),plot(spkh,maxDj,'b-')
    TITLE('Jerk vs. Speed for Driver')
    XLABEL('Speed')
    YLABEL('Jerk')
    subplot(2,1,2),plot(spkh,maxGj,'r-')
    TITLE('Jerk vs. Speed for Main Body')
    XLABEL('Speed')
    YLABEL('Jerk')
% -----
% Plotting Vibration Dosing Value (VDV):
figure(4);
    subplot(2,1,1),plot(spkh,vdvD,'b-')
    TITLE('VDV vs. Speed for Driver')
    XLABEL('Speed')
    YLABEL('VDV')
    subplot(2,1,2),plot(spkh,vdvG,'r--')
    TITLE('VDV vs. Speed for Main Body')
    XLABEL('Speed')
    YLABEL('VDV')
figure(5);
    subplot(2,1,1),plot(spkh,del_Da,'b-')
    TITLE('DAcc. vs. Speed for Driver')
    XLABEL('Speed')
    YLABEL('DAcc.')
    subplot(2,1,2),plot(spkh,del_Ga,'r-')
    TITLE('DAcc. vs. Speed for Main Body')
    XLABEL('Speed')
    YLABEL('DAcc.')
figure(6);
    subplot(2,1,1),plot(spkh,del_Dj,'b-')
    TITLE('DAcc. vs. Speed for Driver')
    XLABEL('Speed')
    YLABEL('DAcc.')
    subplot(2,1,2),plot(spkh,del_Gj,'r-')
    TITLE('DAcc. vs. Speed for Main Body')
    XLABEL('Speed')
    YLABEL('DAcc.')

```

Appendix 'B'

To run the main program file of the MATLAB program in appendix A, the function file which is named LE_8DOF_F.m, includes all the system of equations and space-state representation as per Chapter 3.

LE_8DOF_F.m

```
function dydt = LE_8DOF_f(t,y)
global K_FR K_FL K_RR K_RL K_F1 K_F2 K_R1 K_R2 K_D
global C_FR C_FL C_RR C_RL C_D
global m_FR m_FL m_RR m_RL m_G m_D
global r_x r_y
global a b e d
global I_xx I_yy

% -----
% SELECT TYPE OF HUMP:
yFR=yfr10hcGScr_f(t);          yFL=yFR;
yRR=yrr10hcGScr_f(t);          yRL=yRR;
% -----
% INPUT STIFFNESSE COEF.:
K_F1=175.5e3;   K_FR=19.96e3;   K_F2=175.5e3;   K_FL=19.96e3;
K_R1=175.5e3;   K_RR=17.5e3;    K_R2=175.5e3;   K_RL=17.5e3;
K_D=100e3;
% -----
% INPUT DAMPING COEF.:
C_FR=1290;   C_FL=1290;   C_RR=1620;   C_RL=1620;   C_D=2e3;
% -----
% INPUMT MASSES:
m_FR=40;     m_FL=40;     m_RR=35.5;   m_RL=35.5;   m_G=730;     m_D=75;
% -----
% INPUMT SEAT POSITION:
r_x=0.5;     r_y=0.5;
% -----
% POSITION FOR CENTER OF MASS:
a=0.761;     b=0.761;     e=1.011;    d=1.803;
% -----
% INPUT MOMENTS of Inertia:
I_xx=1230;   I_yy=1230;
% -----
% NOTATIONS OF DIFF. EQUATIONS:
% y(1) = z_FR
% y(2) = z_FL
% y(3) = z_RR
% y(4) = z_RL
% y(5) = z_D
% y(6) = z_G
% y(7) = z_theta_x
% y(8) = z_theta_y
```

```

% y(9) = zdot_FR      = dydt(1)
% y(10) = zdot_FL     = dydt(2)
% y(11) = zdot_RR     = dydt(3)
% y(12) = zdot_RL     = dydt(4)
% y(13) = zdot_D      = dydt(5)
% y(14) = zdot_G      = dydt(6)
% y(15) = zdot_theta_x = dydt(7)
% y(16) = zdot_theta_y = dydt(8)

dydt(1)= y(9);
dydt(2)= y(10);
dydt(3)= y(11);
dydt(4)= y(12);
dydt(5)= y(13);
dydt(6)= y(14);
dydt(7)= y(15);
dydt(8)= y(16);

dydt(9) = ( 1 / m_FR ) * ( ...
- C_FR * ( y(9) - ( y(14) - e * y(16) - a * y(15) ) ) ...
- K_FR * ( y(1) - ( y(6) - e * y(8) - a * y(7) ) ) ...
- K_F1 * ( y(1) - yFR ) );

dydt(10) = ( 1 / m_FL ) * ( ...
- C_FL * ( y(10) - ( y(14) - e * y(16) + b * y(15) ) ) ...
- K_FL * ( y(2) - ( y(6) - e * y(8) + b * y(7) ) ) ...
- K_F2 * ( y(2) - yFL ) );

dydt(11) = ( 1 / m_RR ) * ( ...
- C_RR * ( y(11) - ( y(14) + d * y(16) - a * y(15) ) ) ...
- K_RR * ( y(3) - ( y(6) + d * y(8) - a * y(7) ) ) ...
- K_R1 * ( y(3) - yRR ) );

dydt(12) = ( 1 / m_RL ) * ( ...
- C_RL * ( y(12) - ( y(14) + d * y(16) + b * y(15) ) ) ...
- K_RL * ( y(4) - ( y(6) + d * y(8) + b * y(7) ) ) ...
- K_R2 * ( y(4) - yRL ) );

dydt(13) = ( 1 / m_D ) * ( ...
- C_D * ( y(13) - ( y(14) - r_x * y(16) + r_y * y(15) ) ) ...
- K_D * ( y(5) - ( y(6) - r_x * y(8) + r_y * y(7) ) ) );

dydt(14) = ( 1 / m_G ) * ( ...
- C_FR * ( y(14) - e * y(16) - a * y(15) - y(9) ) ...
- C_FL * ( y(14) - e * y(16) + b * y(15) - y(10) ) ...
- C_RR * ( y(14) + d * y(16) - a * y(15) - y(11) ) ...
- C_RL * ( y(14) + d * y(16) + b * y(15) - y(12) ) ...
- C_D * ( y(14) - r_x * y(16) + r_y * y(15) - y(13) ) ...
- K_FR * ( y(6) - e * y(8) - a * y(7) - y(1) ) ...
- K_FL * ( y(6) - e * y(8) + b * y(7) - y(2) ) ...
- K_RR * ( y(6) + d * y(8) - a * y(7) - y(3) ) ...
- K_RL * ( y(6) + d * y(8) + b * y(7) - y(4) ) ...
- K_D * ( y(6) - r_x * y(8) + r_y * y(7) - y(5) ) );

```



```

dydt(15) = ( 1 / I_xx ) * (...
+ C_FR * ( y(14) - e * y(16) - a * y(15) - y(9) ) * ( a ) ...
- C_FL * ( y(14) - e * y(16) + b * y(15) - y(10) ) * ( b ) ...
+ C_RR * ( y(14) + d * y(16) - a * y(15) - y(11) ) * ( a ) ...
- C_RL * ( y(14) + d * y(16) + b * y(15) - y(12) ) * ( b ) ...
- C_D * ( y(14) - r_x * y(16) + r_y * y(15) - y(13) ) * ( r_y ) ...
+ K_FR * ( y(6) - e * y(8) - a * y(7) - y(1) ) * ( a ) ...
- K_FL * ( y(6) - e * y(8) + b * y(7) - y(2) ) * ( b ) ...
+ K_RR * ( y(6) + d * y(8) - a * y(7) - y(3) ) * ( a ) ...
- K_RL * ( y(6) + d * y(8) + b * y(7) - y(4) ) * ( b ) ...
- K_D * ( y(6) - r_x * y(8) + r_y * y(7) - y(5) ) * ( r_y ) );

dydt(16) = ( 1 / I_yy ) * ( ...
+ C_FR * ( y(14) - e * y(16) - a * y(15) - y(9) ) * ( e ) ...
+ C_FL * ( y(14) - e * y(16) + b * y(15) - y(10) ) * ( e ) ...
- C_RR * ( y(14) + d * y(16) - a * y(15) - y(11) ) * ( d ) ...
- C_RL * ( y(14) + d * y(16) + b * y(15) - y(12) ) * ( d ) ...
+ C_D * ( y(14) - r_x * y(16) + r_y * y(15) - y(13) ) * ( r_x ) ...
+ K_FR * ( y(6) - e * y(8) - a * y(7) - y(1) ) * ( e ) ...
+ K_FL * ( y(6) - e * y(8) + b * y(7) - y(2) ) * ( e ) ...
- K_RR * ( y(6) + d * y(8) - a * y(7) - y(3) ) * ( d ) ...
- K_RL * ( y(6) + d * y(8) + b * y(7) - y(4) ) * ( d ) ...
+ K_D * ( y(6) - r_x * y(8) + r_y * y(7) - y(5) ) * ( r_x ) );

dydt = [dydt(1); dydt(2); dydt(3); dydt(4); dydt(5); dydt(6); dydt(7);
dydt(8); dydt(9); dydt(10); dydt(11); dydt(12); dydt(13); dydt(14);
dydt(15); dydt(16)];

```

Appendix 'C'

One of the hump profiles is shown below representing front and rear tires when passing over 10 humps.

C10h_span_greater_Scr.m

```

car_speed = 20*(1000/3600);
r = 0.10;
car_span = 2.8140;
hump_s = 0.500;
R_tire = 15; % diameter of vehicle tire (inch)
R = R_tire * 2.54 / 100;
th_cr = asin(R / (R+r)); % interfacing angle with vehicle tire
x_star = r * cos(th_cr);
S_cr = 2 * (R+r) * cos(th_cr) - 2 * r;
% S_cr > hump_s;
h_star = R * (1 - sin(th_cr));

t0z = 0.0;
t1z = t0z+(2*x_star)/car_speed;
t2z = t1z+(hump_s-S_cr)/car_speed;
t3z = t2z+(2*x_star)/car_speed;
t4z = t3z+(hump_s-S_cr)/car_speed;
t5z = t4z+(2*x_star)/car_speed;
t6z = t5z+(hump_s-S_cr)/car_speed;
t7z = t6z+(2*x_star)/car_speed;
t8z = t7z+(hump_s-S_cr)/car_speed;
t9z = t8z+(2*x_star)/car_speed;
t10z= t9z+(hump_s-S_cr)/car_speed;
t11z= t10z+(2*x_star)/car_speed;
t12z= t11z+(hump_s-S_cr)/car_speed;
t13z= t12z+(2*x_star)/car_speed;
t14z= t13z+(hump_s-S_cr)/car_speed;
t15z= t14z+(2*x_star)/car_speed;
t16z= t15z+(hump_s-S_cr)/car_speed;
t17z= t16z+(2*x_star)/car_speed;
t18z= t17z+(hump_s-S_cr)/car_speed;
t19z= t18z+(2*x_star)/car_speed;

t0x = car_span/car_speed;
t1x = t0x+(2*x_star)/car_speed;
t2x = t1x+(hump_s-S_cr)/car_speed;
t3x = t2x+(2*x_star)/car_speed;
t4x = t3x+(hump_s-S_cr)/car_speed;
t5x = t4x+(2*x_star)/car_speed;
t6x = t5x+(hump_s-S_cr)/car_speed;
t7x = t6x+(2*x_star)/car_speed;
t8x = t7x+(hump_s-S_cr)/car_speed;
t9x = t8x+(2*x_star)/car_speed;
t10x= t9x+(hump_s-S_cr)/car_speed;

```

```

t11x= t10x+(2*x_star)/car_speed;
t12x= t11x+(hump_s-S_cr)/car_speed;
t13x= t12x+(2*x_star)/car_speed;
t14x= t13x+(hump_s-S_cr)/car_speed;
t15x= t14x+(2*x_star)/car_speed;
t16x= t15x+(hump_s-S_cr)/car_speed;
t17x= t16x+(2*x_star)/car_speed;
t18x= t17x+(hump_s-S_cr)/car_speed;
t19x= t18x+(2*x_star)/car_speed;

i=1;
for t=0.0:0.0001:2
tt(i) = t;

if t < t0z
y01(i) = 0;
elseif t >= t0z & t <= t1z
y01(i) = sqrt(r^2-(car_speed*(t-t0z))^2+(2*car_speed*(t-t0z)*x_star)-
(x_star)^2);
elseif t >= t1z & t <= t2z
y01(i) = 0;
elseif t >= t2z & t <= t3z
y01(i) = sqrt(r^2-(car_speed*(t-t2z))^2+(2*car_speed*(t-t2z)*x_star)-
(x_star)^2);
elseif t >= t3z & t <= t4z
y01(i) = 0;
elseif t >= t4z & t <= t5z
y01(i) = sqrt(r^2-(car_speed*(t-t4z))^2+(2*car_speed*(t-t4z)*x_star)-
(x_star)^2);
elseif t >= t5z & t <= t6z
y01(i) = 0;
elseif t >= t6z & t <= t7z
y01(i) = sqrt(r^2-(car_speed*(t-t6z))^2+(2*car_speed*(t-t6z)*x_star)-
(x_star)^2);
elseif t >= t7z & t <= t8z
y01(i) = 0;
elseif t >= t8z & t <= t9z
y01(i) = sqrt(r^2-(car_speed*(t-t8z))^2+(2*car_speed*(t-t8z)*x_star)-
(x_star)^2);
elseif t >= t9z & t <= t10z
y01(i) = 0;
elseif t >= t10z & t <= t11z
y01(i) = sqrt(r^2-(car_speed*(t-t10z))^2+(2*car_speed*(t-
t10z)*x_star)-(x_star)^2);
elseif t >= t11z & t <= t12z
y01(i) = 0;
elseif t >= t12z & t <= t13z
y01(i) = sqrt(r^2-(car_speed*(t-t12z))^2+(2*car_speed*(t-
t12z)*x_star)-(x_star)^2);
elseif t >= t13z & t <= t14z
y01(i) = 0;
elseif t >= t14z & t <= t15z
y01(i) = sqrt(r^2-(car_speed*(t-t14z))^2+(2*car_speed*(t-
t14z)*x_star)-(x_star)^2);

```

```

elseif t >= t15z & t <= t16z
y01(i) = 0;
elseif t >= t16z & t <= t17z
y01(i) = sqrt(r^2-(car_speed*(t-t16z))^2+(2*car_speed*(t-
t16z)*x_star)-(x_star)^2);
elseif t >= t17z & t <= t18z
y01(i) = 0;
elseif t >= t18z & t <= t19z
y01(i) = sqrt(r^2-(car_speed*(t-t18z))^2+(2*car_speed*(t-
t18z)*x_star)-(x_star)^2);
elseif t >= t19z
y01(i) = 0;
end

if t < t0x
y02(i) = 0;
elseif t >= t0x & t <= t1x
y02(i) = sqrt(r^2-(car_speed*(t-t0x))^2+(2*car_speed*(t-t0x)*x_star)-
(x_star)^2);
elseif t >= t1x & t <= t2x
y02(i) = 0;
elseif t >= t2x & t <= t3x
y02(i) = sqrt(r^2-(car_speed*(t-t2x))^2+(2*car_speed*(t-t2x)*x_star)-
(x_star)^2);
elseif t >= t3x & t <= t4x
y02(i) = 0;
elseif t >= t4x & t <= t5x
y02(i) = sqrt(r^2-(car_speed*(t-t4x))^2+(2*car_speed*(t-t4x)*x_star)-
(x_star)^2);
elseif t >= t5x & t <= t6x
y02(i) = 0;
elseif t >= t6x & t <= t7x
y02(i) = sqrt(r^2-(car_speed*(t-t6x))^2+(2*car_speed*(t-t6x)*x_star)-
(x_star)^2);
elseif t >= t7x & t <= t8x
y02(i) = 0;
elseif t >= t8x & t <= t9x
y02(i) = sqrt(r^2-(car_speed*(t-t8x))^2+(2*car_speed*(t-t8x)*x_star)-
(x_star)^2);
elseif t >= t9x & t <= t10x
y02(i) = 0;
elseif t >= t10x & t <= t11x
y02(i) = sqrt(r^2-(car_speed*(t-t10x))^2+(2*car_speed*(t-
t10x)*x_star)-(x_star)^2);
elseif t >= t11x & t <= t12x
y02(i) = 0;
elseif t >= t12x & t <= t13x
y02(i) = sqrt(r^2-(car_speed*(t-t12x))^2+(2*car_speed*(t-
t12x)*x_star)-(x_star)^2);
elseif t >= t13x & t <= t14x
y02(i) = 0;
elseif t >= t14x & t <= t15x
y02(i) = sqrt(r^2-(car_speed*(t-t14x))^2+(2*car_speed*(t-
t14x)*x_star)-(x_star)^2);

```

```
elseif t >= t15x & t <= t16x
y02(i) = 0;
elseif t >= t16x & t <= t17x
y02(i) = sqrt(r^2-(car_speed*(t-t16x))^2+(2*car_speed*(t-
t16x)*x_star)-(x_star)^2);
elseif t >= t17x & t <= t18x
y02(i) = 0;
elseif t >= t18x & t <= t19x
y02(i) = sqrt(r^2-(car_speed*(t-t18x))^2+(2*car_speed*(t-
t18x)*x_star)-(x_star)^2);
elseif t >= t19x
y02(i) = 0;
end

i=i+1;

end

plot(tt,y01,tt,y02)
```

NOMENCLATURE

- a : Seat position in relation to the center of mass in the negative x-axis (m).
 b : Seat position in relation to the center of mass in the positive x-axis (m).
 e : Seat position in relation to the center of mass in the negative y-axis (m).
 d : Seat position in relation to the center of mass in the positive y-axis (m).
 r_x : Seat position in relation to the center of mass in the pitch-axis (m).
 r_y : Seat position in relation to the center of mass in the roll-axis (m).
 m_{FR} : Mass of the front right wheel (kg).
 m_{FL} : Mass of the front left wheel (kg).
 m_{RR} : Mass of the rear right wheel (kg).
 m_{RL} : Mass of the rear left wheel (kg).
 m_D : Mass of the driver (kg).
 m_G : Mass of the vehicle (kg).
 $(I_G)_{xx}$: Moment of inertia for pitching (kg m²).
 $(I_G)_{yy}$: Moment of inertia for rolling (kg m²).
 z_{FR} : Displacement of the front right wheel with respect to the y-axis (m).
 z_{FL} : Displacement of the front left wheel with respect to the y-axis (m).
 z_{RR} : Displacement of the rear right wheel with respect to the y-axis (m).
 z_{RL} : Displacement of the rear left wheel with respect to the y-axis (m).
 z_D : Displacement of the driver with respect to the y-axis (m).
 z_G : Displacement of the vehicle body with respect to the y-axis (m).
 θ_x : Rotation of the vehicle body with respect to the pitch-axis (m).
 θ_y : Rotation of the vehicle body with respect to the roll-axis (m).

- y_{FR} : Displacement of the front right tire.
 y_{FL} : Displacement of the front left tire.
 y_{RR} : Displacement of the rear right tire.
 y_{RL} : Displacement of the rear left tire.
 \dot{z}_{FR} : Velocity of the front right wheel with respect to the y-axis (m/s).
 \dot{z}_{FL} : Velocity of the front left wheel with respect to the y-axis (m/s).
 \dot{z}_{RR} : Velocity of the rear right wheel with respect to the y-axis (m/s).
 \dot{z}_{RL} : Velocity of the rear left wheel with respect to the y-axis (m/s).
 \dot{z}_D : Velocity of the driver with respect to the y-axis (m/s).
 \dot{z}_G : Velocity of the vehicle body with respect to the y-axis (m/s).
 $\dot{\theta}_x$: Angular velocity of the driver with respect to the pitch-axis (m/s).
 $\dot{\theta}_y$: Angular velocity of the driver with respect to the roll-axis (m/s).
 \ddot{z}_{FR} : Acceleration of the front right wheel with respect to the y-axis (m/s²).
 \ddot{z}_{FL} : Acceleration of the front left wheel with respect to the y-axis (m/s²).
 \ddot{z}_{RR} : Acceleration of the rear right wheel with respect to the y-axis (m/s²).
 \ddot{z}_{RL} : Acceleration of the rear left wheel with respect to the y-axis (m/s²).
 \ddot{z}_D : Seat acceleration (m/s²).
 \ddot{z}_G : Sprung mass (m/s²).
 $\ddot{\theta}_x$: Pitch acceleration (m/s²).
 $\ddot{\theta}_y$: Roll acceleration (m/s²).
 c_{FR} : Damping coefficients for front right wheel.
 c_{FL} : Damping coefficients for front left wheel.
 c_{RR} : Damping coefficients for rear right wheel.
 c_{RL} : Damping coefficients for rear left wheel.

- c_D : Damping coefficients for driver's seat.
 k_{FR} : Stiffness coefficients for front right wheel.
 k_{FL} : Stiffness coefficients for front left wheel.
 k_{RR} : Stiffness coefficients for rear right wheel.
 k_{RL} : Stiffness coefficients for rear left wheel.
 k_D : Stiffness coefficients for driver's seat.
 k_{F1} : Stiffness coefficients for front right tire.
 k_{F2} : Stiffness coefficients for front left tire.
 k_{R1} : Stiffness coefficients for rear right tire.
 k_{R2} : Stiffness coefficients for rear left tire.
 $a_w(t)$: Filtered weighted acceleration.
 t_1 : Initial times of the calculation period.
 t_2 : Final times of the calculation period.
 S_{cr} : Critical spacing.
 S : Spacing between repeated humps.
 r : Radius (or height) of the hump.
 R : Radius of Tire Size.
 R_{T1} : Radius of tire size 13 in (33 cm).
 R_{T2} : Radius of tire size 15 in (38 cm).
 R_{T3} : Radius of tire size 19 in (48 cm).
 S_{cr1} : Critical spacing of radius of tire size R_{T1} .
 S_{cr2} : Critical spacing of radius of tire size R_{T2} .
 S_{cr3} : Critical spacing of radius of tire size R_{T3} .
 h_1 : Height of the hump is 7.5 cm.
 h_2 : Height of the hump is 10 cm.

REFERENCES

- [1] Barak, P., Magic numbers in design of suspensions for passenger cars, Passenger car meeting, SAE paper 911921, 53–88, Tennessee, 1991.
- [2] Bouazara, M., and Richard, M.J., An optimization method designed to improve 3-D vehicle comfort and road holding capability through the use of active and semi-active suspensions, Eur. J. Mech. A/Solids 20 509–520, 2001.
- [3] Bouazara, M., L'influence des paramètres de suspension sur le comportement d'un véhicule, Master's thesis, Université Laval, Canada, 1991.
- [4] Bouazara, M., and Richard, M.J., An optimal design method to control the vibrations of suspensions for passenger cars, in: International Mechanical Engineering Congress and Exposition: The Winter Annual Meeting of ASME, DSC 58, pp. 61–68, Atlanta, 1996.
- [5] BS 6841, Guide for Evaluation of Human Exposure to Whole-Body Mechanical Vibration and Repeated Shocks, British Standard Institution, 1987.
- [6] Crolla, D.A., Semi-active suspension control for a full vehicle model, SAE Technical Paper Series 911904, 45–51, 1992.
- [7] Dupuis, H., and Zerlett, G., The Effects of Whole-body Vibration, Springer, Germany, 1986.
- [8] Khorshid, E., and Alfares, M., A numerical study on the optimal geometric design of speed control humps, Engineering Optimization, Vol. 36, No. 1, 77–100, 2004.
- [9] Fwa, T.F., and Liaw, C.Y., Rational approach for geometric design of speed-control road hump, Transportation Research Record, 66–72, 1992.
- [10] Gobbi, M., and Mastinu, G., Analytical description and optimization of the dynamic behaviour of passively suspended road vehicles, Journal of Sound and Vibration, 245 (3), 457-481, 2001.

- [11] Granlund, J., Whole-Body Vibration when Riding on Rough Roads, Technical Report by Road Engineering Division, National Road Management Division, Sweden, 2000.
- [12] Griffin, M.J., Handbook of Human Vibration. Academic Press, London, United Kingdom, 1990.
- [13] Griffin, M.J., Parsons, K., and Whitham, E., Vibration and comfort, iv. application of experimental results, Ergonomics 25, 721–739, 1982.
- [14] Hrovat, D., Optimal active suspensions for 3d vehicle models, in: Proc. of the American Control Conference, Vol. 2, pp. 1534–1541, Arizona, USA, 1991.
- [15] ISO/DIS 2631-5, Mechanical vibration and shock—evaluation of human exposure to whole-body vibration - part 5: method for evaluation of vibration containing multiple shocks, 2004.
- [16] Kassem, E., and Al-Nassar, Y., Dynamic considerations of speed control humps, Transportation Research-B, 16B (4), 291–302, 1982.
- [17] Maemori, K., Optimum design of speed control humps for vehicles, Trans. Japan Society of Mechanical Engineers, 54 (502C), 1217, Japan, 1988.
- [18] Pedersen, N., Shape optimization of a vehicle speed control bump, Mech. Struct. & Mach., 26 (3), 319–342, 1998.
- [19] Metallidis, P., Verros, G., Natsiavas, S., and Papadimitriou, C., Fault Detection and Optimal Sensor Location in Vehicle Suspensions, Journal of Vibration and Control; 9; 337, 2003.
- [20] Rakheja, S., Computer-aided dynamic analysis and optimal design of suspension systems for off-road tractors, PhD thesis, Concordia University, Canada, 1985.
- [21] Richard, M.J., and Bouazara, M., Effet de la suspension active et semi-active sur le confort et la stabilité des véhicules routiers sous un régime d'excitation aléatoire, in: Canadian Society for Mechanical Engineering, Forum, McMaster University, pp. 227–231, Hamilton, 1996.
- [22] Saadoon, A., On the specifications of the speed hump design, Special Report, Kuwait Ministry of Interior, Transportation Department, 1998.

- [23] Shaaban, A., Abo-Mossalam, Y., Abed and El Chazly, N., The effect of vehicle suspension system components on the ride comfort due to road roughness, Mansoura Engineering Journal, Faculty of Engineering, Mansoura University, 20 (4) 2837–2845, 1995.
- [24] Verros, G., Natsiavas, S., Papadimitriou, C., Design Optimization of Quarter-car Models with Passive and Semi-active Suspensions under Random Road Excitation, Journal of Vibration and Control; 11; 581–606, 2005.
- [25] Watts, G.R., Road humps for the control of vehicle speeds, Laboratory Report # 597, Transport and Road Research Laboratory, Department of Environment and Department of Transport, Crow Thorne, Berkshire, UK, 1973.
- [26] ضوابط ومواصفات المطبات الصناعية, مديرية الصيانة والتشغيل, أمانة الرياض.
- [27] المواصفات العامة لإنشاء الطرق الحضرية, وزارة النقل (المواصلات سابقاً), المملكة العربية السعودية,
- [28] الدليل الموحد لوسائل التحكم المروري, وزارة النقل والمواصلات, المملكة العربية السعودية.

VITA

Name: Ismail Mohammad Yamin Al-Hindi

Place of Birth: Al-Madinah Al-Munawwarah, Saudi Arabia

Education:

1994-1998 Bachelor of Science in Mechanical Engineering from Florida Institute of Technology University, Melbourne, USA.

The degree was granted in December 1998.

2005-2009 Master of Science in Mechanical Engineering from King Fahd University of Petroleum & Minerals, Dhahran, Saudi Arabia.

The degree is granted in May 2009.

Work Experience:

2008 – Present, Northern Area Projects Department, Saudi Aramco.

- ♦ Controlled and executed Third Party Gas Customers for different projects for BI-21-02009, BI-21-00027, and BI-21-00039.
- ♦ Controlled successfully the Detail Design as a lead engineer for BI10-00017/207 Northern Waste Water and Drainage Upgrade in Safaniyah, Tanajib, Abu Ali and Dhahran.
- ♦ Anticipated in procuring LSTK Contract for BI-10-00441/470 for Abu Ali Water Injection Upgrade Projects.
- ♦ Executed project close out and finalized outstanding change orders for BI-10-00096 and BI-3182 in Berri Gas Plant.

- ◆ Procured LSTK Contract for BI-10-00054 Control Sulfur Emissions in BGP, and BI-3205/3183 Load Shedding and Islanding work in RT, UGP, ShGP.

2004 – 2007, Northern Area Projects Department, Saudi Aramco.

- ◆ Handled successfully the Project Proposal completion for BI-10-00054 Control Sulfur Emissions at Berri Gas Plant Project.
- ◆ Performed an excellent job in the execution of BI-3022, Qatif and Abu-Safa Project close-out activities.

2002 – 2004, Yanbu Refinery Department, Saudi Aramco.

- ◆ Developed compressor and pump curves with Reliability Group.
- ◆ Participated in vibration analysis for rotating equipment for preventive maintenance.
- ◆ Developed Corrosion Under Insulation (CUI) Program for Yanbu Refinery using SAES, API 570, API 581 and NACE RP 0198-98.
- ◆ Prepared a Long Form Contract for all the Fuel Oil Tanks.
- ◆ Executed major T&I regeneration programs for Compressors, Vessels and Fin Fans.
- ◆ Participated in Ras Tanura Refinery's CCR Major T&I shutdown.

2000 – 2001, Northern Area Projects Department, Saudi Aramco.

- ◆ Participated in developing Long Form Contract procurement plan, reviewing design packages and addressing construction changes.
- ◆ Executed the construction works for Marjan Flow-lines and Test-lines under BI-8199.

1998 – 1999, Project Support & Controls Department, Saudi Aramco.

- ◆ Prepared Study and Budget Estimates for Offshore Projects BIs.
- ◆ Participated in reviewing ER Estimates and developed Project Change Orders and Company Estimates for Captial BIs and BI-1900.

Certifications:

- ◆ Certified Cost Engineer, **CCE** (2009), Project Cost Management
The Association for the Advancement of Cost Engineering, USA
- ◆ Certified Associate Value Engineering Specialist, **AVS** (2009), Project Value Management
Society of American Value Engineers International, USA
- ◆ Certified Project In Controlled Environment, **PRINCE2** Practitioner (2008),
Project Management
Office of Government Commerce, UK
- ◆ Certified Project Management Professional, **PMP** (2007), Project Management
Project Management Institute, USA